DIE PLASTIDÄRE ATP SYNTHASE UNTER OXIDATIVEM STRESS: KRITISCHE ANGRIFFSZIELE REAKTIVER SAUERSTOFFSPEZIES

Dissertation

Zur Erlangung des akademischen Grades

Doktor der Naturwissenschaften

- Dr. rer. nat. -

vorgelegt von

Dipl.-Biol. Felix Eberhard Buchert

geboren am 17.11.1983 in Görlitz

angefertigt am Institut für Pflanzenphysiologie

Fachbereich 08 (Biologie und Chemie)

Justus-Liebig-Universität Gießen

Gießen, Mai 2012

1. Gutachter:

PD Dr. Christoph Forreiter

Abteilung Biologie, Department Chemie-Biologie

Naturwissenschaftlich-Technische Fakultät der Universität Siegen

Adolf-Reichwein-Straße 2, 57076 Siegen

2. Gutachter:

Prof. Dr. Alfred Pingoud

Institut für Biochemie

FB08 der Justus-Liebig-Universität Gießen

Heinrich-Buff-Ring 58-62, 35392 Gießen

THE CHLOROPLAST ATP SYNTHASE UPON OXIDATIVE STRESS: CRITICAL TARGETS OF REACTIVE OXYGEN SPECIES

A thesis submitted in partial fulfillment of the requirements

for the degree Doctor of Science

- Dr. rer. nat. -

Dipl.-Biol. Felix Eberhard Buchert

born on 17th of November 1983 in Görlitz

The Department of Plant Physiology

Faculty 08 (Biology and Chemistry)

Justus-Liebig-University Giessen

Giessen, May 2012

Table of contents

PEER-REVIEWED PUBLICATIONS 1

ZUSAMMENFASSUNG 2

SUMMARY 3

1 INTRODUCTION 4

1.1 CHLOROPLAST F-ATP SYNTHASE 4
1.2 REACTIVE OXYGEN SPECIES 7
1.3 PURPOSE OF THE WORK 9

2 MATERIAL AND METHODS 11

2.1 REAGENTS 11
2.2 METHODS 12
2.2.1 Thylakoid membrane preparation 12
2.2.2 Isolation of CF1, subunit dissection and reassembly 12
2.2.3 Mass spectrometry analysis 12
2.2.4 Site-directed mutagenesis 13
2.2.5 Protein expression and purification 14
2.2.6 Hybrid F1 assembly 14
2.2.7 Redox-modulation of thylakoid membranes 15
2.2.8 Trypsin-activation of thylakoid membrane-bound CF1 15
2.2.9 Redox-modulation of soluble F1 16
2.2.10 Treatment with reactive oxygen species 16
2.2.11 Simultaneous measurement of electron transfer and membrane energization 16
2.2.12 Measurement of proton translocation 17
2.2.13 ATP hydrolysis and synthesis measurements 17
2.2.14 Alkalization of thylakoid suspensions 18
2.2.15 Alignment of F1 γ subunits 18

3 RESULTS 19

3.1 *IN SITU* AFFECTION OF CF1CFO BY SINGLET OXYGEN 19
3.1.1 Semi-quantitative detection of singlet oxygen release by Rose Bengal illumination 19
3.1.2 Influence of singlet oxygen on membrane integrity 19
3.1.3 Effect of singlet oxygen on MgATP-dependent proton translocation by CF1CFo 23
3.1.4 Effect of singlet oxygen on sulfite-stimulated MgATPase by isolated thylakoids 24
3.1.5 Effect of γ-cysteine redox state on the impact of singlet oxygen 26
3.1.6 Impact of singlet oxygen on ATP synthesis by isolated thylakoids 28
3.2 CF1 *IN VITRO*: ISOLATION, MOLECULAR DISSECTION AND AFFECTION BY SINGLET OXYGEN 29
3.2.1 Isolation of the CF1 portion from spinach and reconstitution to the membrane 29
3.2.2 Treatment of the isolated CF1 with singlet oxygen 31

3.2.3 Molecular dissection and reassembly of the spinach CF1 portion 33
3.3 MAPPING OF PUTATIVE ROS TARGETS AND MASS SPECTROMETRIC ANALYSIS OF CF1 38
3.3.1 Mapping of putative targets by using a model structure of the CF1 γ subunit 38
3.3.2 Mass spectrometry analysis of CF1 oxidation 40
3.4 THE HYBRID F1: SITE-DIRECTED MUTAGENESIS, EXPRESSION, PURIFICATION AND ASSEMBLY 51
3.5 THE HYBRID F1: MUTANT CHARACTERIZATION OF CATALYTIC PROPERTIES 53
3.5.1 The effect of oxyanions on MgATP hydrolysis 53
3.5.2 The effect of γ disulfide redox-modulation on MgATP hydrolysis 54
3.6 THE HYBRID F1: MGATPASE UPON EXPOSURE TO SINGLET OXYGEN 55
3.7 THE HYBRID F1: MGATPASE UPON EXPOSURE TO HYDROGEN PEROXIDE 59
3.8 THE HYBRID F1: MGADP BINDING PROPENSITY UPON EXPOSURE TO ROS 61

4 DISCUSSION 63

4.1 *IN SITU* AFFECTION OF CF1CFO BY SINGLET OXYGEN 63
4.2 CF1 *IN VITRO*: ISOLATION, MOLECULAR DISSECTION AND AFFECTION BY SINGLET OXYGEN 65
4.3 MAPPING OF PUTATIVE ROS TARGETS AND MASS SPECTROMETRIC ANALYSIS OF CF1 66
4.4 THE HYBRID F1: MUTANT CHARACTERIZATION OF CATALYTIC PROPERTIES 67
4.5 THE HYBRID F1: MGATPASE UPON EXPOSURE TO SINGLET OXYGEN 68
4.6 THE HYBRID F1: MGATPASE UPON EXPOSURE TO HYDROGEN PEROXIDE 69
4.7 THE HYBRID F1: MGADP BINDING PROPENSITY UPON EXPOSURE TO ROS 70
4.8 PERSPECTIVE 71

5 ABBREVIATIONS 73

6 REFERENCES 74

7 ACKNOWLEDGEMENTS 83

STELLUNGNAHME 84

Peer-reviewed publications

Parts of the work have been published / are in the process of being published.

I. F. Buchert, C. Forreiter, Singlet oxygen inhibits ATPase and proton translocation activity of the thylakoid ATP synthase CF1CFo, FEBS Letters, Vol. 584, No 1, pp. 147-152, January, 2010

II. F. Buchert, Y. Schober, A. Römpp, M. L. Richter, C. Forreiter, Reactive oxygen species affect ATP hydrolysis by targeting a highly conserved amino acid cluster in the thylakoid ATP synthase γ subunit (submitted, March, 2012)

Zusammenfassung

Gegenstand der Arbeit ist die Untersuchung des Einflusses von reaktiven Sauerstoffspezies auf die Enzymaktivität der plastidären ATP-Synthase *in situ* und *in vitro*. An isolierten Thylakoiden aus Spinat wurde eine verminderte katalytische Aktivität nach Kontakt mit Singulett-Sauerstoff gemessen. So konnte gezeigt werden, dass von behandelten Thylakoiden sowohl weniger ATP synthetisiert als auch hydrolysiert wurde. Zudem wiesen die Proben einen eingeschränkten Protonentransport in das Thylakoidlumen nach ATP-Zugabe auf. Die Identifizierung spezifischer Angriffsstellen für reaktive Sauerstoffspezies war zentraler Gegenstand der Studie. Demnach wurde der beobachtete Aktivitätsabfall in Abhängigkeit vom Redoxzustand des Enzyms auf Strukturänderungen zurückgeführt. Die Aufreinigung und Analyse der löslichen CF1-Komponente deutete darauf hin, dass die Aktivitätsabnahme durch Singulett-Sauerstoff *in vitro* der Abnahme des Enzyms *in situ* ähnelte. *Cross-Links* zwischen regulatorischen Untereinheiten von CF1, die ursprünglich für den Abfall durch Singulett-Sauerstoff verantwortlich gemacht wurden, konnten durch graduelle Demontage ausgeschlossen werden. Besonderheiten, die mittels Strukturmodellanalyse aufgezeigt werden konnten, deuteten darauf hin, dass die γ Untereinheit von CF1 funktionelle Angriffsziele für Singulett-Sauerstoff enthält. Begleitend dazu ergaben massenspektrometrische Untersuchungen, dass ein konserviertes *Cluster* in der γ Untereinheit, bestehend aus Methioninen und Cystein, durch Singulett-Sauerstoff und Wasserstoffperoxid oxidiert wurde. Eine Analyse entsprechender Punkt-Mutationen an den Zielaminosäuren erfolgte in einem Assemblierungssystem von rekombinanten Untereinheiten aus photosynthetischen ATP-Synthasen. So konnte gezeigt werden, dass die untersuchten Mutanten katalytische Veränderungen aufwiesen, wie beispielsweise Bindungsstärke von MgADP oder Redox-Regulierung der Enzymaktivität. Es wurden dabei Hinweise für Interaktionen innerhalb des *Clusters* gefunden. Zudem hatte die interagierende Gruppe an Aminosäuren weitreichende Einflüsse auf funktionelle Strukturen im Enzym. Letztendlich wurde die wesentliche Zielsetzung der Studie erfüllt, indem mittels der Mutanten gezeigt werden konnte, dass eine Oxidation der postulierten Angriffsziele in der γ Untereinheit durch Wasserstoffperoxid zur Aktivitätsabnahme beitrug. Gleiches galt für Singulett-Sauerstoff, jedoch deuten die Daten auf ein Zusammenspiel mit weiteren Resten hin.

Summary

This study examines the impact of reactive oxygen species on enzymatic activity of the chloroplast ATP synthase *in situ* and *in vitro*. Isolated spinach thylakoids were shown to be less catalytically active upon treatment with singlet oxygen. It was demonstrated that exposed thylakoids lost their capacity to synthesize and hydrolyze ATP and to acidify the thylakoid lumen in an ATP-dependent manner. A central element of the study was the identification of specific target sites which could be solved in the course of the project. Structural predictions upon enzymatic redox-regulation served as a first platform for this approach. Purification of soluble catalytic CF1 protein revealed that ATPase activity *in vitro* attenuated by singlet oxygen in a comparable manner to the reaction *in situ*. With the help of a stepwise disassembly approach it could be shown that initially suggested inter-subunit cross-links between regulatory subunits were not responsible for singlet oxygen-induced loss of activity. Instead, the CF1 γ subunit seemed to be a promising candidate that harbored functional targets responsible for activity attenuation. *In silico* analysis proposed a γ subunit methionine-cysteine cluster to form a highly conserved set of potential targets of various reactive oxygen species. Further mass spectrometry analysis revealed that these residues were susceptible to singlet oxygen and hydrogen peroxide. Several point mutations within in the cluster were analyzed using a recombinant photosynthetic F-ATP synthase assembly system. In an extensive biochemical mutant characterization screen it could be demonstrated that some mutants displayed an aberration of catalytic properties, such as MgADP binding propensity and activity regulation by the γ subunit redox state. The cluster residues were ascribed to mutually interact while having an effect on remote functional domains within the enzyme. Finally, it could be shown that oxidation of the cluster was responsible for hydrogen peroxide-induced activity attenuation. It is very likely that additional residues participate in singlet oxygen-dependent loss of activity.

1 Introduction

1.1 Chloroplast F-ATP synthase

The chloroplast ATP synthase, sometimes referred to as thylakoid ATP synthase, is closely related to its bacterial and mitochondrial homologs (reviewed in McCarty et al. 2000; Richter 2004). Due to high overall structural similarity and amino acid homology in functionally important domains, it is assumed that F-ATP synthases share a common ancestor (Table 1).

Table 1: Nomenclature of equivalent ATP synthase subunits.
[a]ATP synthase from *E. coli* and *Bacillus* PS3 have two identical subunits b. Cyanobacteria and purple non-sulfur bacteria have an extra homolog known as b'. Taken from (Groth and Strotmann 1999; Walker 1998).

type	bacteria	chloroplasts	mitochondria
F1	α	α	α
	β	β	β
	γ	γ	γ
	δ	δ	OSCP
	ε	ε	δ
	-	-	ε
Fo	a	IV (or a)	a (or ATPase 6)
	b[a]	I and II (or b and b')	b
	c	III (or c)	c
Extra	-	-	F6
	-	-	inhibitor
	-	-	A6L
	-	-	d
	-	-	e
	-	-	f
	-	-	g

Like all F-type ATP synthase members, the chloroplast enzyme is composed of two functional portions. It is believed, that those portions evolved by established interplay of an ATP-dependent helicase (Gomis-Ruth et al. 2001) with a membrane protein translocase (Mulkidjanian et al. 2007). In a reversible process, ATP is synthesized or hydrolyzed. These processes are accomplished by two coupled portions, the peripheral membrane protein complex F1 and the integral membrane-spanning protein complex Fo. During ATP synthesis or hydrolysis by F1, an electrochemical potential gradient is utilized or generated by H^+ translocation through Fo. The chloroplast Fo (CFo) portion from spinach (*Spinacia oleracea*) consists of four different subunits with a stoichiometry of $I_1II_1III_{14}IV_1$. The copy number of subunit III is species-specific. The chloroplast F1 (CF1) is an assembly of five subunits, having a stoichiometry of $\alpha_3\beta_3\gamma_1\delta_1\varepsilon_1$ (Figure 1).

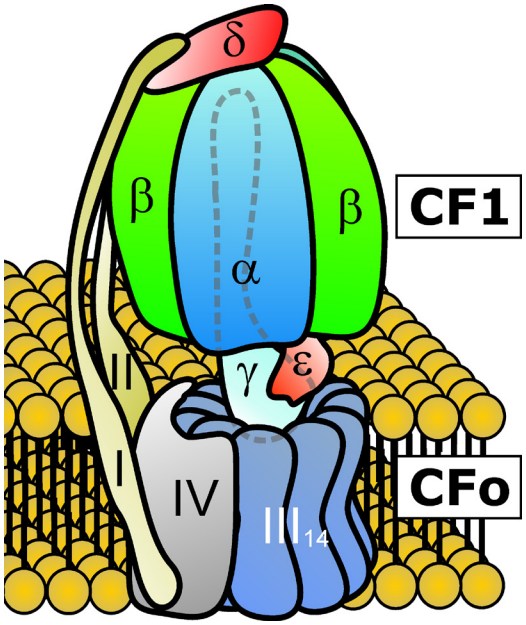

Figure 1: Proposed subunit organization of the chloroplast ATP synthase complex.

Enzyme activity is dependent on divalent cations (Digel et al. 1998) and tightly coupled to rotation of both, the subunit III-ring (Sambongi et al. 1999) and the central stalk, consisting of γ and ε subunits (Kato-Yamada et al. 1998). According to ATP synthesis mode, the ring of subunit III is often referred to as the motor fuelled by the proton motive force (pmf). The pmf is composed of the electric field and the transmembrane H^+ gradient (ΔpH). A crucial feature of the motor is the mechanical coupling to the stalk region of the enzyme. Coupling to subunit III ring is accomplished by the foot region of the γ subunit and the N-terminal domain of the ε subunit (Cingolani and Duncan 2011), the equivalent domain of the δ subunit in mitochondria. ATP synthesis and hydrolysis are restricted to the three catalytic nucleotide binding sites located at the subunit interfaces in the $\alpha_3\beta_3$ hexameric ring. With a total of six, three catalytic sites are formed by β subunit residues and three non-catalytic sites are found on the α subunit at alternating subunit interfaces (Abrahams et al. 1994; Girault et al. 1988). Rotation of the stalk affects catalytic domains and imposes binding site cooperativity. Stalk rotation by 120°, which can be further resolved in substeps (Pu and Karplus 2008), imposes three binding site conformations during a complete rotation. According to substrate affinity, binding site conformations can be discriminated between open, loose and tight. During ATP synthesis, substrates are bound by the open site. Then, the binding pocket converts to a loose site, sequestering the substrates. Finally, ATP is synthesized upon tight site formation and released afterwards (open site). The cycle of interconversion is part of the *binding change mechanism*

proposed by Boyer (1993) and the energy-requiring step is binding of the substrates and release of the products.

A special feature of higher plant CF1 is an additional regulatory domain in the γ subunit (Figure 2A) consisting of about 40 amino acids (Richter 2004). The regulatory core element is a disulfide forming pair of cysteines, designated as C199 and C205 in spinach. Reduction of the γ disulfide elevates ATP hydrolysis and synthesis probably via an inter-domain movement within the γ subunit. It is believed that reduction imprints an open conformation within the dithiol domain (Figure 2C), whereas in the oxidized state the disulfide results in a closed compact structure (Figure 2D). Concurrently, disulfide formation might coordinate an additional regulatory interplay between γ subunit and the C-terminus of the ε subunits, wrapping around parts of the γ subunit protrusion.

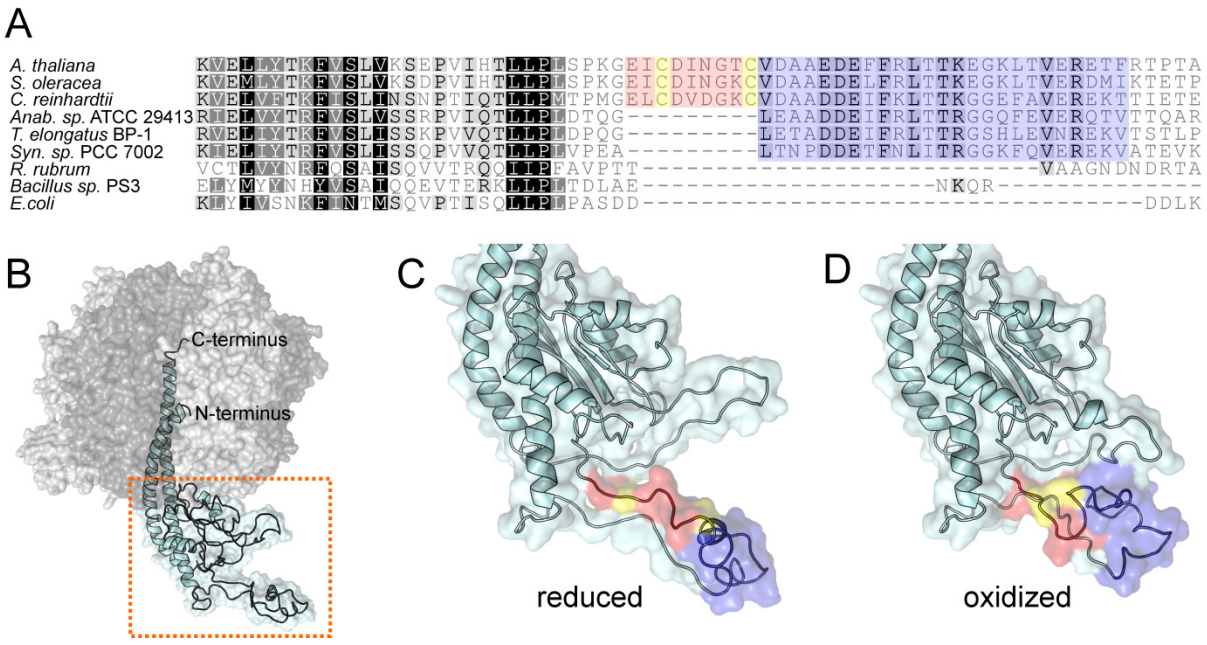

Figure 2: The γ subunit redox region is unique to higher plants and supposedly a flexible structural domain. (A) Sequence alignment excerpt of F1 γ subunits around the redox region (red) containing 9 amino acids unique to higher plant chloroplasts. The core regulatory element is composed of two cysteines (yellow) that are involved in redox-regulation. An insert region (blue) can also be found in cyanobacterial γ subunits (Sunamura et al. 2010). (B) Alignment of crystal structures from spinach CF1 α (light grey) and β (dark grey) subunits, and the γ subunit homology model (cyan) was carried out as described under 2.2.15. Terminal ends of the γ subunit are indicated. The CF1 γ segment protruding from the $\alpha_3\beta_3$ hexamer is highlighted by a dashed box. The segment contains the redox region which is believed to alter its configuration (Richter et al. 2005). Dithiol formation upon reduction imprints an open conformation (C), whereas closed conformation is caused by disulfide formation upon oxidation (D). The color coding is taken from (A).

It is assumed that catalytic activity of CF1 is tightly redox-regulated to prevent futile ATP hydrolysis in the dark (Figure 3), when ATP synthesis is inactive due to low pmf (Mills et al. 1996).

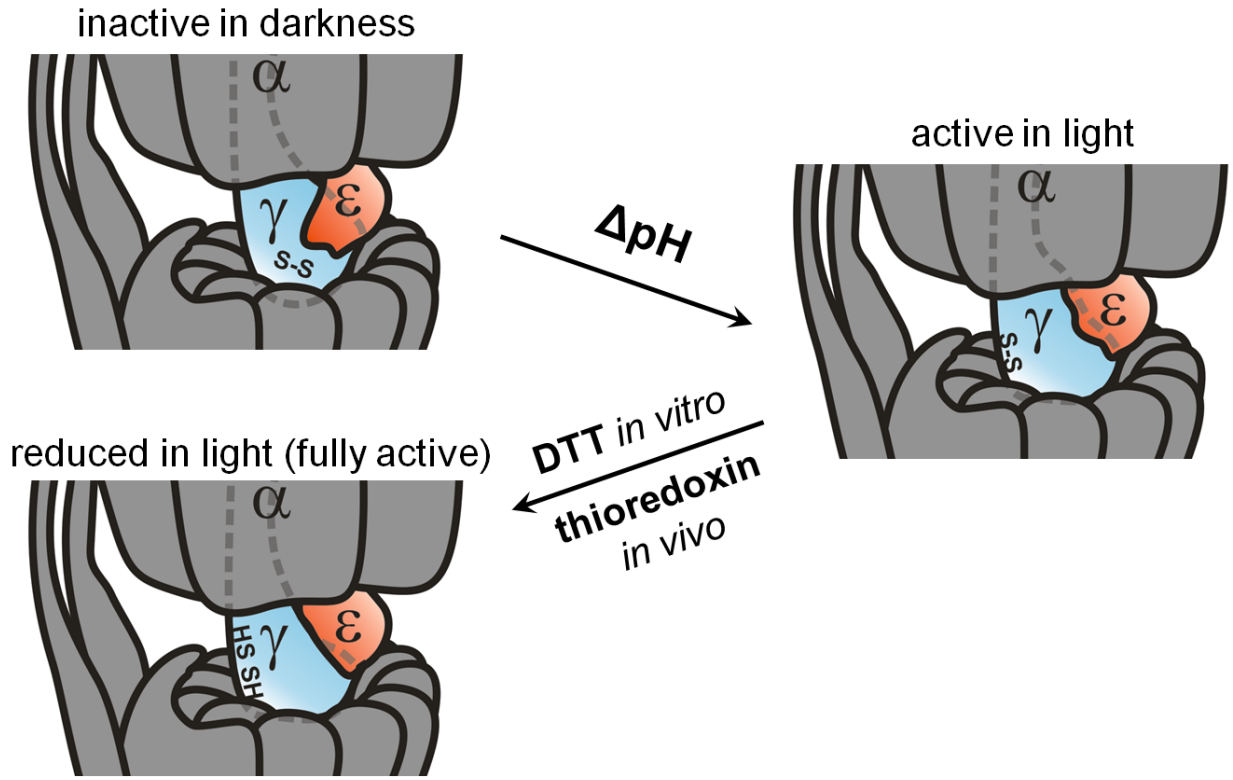

Figure 3: Model of activity regulation in chloroplast F-ATP synthase. The disulfide-forming pair of cysteines is buried in darkness and the enzyme is inactive due to tight interplay between γ and ε subunits. Upon illumination, the generated ΔpH is believed to cause structural changes between the two subunits, thus loosening the strength of interaction. Structural alterations within the γ subunit result in solvent exposure of the disulfide. In light the enzyme is active and enhanced activities are obtained by reduction and cleavage of the disulfide bridge, resulting in structural changes of the γ subunit and probably the ε subunit as well. The figure is adapted from Evron et al. (2000).

1.2 Reactive oxygen species

Evolution of oxygenic photosynthesis, resulting in Great Oxygenation Event several billion years ago (Hohmann-Marriott and Blankenship 2011), ever since was a potential harm to anaerobic and aerobic organisms as well. While hazardous consequences for the former are perfectly obvious, the downside of oxygen production for aerobic organisms is not obvious at first glance. Unambiguously, the innovation of splitting highly abundant water freed photosynthesis to invade new environments. As a consequence of downstream evolutionary events, accumulation of oxygen literally changed the planet by establishing aerobic respiration (Dismukes et al. 2001). Nevertheless, chemical properties of the molecule unavoidably cause formation of reactive oxygen species (ROS) as by-products of photosynthesis (Apel and Hirt 2004; Glaeser et al. 2011) and aerobic respiration as well (Adam-Vizi and Chinopoulos 2006). Triplet molecular oxygen ($^3O_2$) in its ground state is a bioradical, containing two outermost parallel-spinning

valence electrons that occupy separate orbitals. To oxidize a nonradical atom or molecule, $^3O_2$ needs to react with a partner, providing a pair of electrons with parallel spins and fitting into free electron orbitals of $^3O_2$. Pairs of electrons in most organic molecules typically have opposite spins (Cadenas 1989), thus imposing a restriction on the reaction with $^3O_2$. However, ground state $^3O_2$ can be converted to ROS (Figure 4) by energy transfer or by electron transfer reactions (reviewed in Apel and Hirt 2004). The former reaction yields singlet oxygen ($^1O_2$), whereas the latter results in sequential reduction to superoxide ($O_2^{\bullet-}$), hydrogen peroxide (H_2O_2), and hydroxyl radicals ($OH^{\bullet}$).

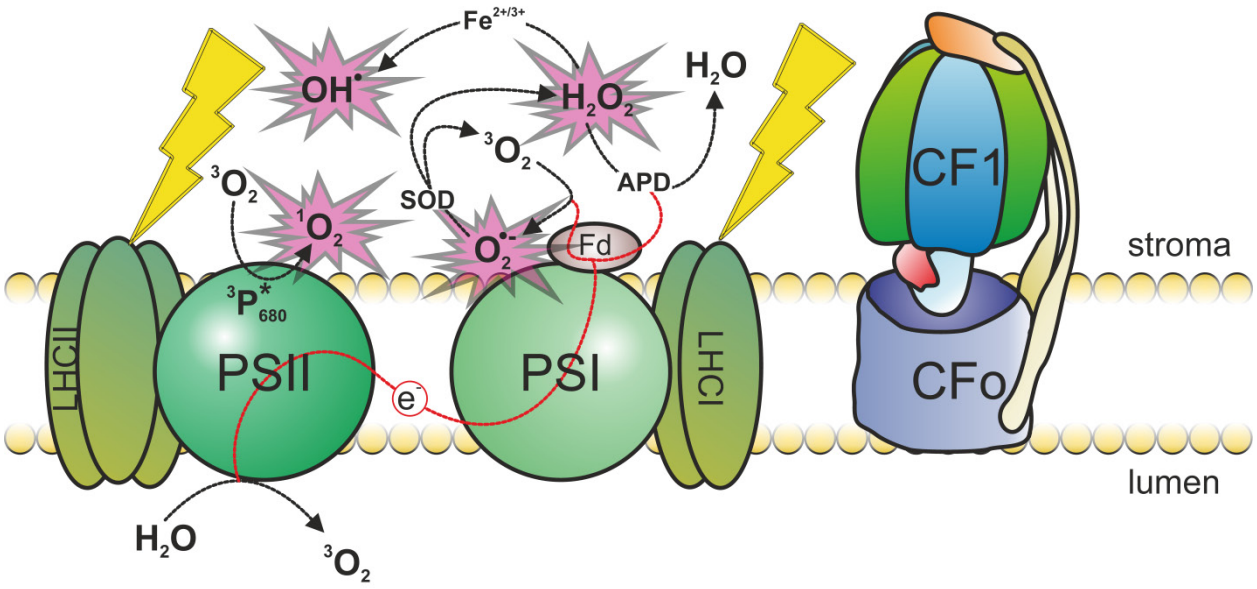

Figure 4: Sites of ROS generation in chloroplasts. Ground state triplet oxygen ($^3O_2$) forms singlet oxygen ($^1O_2$) at photosystem II (PSII) by energy transfer from triplet excited chlorophyll of PSII reaction center ($^3P^*_{680}$). In the Mehler reaction at photosystem I (PSI), superoxide ($O_2^{\bullet-}$) is formed by electron transfer to $^3O_2$ via ferredoxin (Fd). Following detoxification by superoxide dismutase (SOD), hydrogen peroxide (H_2O_2) is formed. Ascorbate peroxidase (APD) consumes H_2O_2, yielding water. The scavenging is also referred to as water-water cycle, according to electron circuit. By various peroxidases (not shown) and iron-catalyzed Haber-Weiss reaction, hydroxyl radicals ($OH^{\bullet}$) are generated. Light harvesting complex I and II (LHCI, LHCII), and the ATP synthase (CF1CFo) are shown.

In plants, especially under high light conditions, electron transfer chain is frequently overloaded. As a consequence, triplet excited pigments are generated. Excited pigment intermediates contain outer electrons spinning in a parallel orientation, thus facilitating formation of ROS and other radicals. The mode of action is the same for artificial *in vitro* photosensitizers (DeRosa and Crutchley 2002), such as Rose Bengal (RB). However, *in vivo* ROS are scavenged by various antioxidative defense mechanisms (Mittler 2002), but the equilibrium between production and scavenging is permanently perturbed upon environmental changes. ROS react with lipids, nucleic acids and proteins. Therefore, these highly reactive molecules can damage the photosynthetic apparatus and promote photoinhibition (Nishiyama

et al. 2006). The most prominent ROS formed under high light conditions is H_2O_2, mainly released by dismutation at PSI. H_2O_2 is considered to be a weak oxidant (Imlay 2003), acting as a signal for genetically controlled stress-responses (Laloi et al. 2007; Neill et al. 2002). There are indications that transport of H_2O_2 is facilitated via aquaporins (Bienert et al. 2006), enabling the molecule to diffuse rapidly within the photosynthetic cell. In contrast, the damaging potential of $^1O_2$ is much higher (Davies 2005). For this reason $^1O_2$ is often referred to as the major ROS involved in photo-oxidative damage (Triantaphylides et al. 2008). It is mainly produced by triplet chlorophyll during energy transfer at PSII. However, $^1O_2$ is also formed at other sites where triplet chlorophyll molecules appear, such as the antennae of light harvesting complex (Niyogi 1999). The transport mechanism for $^1O_2$ is still unclear, but recent studies suggest that several cellular compartments can be reached, distant from its origin at PSII (Fischer et al. 2007). Like H_2O_2, $^1O_2$ is considered to be a signaling molecule (Kim et al. 2008a). Recent findings that ascribe ROS to molecular messengers are in good correspondence with the idea that these reactive molecules are also considered to play a role in evolution (Dowling and Simmons 2009).

1.3 Purpose of the work

The idea of the work presented here originated from previous observations obtained in the Arabidopsis *flu* mutant by Mahler et al. (2007). This mutant accumulates free protochlorophyllide in darkness due to an absent feedback inhibition, mediated by the nuclear encoded FLUORESCENT protein (op den Camp et al. 2003). Upon re-illumination, free protochlorophyllide acts as a photosensitizer for $^1O_2$ generation. Therefore, the *flu* mutant is a versatile tool to examine $^1O_2$-specific effects in a non-invasive manner (Kim et al. 2008a). Mahler et al. (2007) could show that thylakoid protein pattern was altered 15 min after $^1O_2$ formation already. In particular, a new CF1 γ subunit isoform was detected in a two-dimensional polyacrylamide gel electrophoresis approach. The authors concluded that immediateness of the observation indicated a direct $^1O_2$ impact on the γ subunit, rather than genetically induced post-translational modifications. Initial mass spectrometric analysis revealed a $^1O_2$-specific alteration of a γ-peptide between γF176 and γK195. Furthermore, it could be demonstrated that re-illuminated mutants showed enhanced non-photochemical quenching (NPQ). In higher plants, this mechanism evolved to protect the photosynthetic machinery by managing the light capturing by PSII (Demmig-Adams and Adams 1992; Niyogi 2000). Three quenching components account for NPQ, termed photoinhibition-related (qI), state transition-related (qT), and energy-dependent quenching (qE). The latter is triggered by the thylakoid ΔpH, whereas acidic lumen pH is an activatory parameter (Bratt et al. 1995; Muller et al. 2001; Yamamoto 1979). It could be shown that NPQ is modulated by modification of thylakoid membrane proton

efflux conductance (gH^+) through ATP synthase (Kanazawa and Kramer 2002; Takizawa et al. 2008).

In order to support *in vivo* observations, the initial objective of my work was to find out if $^1O_2$ affects enzymatic activity of CF1CFo *in situ*. A spinach thylakoid assay system enabled biochemical analysis of the membrane-bound enzyme under oxidative stress. Since oxidative enzyme affection has not been extensively studied yet, my project was intended to gain detailed information about specific target sites for $^1O_2$ and other ROS. Expected gain of knowledge could help to design *in vivo* studies with ROS-tolerant F-ATP synthase in the future. First of all, catalytically active CF1 was isolated and analyzed *in vitro*. Target subunit delimitation was accomplished by stepwise molecular subunit dissection and reassembly. This biochemical approach allowed exclusive exposure of particular enzyme building blocks and elimination of interfering regulatory subunits, revealing potential targets within the γ subunit. *In silico* target mapping and mass spectrometry analysis proposed a sulfurous γ subunit amino acid cluster. Extensive γ subunit mutant analysis of assemblies containing native CF1 α and β subunits is rather complicated. Therefore, for the first time, a previously established recombinant assembly system served as a tool to monitor a broad range of mutant enzymes in regard to ROS response. Detailed ROS target site information is provided in the site-directed mutant screens.

2 Material and methods

2.1 Reagents

chemical	manufacturer
9-AA	Sigma Aldrich
Aceton	AppliChem
Acetonitril	Uvasol
ACMA	Sigma Aldrich
ADP	AppliChem
Ammonium bicarbonate	Sigma Aldrich
Ammonium chloride	AppliChem
Ammonium heptamolybdate	Merck
Ampicillin	AppliChem
ATP	AppliChem
*Bam*HI	New England Biolabs
Bovine serum albumin	AppliChem
Chloramphenicol	AppliChem
Chloroform	AppliChem
Coomassie Brilliant Blue R-250	AppliChem
Copper(II) chloride	Merck
DCMU	Sigma Aldrich
*Dpn*I	New England Biolabs
DTT	AppliChem
*Eco*RI	New England Biolabs
EDTA - Disodium salt (analytical grade)	Serva
Ethanol	AppliChem
Ferrous nitrate, hexahydrate	Serva
Formic acid (puriss. pa)	Fluka
Glycerol	Roth
Gramicidin D	AppliChem
H_2O, HPLC grade	Fluka
H_2O_2 solution	AppliChem
Iron(II) sulfate	Merck
Magnesium chloride	AppliChem
MES	AppliChem
*Nco*I	New England Biolabs
Phusion DNA polymerase	Fisher Scientific
Plas/mini Isolation Spin-Kit	AppliChem
Potassium ferricyanide	AppliChem
Potassium phosphate	Sigma Aldrich
Pyocyanine (purified from photo-oxidized Phenazine methosulfate)	Serva
RB	AppliChem
RNO	Sigma Aldrich
Sodium chloride	Fluka
Sodium sulfite	Fluka
Sucrose	AppliChem
Sulfuric acid	Merck
Superflow Ni-NTA agarose	Qiagen
T4 DNA ligase	New England Biolabs
T4 Polynucleotide Kinase	New England Biolabs
Tricine	AppliChem
Tris	AppliChem
Trypsin (Sequencing Grade Modified Trypsin, porcine)	Promega
Urea (ultra pure)	Roth
Venturicidin	Sourcon-Padena

2.2 Methods

2.2.1 Thylakoid membrane preparation

Preparation procedure was basically performed as previously described (McCarty 2006). Fresh leaves of market spinach (*Spinacia oleracea*) were rinsed with water and larger midribs were removed. Isolation was performed at 4 °C. 10 g of leaf material was ground for 5 s in a pre-cooled Waring Blendor using 50 mL of homogenization buffer containing 400 mM sucrose, 20 mM Tricine-NaOH (pH 8.0) and 10 mM NaCl. The homogenate was passed through 4 layers of Micracloth and centrifuged for 10 min at 5000×*g*. The resulting pellet was resuspended in a small volume of homogenization buffer to determine chlorophyll (Chl) content (Arnon 1949). Afterwards, thylakoids were diluted either to 1 mg Chl mL^{-1} or 4 mg Chl mL^{-1} for further experiments. In some experiments, thylakoids were stripped of CF1 and the membranes were stored at -80 °C in a buffer containing 400 mM sucrose, 10 mM Tricine-NaOH (pH 8.0), 10 mM NaCl and 10 mg mL^{-1} bovine serum albumin (Kamienietzky and Nelson 1975). The membrane vesicles were later used for CF1 reconstitution experiments (Cruz et al. 1995).

2.2.2 Isolation of CF1, subunit dissection and reassembly

Isolation of catalytically active spinach CF1 (Shapiro and McCarty 1990), followed by the release of δ and ε subunit (Richter et al. 1986), was performed according to published procedures. By following published protocols, further dissection yielded $\alpha_3\beta_3$ hexamer (Gao et al. 1995) which was reassembled afterwards to obtain CF1 (He et al. 2008; Sokolov et al. 1999). Determination of protein, using bovine serum albumin as a standard, was carried out according to the methods of Bradford (1976). Immunodetection of the γ subunit was performed with antibodies that were a generous gift from Dr. Wolfgang Junge.

2.2.3 Mass spectrometry analysis

ROS treated soluble spinach CF1 (see section 2.2.10) was frozen in liquid nitrogen and kept on ice. The protocol, following raw data processing, was carried out by Yvonne Schober (Institute of Inorganic and Analytical Chemistry, Justus-Liebig-University Giessen): Analysis of the spectra was done with the help of Y. Schober and Dr. Andreas Römpp (Institute of Inorganic and Analytical Chemistry, Justus-Liebig-University Giessen).

CF1 was digested using modified trypsin at a 1:30 enzyme/protein ratio (w/w) at 37 °C for 15 h. In addition, a purification step using C18 Zip Tips (Varian, Lake Forest, USA) was applied according to the manufacturer's recommendations. Measurements of all samples were accomplished on an Ultimate binary nano HPLC pump/autosampler system for HPLC analysis (LCPackings/Dionex, Idstein, Germany). 5 µL of the sample were pre-focused on a trap column (Dionex, C18 PepMap, inner diameter 300 µm, length 5 mm) and separated on a fused-silica C18 PepMap100 capillary column (Dionex, 3 µm, 100 Å; inner diameter 75 µm; length 150 mm). The flow rate was 0.2 µL min^{-1}. The nanoHPLC system was coupled either to a nanoelectrospray interface of a LTQ Orbitrap Discovery mass spectrometer or a LTQ FT Ultra mass spectrometer (both Thermo Fisher Scientific GmbH, Bremen, Germany). Survey MS scans with a high mass accuracy better than 2 ppm were measured on both instruments. The three most intense peaks in the survey scan were chosen for fragmentation in ion trap ms mode. Collision induced dissociation was used for fragmentation in the ion trap. Each sample was measured three times. LC-ESI-MS/MS data were searched against the UniProt database (www.uniprot.org) of spinach CF1 using Proteome Discoverer 1.2 (Thermo Fisher Scientific GmbH, Bremen, Germany) based on the SEQUEST search algorithm. Mass tolerance for precursor ions was set to 2 ppm, mass tolerance for fragment ions was set to 0.8 u. Two missed cleavages were allowed in order to account for incomplete digestion. Oxidation was allowed as post translational modification. Peptides with a "peptide probability" (SEQUEST parameter) of 50 and higher were considered as significant identifications. Peptides of interest where manually inspected, based on fragment ion spectra and the specific location of oxidized amino acid residues was verified.

2.2.4 Site-directed mutagenesis

All mutations were performed using template plasmids pET8c-γ.BB1 and pET8c-*Rr*.β. The former pET expression vector carried a *Bam*HI/*Nco*I-ligated cDNA coding for spinach wild type CF1 γ subunit (Sokolov et al. 1999). In the latter pET vector *Eco*RI/*Bam*HI-ligated cDNA coded for wild type *Rhodospirillum rubrum* β subunit (Nathanson and Gromet-Elhanan 1998). Phosphorylation of 5'-end abutting oligonucleotides, PCR reaction, restriction digest of the template DNA, ligation of the amplified pET vector and transformation into *E. coli* XL1-Blue cells, followed by selection for ampicillin resistance (100 µg mL^{-1}), were carried out according to the manufacturer's instructions. Oligonucleotide sequences carrying the mutations are shown in Table 2. Sequencing was performed by GATC Biotech (Konstanz, Germany). Additionally, a previously published plasmid (Samra et al. 2006) was used, coding for an alanine substitution of disulfide-forming regulatory cysteines (γC199+205A).

Table 2: Oligonucleotides used for site-directed mutagenesis.
[a]pET vectors carrying the CDS of *Spinacia oleracea atpC* (γ) and *Rhodospirillum rubrum atpD* (β) were used as templates. [b]Underlined and latin bases indicate mutations and wobble base pairing, respectively.

primer	mutation[a]	oligonucleotide sequence (5'-3')[b]
FB005	γM23L	ATCACCGAAGCACTGAAGCTCGTCGCC
FB009	γC89A	ATTAAACCCGCCCGCAAGACCACGGTC
FB013	γM95L	GGTTTAATAATCTGTTGCTGAAGAAGG
FB002	γH187Q	AATCAGACCCAGTAATCCAGACCCTACTCC
FB007	γM279L+γM282L	CTTGCTGCGAGGCTGACTGCTCTGAGTAATGCTACTG
FB020	βY341F	*A*CTGGGCATCTTCCCGGCCGTC
FB022	βH363Q+βY364F	GTTCAAGGTGGCCCGCGAAGTTC

2.2.5 Protein expression and purification

All backbone plasmids were a generous gift from Dr. Mark Richter. Wild type and mutant constructs were expressed by following the same protocol. The pET plasmids carrying recombinant spinach CF1 γ subunit were transformed into expression host *E. coli* BL21(DE3)/pLysS (Studier and Moffatt 1986). Previously published pET expression vectors, carrying *Rhodospirillum rubrum* F1 α subunit with an N-terminal His-tag (Tucker et al. 2004) and wild type *Rhodospirillum rubrum* β subunit (Nathanson and Gromet-Elhanan 1998), were transformed into expression host *E. coli* BL21-Gold(DE3)/pRARE. Cells were selected for ampicillin (100 µg mL^{-1}) and chloramphenicol (34 µg mL^{-1}) resistance. Cell suspensions were passed three times through a French press at 10000 psi for lysis. Inclusion bodies were purified as described elsewhere (Sokolov et al. 1999) by several centrifugation washing steps for 10 min at 5000×*g* in a buffer containing 50 mM Tris-HCl (pH 8.0) and 2 mM EDTA. Storage was carried out at -80 °C in 25 mM Tris-HCl (pH 8.0), 1 mM EDTA, 50% (v/v) glycerol.

2.2.6 Hybrid F1 assembly

Assembly of a catalytically active hybrid F1 $\alpha^{R}{}_{3}\beta^{R}{}_{3}\gamma^{C}$ core complex consisting of RrF1 α_{6xHis} (α^{R}) and β (β^{R}) subunits and spinach CF1 γ (γ^{C}) subunit was performed based on a method described elsewhere (He et al. 2007). Briefly, inclusion bodies of the subunits were solubilized in 8 M urea, centrifuged at 16,000 rpm and 4 °C for 30 min and mixed at a ratio of α^{R}:β^{R}:γ^{C} = 5:5:3 by weight. The subunit mix was diluted to 0.1 mg protein mL^{-1} in refolding buffer containing 4 M urea, 50 mM Tris-HCl (pH 8.0), 50 mM NaCl, 50 mM $MgCl_2$, 50 mM ATP, 20 mM DTT, 20% glycerol and dialyzed in two steps at 4 °C against 10 volumes dialysis buffer containing 50 mM Tris-HCl (pH 8.0), 50 mM NaCl, 20% glycerol. The dialyzed protein was applied to a Ni-NTA

affinity column equilibrated with 50 mM Tris-HCl (pH 8.0), 50 mM NaCl, 1 mM ATP (TNA buffer), washed and eluted in TNA buffer including 300 mM imidazole. Eluted protein was precipitated by adding solid ammonium sulfate (50% saturation) and desalted after centrifugation via Sephadex G50 spin columns (Penefsky 1977). Assemblies were stored in aliquots at -80 °C in TAG buffer containing 50 mM Tris-HCl (pH 8.0), 1 mM ATP, 20% (v/v) glycerol. Due to surface properties of spinach CF1 α subunit, assembly of recombinant CF1 $\alpha_3\beta_3\gamma$ from inclusion bodies cannot be carried out (personal communications with Dr. Mark Richter and Dr. Toru Hisabori). Therefore, the hybrid F1 assembly system was used for mutant screening in this work.

2.2.7 Redox-modulation of thylakoid membranes

Thylakoids (100 µg Chl mL^{-1}) were illuminated (900 W m^{-2} / ca. 4.2 mmol m^{-2} s^{-1} PAR; Philips 7158; Philips, Hamburg, Germany) between 1 and 3 min at 25 °C in the presence of 50 mM Tricine-NaOH (pH 8.0), 50 mM NaCl, 5 mM $MgCl_2$, 25 µM pyocyanine and 10 mM DTT to reduce regulatory γ-cysteines. Those thylakoids will be referred to as “activated thylakoids”. Alternatively, in some experiments reduced or oxidized thylakoids were obtained by incubating membrane preparations (1 mg Chl mL^{-1}) for 30 min at room temperature with 10 mM DTT (“reduced thylakoids”) and 100 µM $CuCl_2$ (“oxidized thylakoids”), respectively (Samra et al. 2006).

2.2.8 Trypsin-activation of thylakoid membrane-bound CF1

Where indicated, oxidized or reduced thylakoids were used for trypsin treatment as described previously (McCarty 2005). Thus, compared to their non-trypsinized counterparts, enhanced MgATPase activities can be obtained since trypsinized γ subunit is not longer inhibited by the ε subunit (Hightower and McCarty 1996; Soteropoulos et al. 1992). Assay conditions during illumination were identical as for “activated thylakoids” except the presence of trypsin and absence of DTT. Thylakoids (100 µg Chl mL^{-1}) were incubated for 1 min with 5 µg mL^{-1} of freshly prepared trypsin in the light (900 W m^{-2}; 25 °C). After illumination, 6-fold excess of trypsin inhibitor (by weight) was added.

2.2.9 Redox-modulation of soluble F1

Desalted (Penefsky 1977) ammonium sulfate precipitates of dissected/reassembled CF1 were reduced and oxidized at the conditions indicated. In some experiments 0.29 µM hybrid F1 was incubated in TAG buffer for 60 min and 37 °C in the presence of 10 mM DTT (reduction) and 100 µM $CuCl_2$ (oxidation), respectively.

2.2.10 Treatment with reactive oxygen species

Illumination for 1 min (900 Wm^{-2}; 25 °C) of thylakoids was performed in the presence of different concentrations of RB as a potential photosensitizer for $^1O_2$ formation (DeRosa and Crutchley 2002). In some experiments, $^1O_2$ formation was semi-quantitatively monitored by absorbance quenching of *p*-nitrosodimethylaniline (RNO) in an illuminated mixture containing 50 mM Tricine-NaOH (pH 8.0), 50 mM NaCl, 5 mM $MgCl_2$, 25 µM RNO, 10 mM L-histidine and 2.5 µM RB (Telfer et al. 1994). Thylakoids were assayed for MgATPase immediately after illumination. For control experiments, activated thylakoids were kept for 1 min with 10 µM RB in the dark. Unless indicated, 0.29 µM soluble chloroplast and hybrid F1 were illuminated for various periods in the presence of 2 µM RB. H_2O_2 experiments were carried out by incubating soluble enzyme for 60 min at 37 °C and various concentrations of H_2O_2. added from a stock solution. Several compounds activate H_2O_2, yielding $OH^{\bullet}$ via Fenton chemistry (Lin and Wu 2005). Therefore, any catalysts were omitted in the assay resulting in rather high concentrations of H_2O_2 applied. The reaction was quenched for 30 min at 25 °C by 12.5-fold dilution in 50 mM Tris-HCl (pH 8.0) and 10 mM L-methionine. During ROS treatment, CF1 was kept in TA buffer containing 50 mM Tris-HCl (pH 8.0) and 1 mM ATP. Hybrid F1 was kept in TAG buffer during ROS exposure. In some experiments $^1O_2$ was generated in 50 mM MES-KOH (pH 6.0), 1 mM ATP, 20% (v/v) glycerol.

2.2.11 Simultaneous measurement of electron transfer and membrane energization

The assay was performed as described elsewhere (Evron and McCarty 2000). In advance, thylakoids (100 µg Chl mL^{-1}) were illuminated for 1 min (900 W m^{-2}; 25 °C) in a mixture containing 50 mM Tricine-NaOH (pH 8.0), 50 mM NaCl and RB at different concentrations. For fluorescence measurements, a reaction mixture (2 mL) was assayed containing 50 mM Tricine-NaOH (pH 8.0), 50 mM NaCl, 0.2 mM ferricyanide, 2 µM 9-aminoacridine (9-AA) and thylakoids equal to 10 µg Chl. Measurements were performed using a FluoroMax-4 device (HORIBA Jobin Yvon, New Jersey, USA). A grey filter (T = 10%) and a filter with T_{max} at 400 nm were placed in

front of the excitation beam (399 nm, slit bandwidth 0.5 nm) and emission beam (430 nm, slit bandwidth 8 nm), respectively. Electron transfer was stimulated by illuminating samples with actinic red light (140 µmol m^{-2} s^{-1} PAR) for 4 min while 9-AA fluorescence and ferricyanide reduction were monitored. In some experiments, membranes were uncoupled with 2 µM gramicidine D and 4 mM NH_4Cl. Obtained data was used to calculate ΔpH values as described elsewhere (Schuldiner et al. 1972) assuming a ratio of external volume to internal thylakoid volume of 2500 to 1 in a reaction mixture with thylakoids equal to 20 µg of Chl mL^{-1} (McCallum and McCarty 2007).

2.2.12 Measurement of proton translocation

H^+ translocation by activated thylakoids was estimated by 9-amino-6-chloro-2-methoxyacridine (ACMA) fluorescence measurements performed as described elsewhere (McCarty 2005). A grey filter (T = 10%) was placed in front of the excitation beam (410 nm, slit bandwidth 0.75 nm). Emission was recorded at 475 nm (slit bandwidth 2.5 nm). Thylakoids, equal to 10 µg Chl, were assayed in a mixture containing 50 mM Tricine-NaOH (pH 8.0), 5 mM NaCl, 1.5 mM $MgCl_2$ and 2 µM ACMA. Quenching was initiated by adding 3 mM ATP. After reaching steady state fluorescence, 3 mM NH_4Cl were applied to dissipate any ΔpH. In some experiments 5 mM sulfite was added. Results, which represent ATP-dependent portion of the ACMA quenching, are reported as ΔF/F.

2.2.13 ATP hydrolysis and synthesis measurements

Sulfite-stimulated MgATP hydrolysis was monitored by measuring the release of inorganic phosphate (Pi) photometrically (Taussky and Shorr 1953). Activated/trypsinized thylakoids, equal to 6 µg Chl, or reduced/oxidized thylakoids, equal to 20 µg Chl, were incubated for 5 min at 37 °C in a medium containing 50 mM Tricine-NaOH (pH 8.0), 10 mM NaCl, 1.5 mM $MgCl_2$ and 3 mM ATP. Activated/trypsinized thylakoids were assayed in presence of 20 mM Na_2SO_3, whereas reduced/oxidized thylakoids were assayed at 40 mM Na_2SO_3. Photophosphorylation (McCarty 2005) after $^1O_2$ exposure was assayed using an RG2 transmission filter (Schott, Mainz, Germany) to avoid continuous excitation of RB. Light absorbance of RB (Telfer et al. 1994) was minimized by the RG2 filter. MgATP hydrolysis by dissected/reassembled CF1 and hybrid F1 assemblies was carried out for 2 min and 37 °C in a 0.5 mL reaction volume containing 2 – 5 µg of protein in 50 mM Tris-HCl (pH 8.0), 25 mM Na_2SO_3, 5 mM ATP, 2.5 mM $MgCl_2$. Sodium sulfite was omitted in some experiments. CaATP hydrolysis was carried out for 2

min and 37 °C in 50 mM Tris-HCl (pH 8.0), 5 mM $CaCl_2$ and 5 mM ATP. ATPase reaction was stopped by adding trichloroacetic acid. Colorimetric measurements were performed at 740 nm (UV mini-1240; Shimadzu, Duisburg, Germany). One measurement represents the difference between the Pi release of an incubated sample and Pi at t = 0.

2.2.14 Alkalization of thylakoid suspensions

Some experiments were carried out to monitor membrane integrity upon RB treatment. ΔpH of the external reaction mixture was recorded using an InLab Micro pH electrode (Mettler Toledo, Giessen, Germany). Thylakoid membranes (100 µg Chl mL^{-1}) were kept in a weakly buffered medium containing 0.5 mM Tricine-NaOH (pH 8.0), 100 mM sucrose, 50 mM NaCl and 10 µM pyocyanine. Illumination was carried out for 1 min (900 W m^{-2}; 25 °C).

2.2.15 Alignment of F1 γ subunits

Multiple sequence alignment and phylogenetic tree calculations were done using ClustalW (Larkin et al. 2007) and Geneious (Drummond et al. 2011), respectively. Visualization of structural alignments was performed using PyMOL/CEalign (DeLano and Lam 2005; Shindyalov and Bourne 1998). The homology model of spinach CF1 γ subunit (Richter et al. 2005) and the crystal structure of spinach CF1 α and β subunits (Groth and Pohl 2001; PDB ID: 1FX0) were aligned to a template structure (Cingolani and Duncan 2011; PDB ID: 3OAA) of corresponding *E. coli* F1 subunits.

3 Results

3.1 *In situ* affection of CF1CFo by singlet oxygen

3.1.1 Semi-quantitative detection of singlet oxygen release by Rose Bengal illumination

Several probes are used for semi-quantitative $^1O_2$ detection approaches. RNO is bleached to the nitro form caused by the *trans*-annular peroxide product of $^1O_2$ reaction with histidine in the assay (Telfer et al. 1994). The results in Figure 5 suggested that illumination of RB exclusively caused a more or less linear release of $^1O_2$. However, estimation of $^1O_2$ concentration in the samples was not possible with this technique.

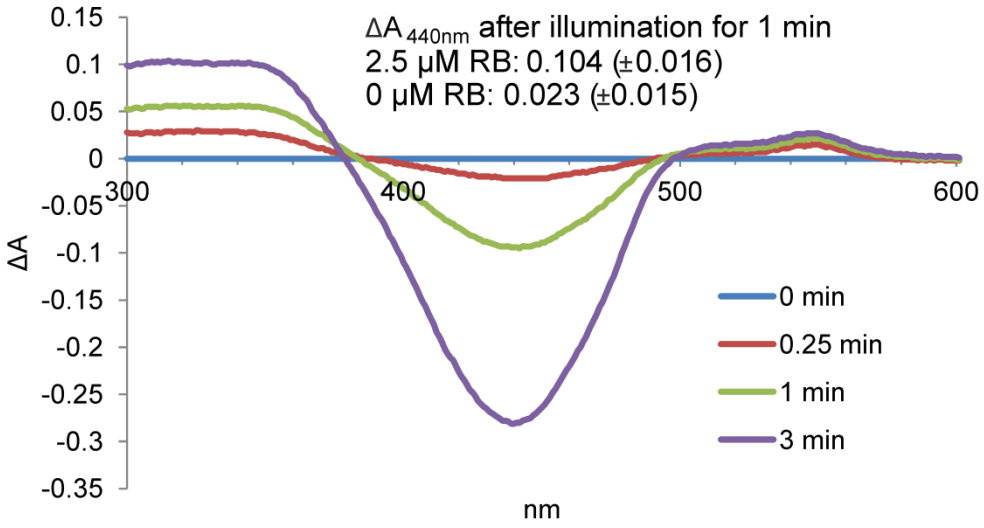

Figure 5: Estimation of RB-induced $^1O_2$ release monitored by RNO absorbance quenching. $^1O_2$ was exclusively released by RB, as detected by ΔA_{440nm} (n = 3, ±SD), in a linear fashion. Assays were carried out as described in section 2.2.10.

3.1.2 Influence of singlet oxygen on membrane integrity

$^1O_2$ has a strong potential to interact with various molecules, particularly lipids (Davies 2004; Girotti and Kriska 2004; Martinez et al. 2003). Therefore, it was essential to ensure thylakoid membrane integrity after and during $^1O_2$ exposure before evaluating any H^+ translocation activity of CF1CFo. According to Evron and McCarty (2000), a simultaneous assay of electron transfer and light-dependent thylakoid lumen acidification was carried out. The latter measurement allowed calculations of ΔpH generated upon illumination (McCallum and McCarty 2007; Schuldiner et al. 1972). The assay of electron transfer in illuminated thylakoid membranes is based on the color change of the yellow ferricyanide to colorless ferrocyanide upon reduction.

Since absorbance of ferricyanide (Figure 6) superimposes the 9-AA fluorescence emission spectrum, an increase of 9-AA fluorescence at 430 nm could be observed during electron transfer (Figure 7).

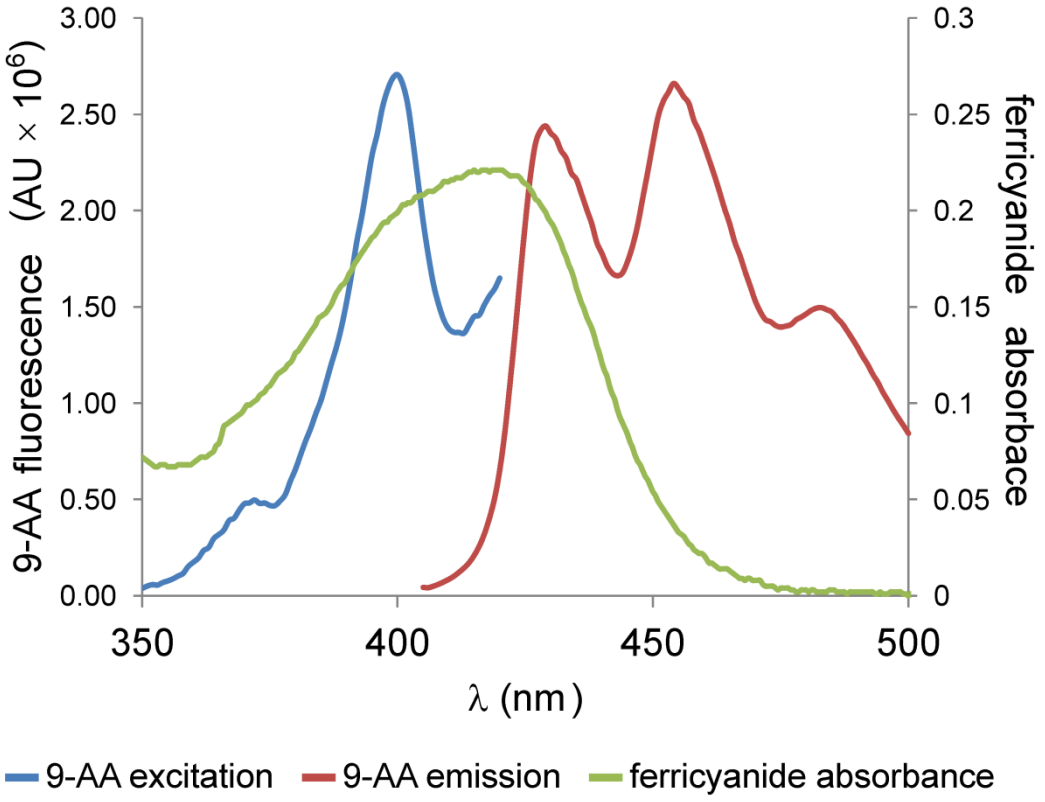

Figure 6: Fluorescence and absorbance spectra of 2 µM 9-AA in 50 mM Tricine-NaOH (pH 8.0), showing the excitation spectrum in blue and the emission spectrum in red. The absorbance spectrum of 0.2 mM ferricyanide of a separate measurement is shown in green. Further assay conditions are described in section 2.2.11.

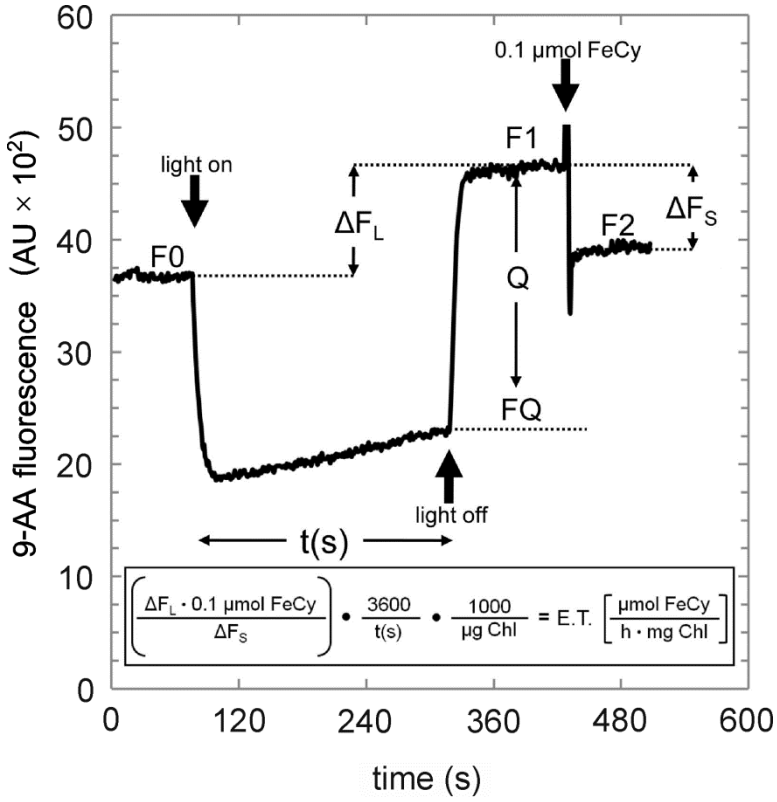

Figure 7: Fluorescence kinetics of simultaneous H^+ translocation and electron transfer measurement. Light-induced fluorescence quenching of 9-AA and reduction of ferricyanide (FeCy) and were assayed according to previous reports (Evron and McCarty 2000). Initial 9-AA fluorescence (F0) was quenched after switching on actinic red light. The fraction of total fluorescence that was quenched (Q= (F1 – FQ) / F1) was used for calculation of ΔpH (Schuldiner et al. 1972). FQ, 9-AA fluorescence before switching off the light; F1, 9-AA fluorescence after illumination; F2, 9-AA fluorescence after addition of 0.1 µmol FeCy; ΔF_L, the relative increase in fluorescence caused by FeCy reduction (ΔF_L = 1 – F0 / F1); ΔF_S, the decrease in 9-AA fluorescence after addition of 0.1 µmol FeCy standard (ΔF_S = 1 – F2 / F1); t, the illumination time in seconds. The equation converts ΔF_L into the rate of FeCy reduction (µmol FeCy reduced h^{-1} mg Chl^{-1}). Figure and legend according to Evron and McCarty (2000).

Electron transfer rates were determined and ΔpH of illuminated thylakoids in presence of different RB concentrations were calculated (Figure 8). Only a small increase of electron transfer rate was observed upon treatment with up to 10 µM RB. Since electron transfer under continuous illumination correlates with H^+ efflux through thylakoid membranes (Davenport and McCarty 1984; Hangarter et al. 1987), uncoupled membranes showed roughly 2.5-fold electron transfer rates compared to membranes that were not exposed to $^1O_2$. A reversed, but expected result was observed by analyzing thylakoid membrane energization at increasing RB concentrations. The extent of generated ΔpH was marginally reduced at increasing concentrations of RB. This was in strong contrast to uncoupled membranes, showing no light-induced 9-AA quenching. It was suggested that, up to a concentration of 10 µM RB, treated thylakoid membranes remained integer. The outcome of simultaneous assay was in line with an analysis of medium pH alkalization during illumination of thylakoids in the presence of RB (Figure 9). Samples that were treated with up to 50 µM RB (not shown) resembled DCMU

treated samples, where electron transfer between PSII and PSI was inhibited. Therefore, RB concentration applied in the experiments did not exceed 10 µM.

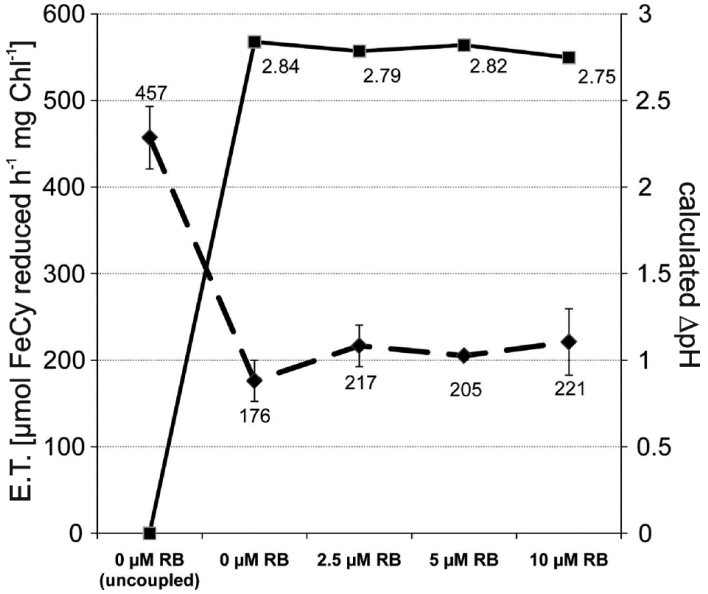

Figure 8: Measured electron transfer rates (E.T.) and calculated ΔpH of thylakoids exposed to $^1O_2$ according to Figure 7. Assay conditions as described in section 2.2.11 (*n* = 3, ± SE). Dashed line: E.T. of thylakoids illuminated with different RB concentrations or uncoupled with 2 µM gramicidine D and 4 mM NH_4Cl prior to assay. E.T. are expressed in µmol ferricyanide reduced h^{-1} mg Chl^{-1}; Solid line: calculated ΔpH of assayed thylakoids.

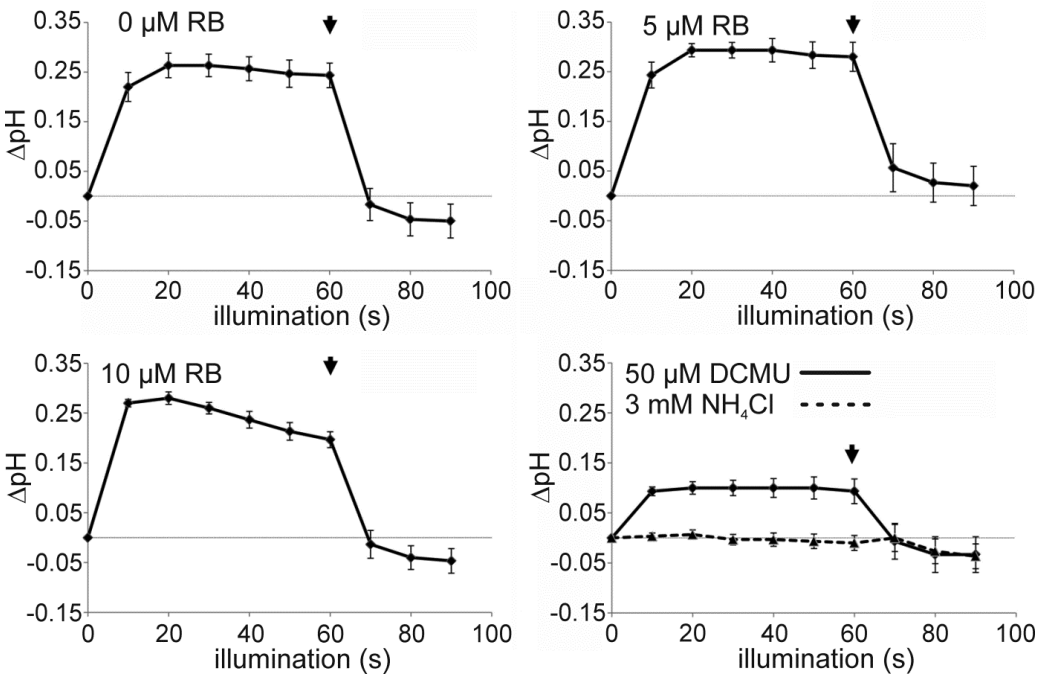

Figure 9: Membrane integrity in the presence of different concentrations of RB. The assay was carried out according to section 2.2.14. A 4 mL reaction mixture was illuminated for 1 min and subsequently. Addition of 3 mM NH_4Cl (black arrows) disintegrated the generated ΔpH. For control, a mixture lacking thylakoids was treated in the same manner. Results were corrected with controls (*n* = 3, ± SE).

3.1.3 Effect of singlet oxygen on MgATP-dependent proton translocation by CF1CFo

To find out, if the impact of $^1O_2$ on the γ subunit of CF1CFo (Mahler et al. 2007) correlates with an altered H^+ translocation activity, proton translocation by isolated spinach thylakoids was assayed. ACMA fluorescence quenching, initiated by addition of ATP to a thylakoid suspension, was monitored to analyze ATP-dependent thylakoid lumen acidification (Figure 10). By calculating ΔF/F ratios after uncoupling the membranes, unspecific fluorescence changes upon ATP addition had no effect (McCarty 2005).

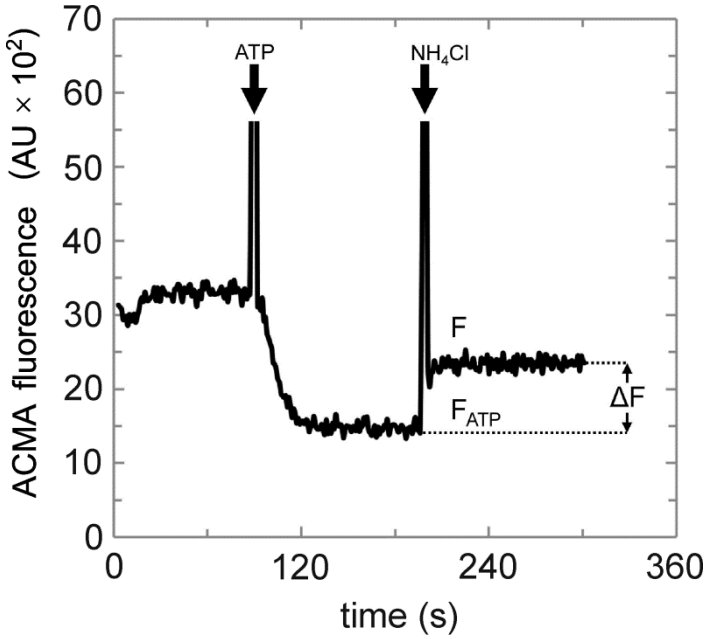

Figure 10: ATP-driven ACMA quenching of activated thylakoids. ΔF/F calculation from unprocessed fluorescence data. Black arrows indicate addition of 3 mM ATP and 3 mM NH_4Cl, respectively. To exclude any unspecific quenching, ΔF/F represents the difference between steady-state fluorescence after addition of ATP (F_{ATP}) and uncoupler (F) divided by F.

As outlined in Figure 11A, within 1 min of $^1O_2$ exposure the ability of CF1CFo to generate an ATP-driven ΔpH dropped dramatically at increasing concentrations of RB. Control samples kept in the dark showed comparable ΔF/F values as activated thylakoids without RB. Therefore, measurement artifacts due to fluorescence interference of ACMA and RB could be ruled out. Addition of sulfite to overcome MgATPase inhibition due to tightly bound MgADP (Digel et al. 1996; Du and Boyer 1990) had no effect on the rate of inactivation by $^1O_2$ (Figure 11B). Sulfite is able to increase ΔF/F of trypsin-treated membranes (McCarty 2005) that show increased trypsin-mediated H^+ leakage (McCallum and McCarty 2007).

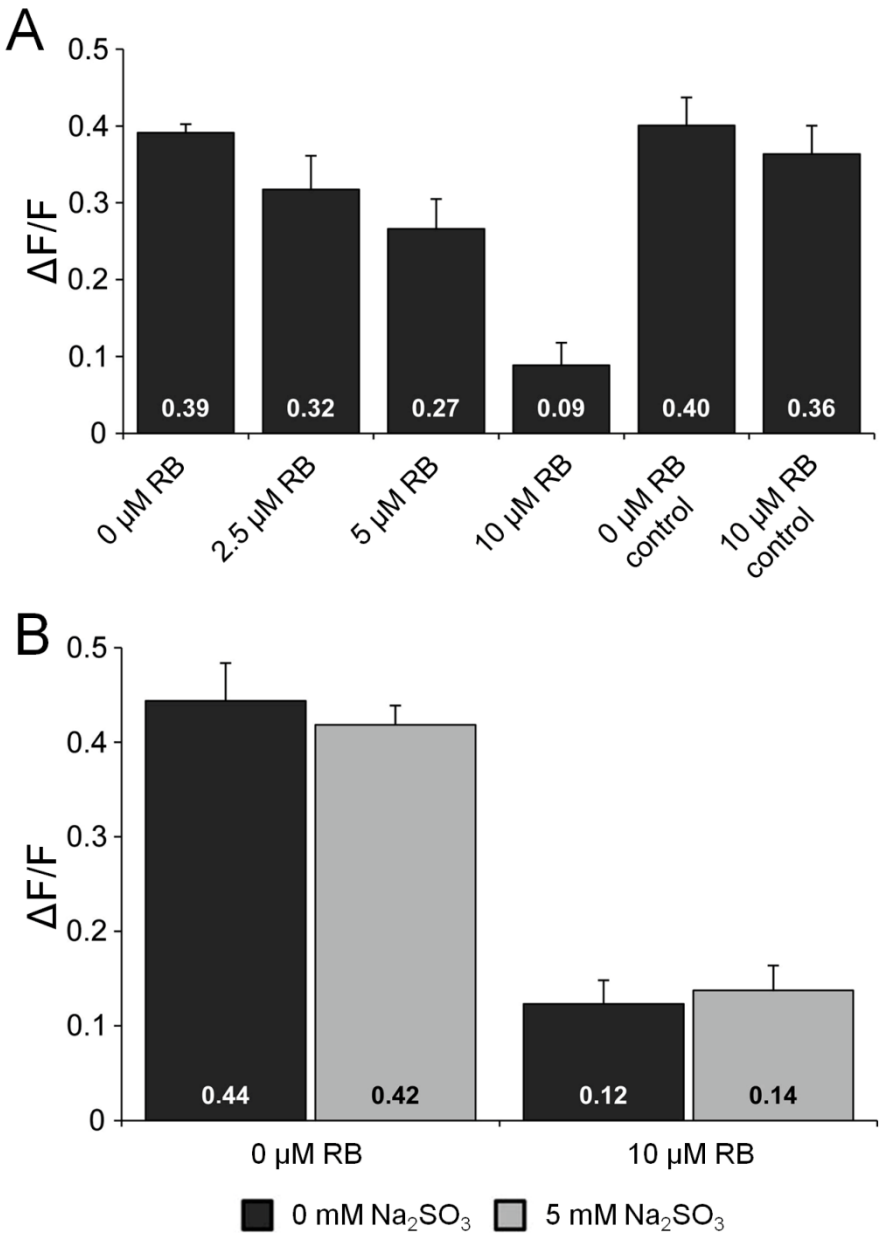

Figure 11: ATP-driven ACMA quenching by activated thylakoids exposed to $^1O_2$. Activation and assay conditions as described in section 2.2.12. Values were obtained from raw data presented in Figure 10 (n = 3, ± SE) and expressed as ΔF/F. (A) ΔF/F in absence of sulfite after thylakoid exposure to $^1O_2$. In control experiments, activated thylakoids were kept 1 min in darkness in the absence or presence of RB. (B) Effect of 5 mM Na_2SO_3 on ΔF/F of $^1O_2$-exposed thylakoids.

3.1.4 Effect of singlet oxygen on sulfite-stimulated MgATPase by isolated thylakoids

In a second approach MgATP hydrolysis by thylakoid membranes was measured. In line with results demonstrating H^+ translocation decline (Figure 11), a gradual $^1O_2$-induced decrease of Pi release by activated thylakoids was observed (Figure 12).

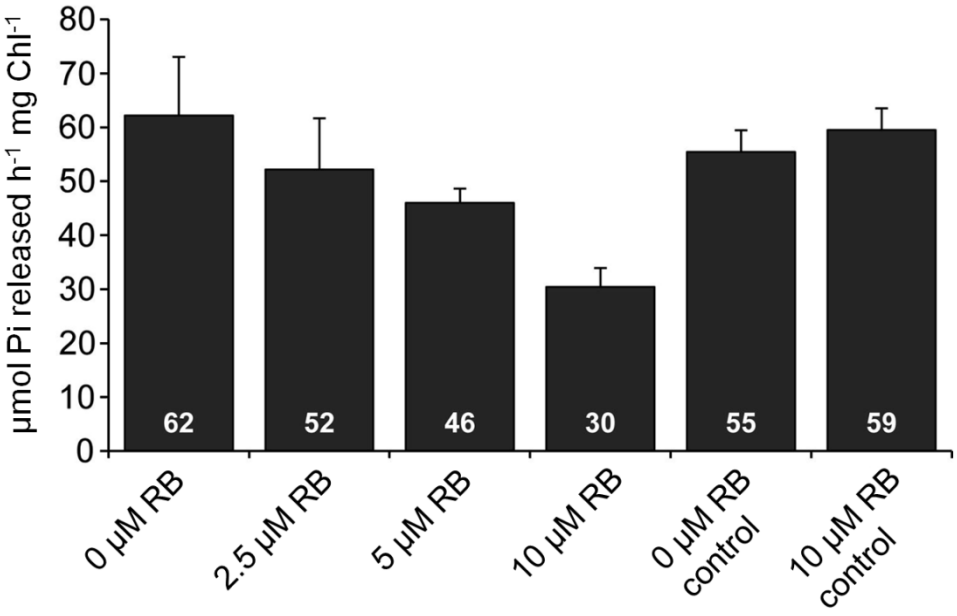

Figure 12: MgATPase activity of activated thylakoids exposed to $^1O_2$. Activated thylakoids, equivalent to 6 µg Chl, were assayed in the presence of 20 mM Na_2SO_3 as described in section 2.2.13. In control experiments, activated thylakoids were kept 1 min in darkness in the absence or presence of RB. ATPase rates are expressed as µmol Pi released h^{-1} mg Chl^{-1} (*n* = 3, ± SE).

Interestingly, a certain uncoupling of H^+ translocation and Pi release was observed. Upon treatment with 10 µM RB, the latter resulted in 50% reduction (Figure 12), whereas the former was reduced to 33% (Figure 11B). In both experiments, sulfite was present to overcome ADP inhibition. Therefore, values free from $^1O_2$-mediated uncoupling artifacts were obtained. Accordingly, observed decline of Pi release and ATP-dependent H^+ translocation was caused exclusively by $^1O_2$. Sulfite-stimulated MgATP hydrolysis was also assayed under uncoupling conditions in the presence of 2 µM gramicidine D and 4 mM NH_4Cl (not shown). In line with previous reports, uncoupling of activated thylakoids had little effect on Pi release by MgATP hydrolysis in the presence of sulfite (Bakker-Grunwald and van Dam 1973; Gräber et al. 1977; Junge 1970). Due to the experimental setup, thylakoids were illuminated in the presence of DTT for only 1 min. In literature (McCarty 2006) higher MgATPase activities around 150 µmol Pi released h^{-1} mg Chl^{-1} could be observed after 3 min of illumination. An illumination step for 1 min in the presence of 10 mM DTT resulted in a roughly 6-fold increase of MgATPase compared to non-illuminated samples. This indicated that the procedure was sufficient to obtain “activated thylakoids” which are reduced to a certain extent (not shown). Samples that were illuminated for 3 min showed comparable ATP hydrolysis rates as reported in literature (see Figure 15 below).

3.1.5 Effect of γ-cysteine redox state on the impact of singlet oxygen

Mahler et al. (2007) could show that $^1O_2$ specifically interacts with the γ subunit of CF1CFo. Furthermore, it is known that the γ subunit plays a dominant role in H^+ gating (Evron and Pick 1997). There exists evidence that structural changes of γ and ε subunits occur in dependence on the γ-redox state (Johnson and McCarty 2002; McCarty and Fagan 1973; Richter 2004; Richter and Gao 1996; Richter and McCarty 1987; Schumann et al. 1985). In Figure 13A reduced and oxidized thylakoids were exposed to $^1O_2$. The data indicated that oxidized thylakoids were nearly 3-fold more severely affected by $^1O_2$ than MgATPase by reduced thylakoids.

To get additional insight on the mechanism of $^1O_2$ interaction, trypsin was used as an artificial ATPase activator of CF1CFo. Trypsin treatment of thylakoids minimizes the inhibitory effect of the ε subunit on ATP hydrolysis by cleaving the γ subunit at specific sites (Hightower and McCarty 1996; Richter et al. 2000; Soteropoulos et al. 1992). Experiments were carried out with membranes containing either oxidized or reduced γ-cysteines. Again, MgATPase by oxidized trypsin-treated thylakoids was more affected by $^1O_2$ (Figure 13B). The residual activities after exposure to $^1O_2$ were simliar to a certain extent, no matter if trypsin was applied (Figure 13B) or not (Figure 13A). Reduced thylakoids, that were washed prior assay to get rid of DTT, showed unaltered residual MgATPase as non-washed thylakoids (not shown). This suggested that traces of DTT in the suspension had no severe effect on the impact of $^1O_2$ generated by illumination of RB.

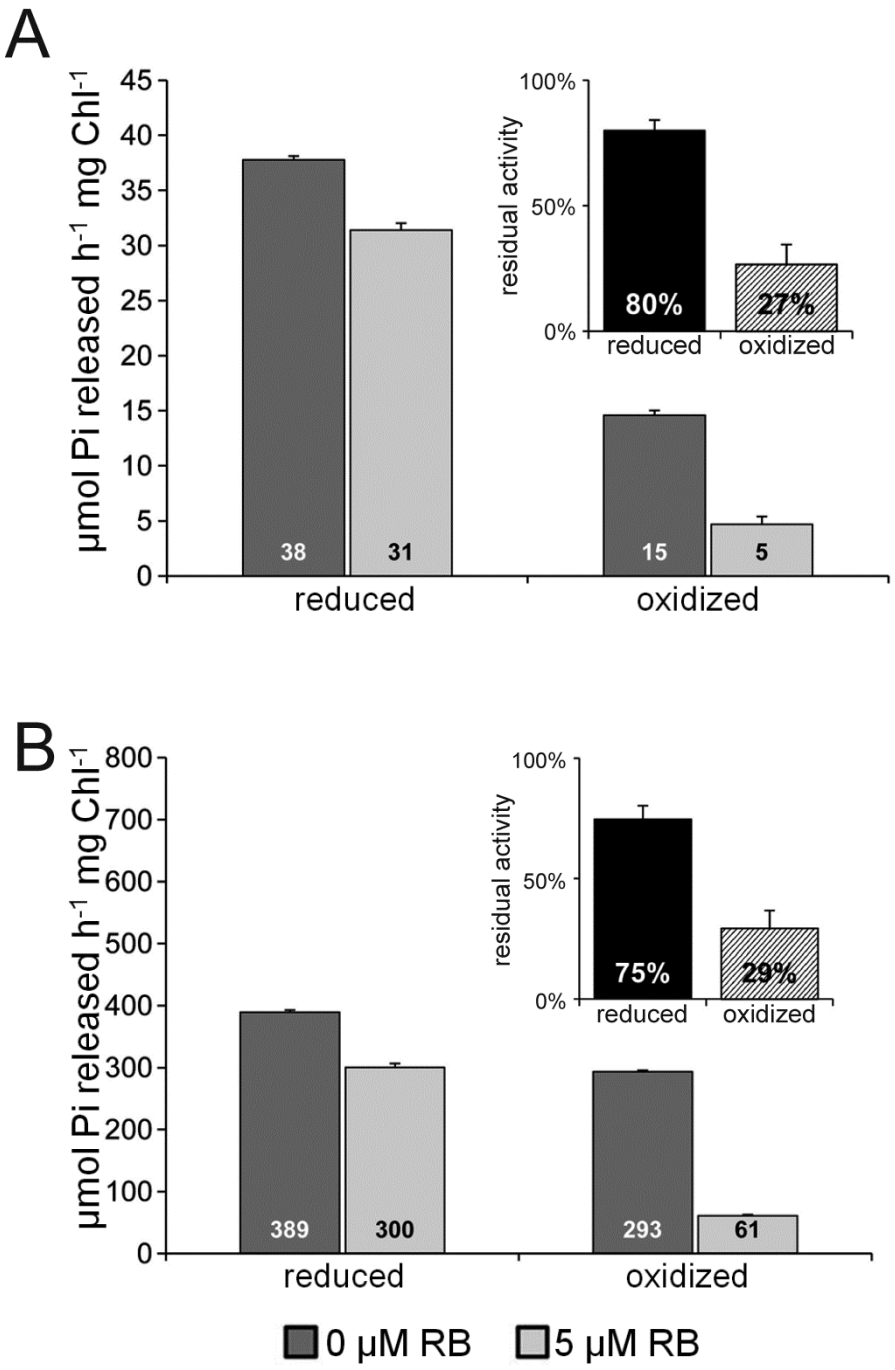

Figure 13: MgATPase activity of reduced and oxidized thylakoids exposed to $^1O_2$ (*n* = 3, ± SE). Reduced and oxidized thylakoids were prepared by incubating membrane preparations as described in section 2.2.7. MgATPase activity is expressed as µmol Pi released h^{-1} mg Chl^{-1}. Trypsin treated thylakoids showed enhanced MgATPase. Independently of trypsin treatment, more deleterious $^1O_2$ impact in oxidized samples was observed. (A) Non-trypsinized preparations were illuminated with RB and assayed immediately in the presence of 40 mM Na_2SO_3. (B) Trypsin activated thylakoids were prepared prior $^1O_2$ generation (section 2.2.8) and assayed in the presence of 20 mM Na_2SO_3. The insets represent residual ATPase activity of three experiments (± SE) after treatment with 5 µM RB.

A similar result as reported in Figure 13 was observed when ATP-dependent H^+ translocation by trypsin-treated thylakoids was assayed (Figure 14). After exposure to $^1O_2$ generated by 5 µM RB, ΔF/F values of oxidized thylakoids dropped twice as much as those of reduced thylakoids. Trypsin treatment was crucial since only small initial ΔF/F values of oxidized thylakoids were observed (not shown), thus making the analysis of a $^1O_2$-dependent effect difficult. Poor ΔF/F values of oxidized thylakoids corresponded to previous observations (McCarty 2005).

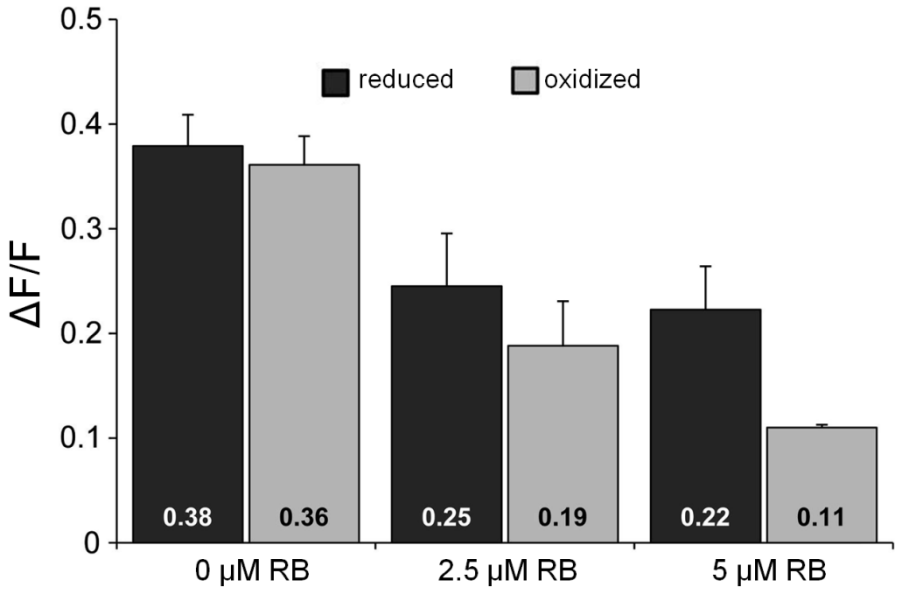

Figure 14: ATP-driven ACMA quenching of reduced and oxidized trypsin-treated thylakoids exposed to $^1O_2$. Decline of ΔF/F is shown after exposure of thylakoids to $^1O_2$ (*n* = 3, ± SE). Trypsin-activated membranes (section 2.2.8) were assayed in presence of 5 mM Na_2SO_3, whereas non-trypsinized membranes were analyzed as described in section 2.2.12.

3.1.6 Impact of singlet oxygen on ATP synthesis by isolated thylakoids

Extending the MgATP hydrolysis approach (Figure 12, Figure 13) revealed that both, ATP hydrolysis and ATP synthesis by spinach thylakoid membranes attenuated upon exposure to $^1O_2$ (Figure 15). The quantitative impact on both activities was comparable, resulting in residual ATP hydrolysis of 72% and ATP synthesis of 70% after treatment with 10 µM RB.

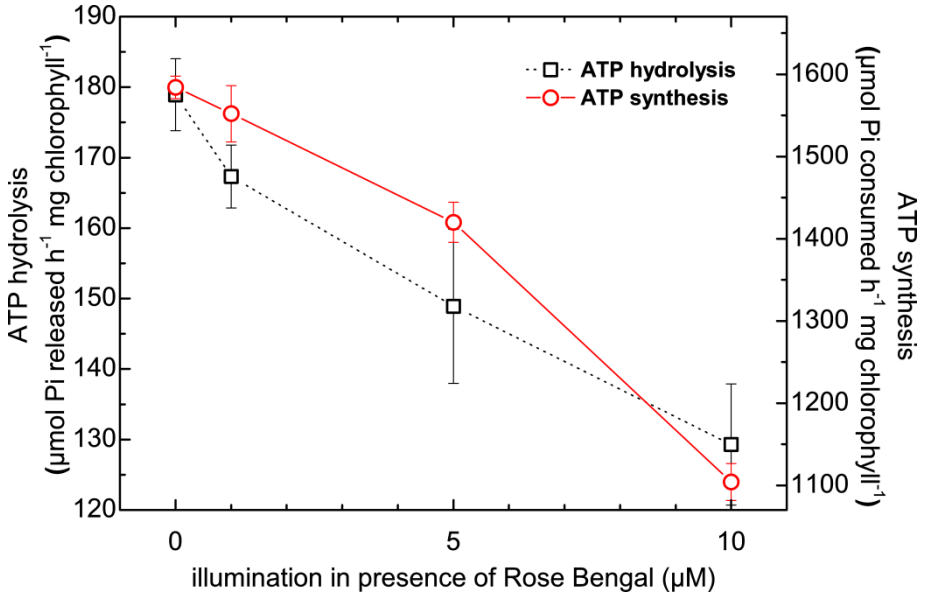

Figure 15: $^1O_2$ lowered enzyme activity *in situ* (*n* = 3, ± SE). CF1CFo of isolated spinach thylakoid membranes was assayed for ATP synthesis (photophosphorylation) and sulfite-stimulated MgATP hydrolysis. Prior 30 s RB illumination procedure, membranes were activated by illumination for 3 min in presence of DTT.

3.2 CF1 *in vitro*: Isolation, molecular dissection and affection by singlet oxygen

3.2.1 Isolation of the CF1 portion from spinach and reconstitution to the membrane

Loss of enzyme activity might be caused either by unspecific or specific protein oxidation. Regarding the latter, affection of particular residues of either CF1 or CFo might be involved. In order to prove involvement of the catalytically active portion in $^1O_2$-induced activity attenuation, membranes were stripped of CF1 according to a previously published protocol (Shapiro and McCarty 1990). The protein complex was removed from a diluted thylakoid membrane suspension by EDTA, followed by an anion exchange chromatography purification protocol (Figure 16).

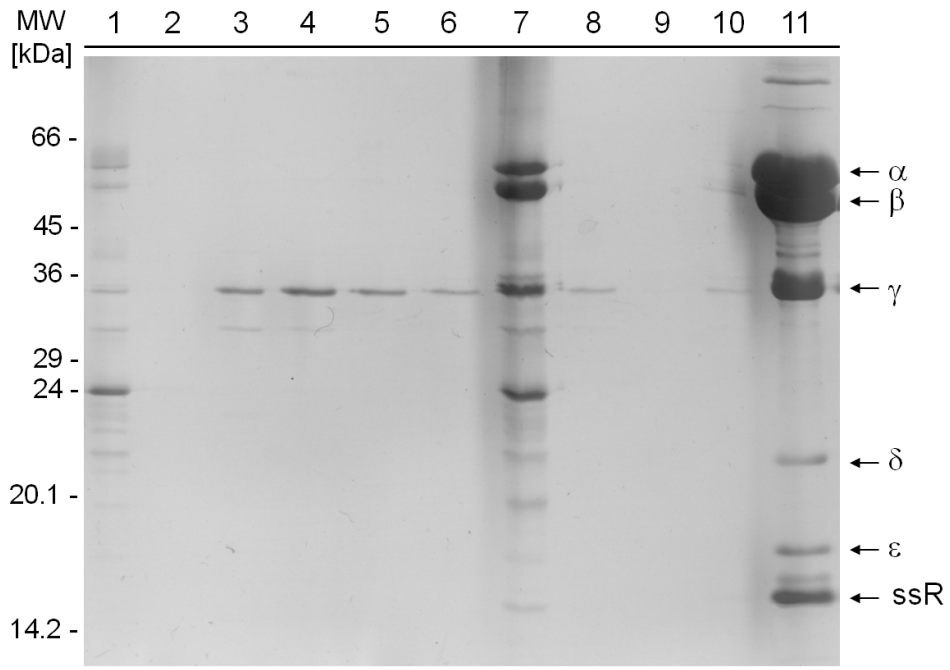

Figure 16: Purification of spinach CF1 visualized by SDS-PAGE. Silver-stained gels contained in lanes 1: EDTA-treated thylakoids stirred with DEAE-cellulose; 2: flow through-collected DEAE-cellulose slurry on miracloth; 3-6: washing step flow through of DEAE-cellulose slurry on miracloth at increasing NaCl (50 mM, 100 mM, 125 mM, 150 mM); 7: Slurry used for pouring of column; 8-10: clear flow through at 400 mM NaCl (void volume fractions); 11: green flow through at 400 mM NaCl containing pure CF1 and minor contaminations, such as the small subunit of RuBisCO (ssR).

Similarly to EDTA treated membranes, thylakoids incubated with sodium bromide are devoid of CF1 (Kamienietzky and Nelson 1975) since these membranes showed no MgATPase and lacked proteins resembling CF1 α, β and γ subunits (Figure 17A). The membranes were isolated in preparation of a reconstitution approach (Cruz et al. 1995) which was intended to be carried out with reassembled CF1 harboring ROS-tolerant recombinant subunits. The quality of the preparation allowed MgATPase assays upon reconstitution with CF1 (Figure 17A) and H^+ translocation measurements (Figure 17B) since the membranes were integer and capable to generate a ΔpH.

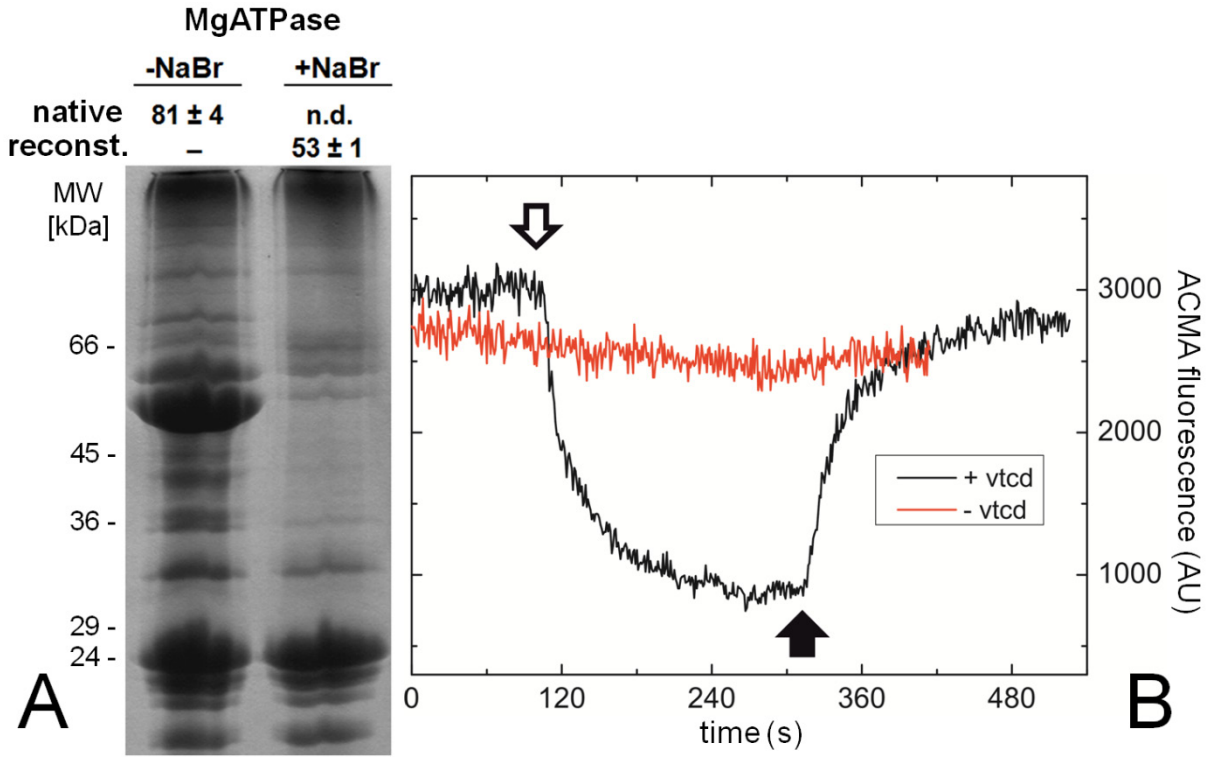

Figure 17: Preparation of CF1-deficient membranes by sodium bromide treatment. (A) Samples, equivalent to 10 µg Chl, were separated by SDS-PAGE and stained with Coomassie. NaBr caused loss of two dominant bands between 45 and 66 kD and bands at approximately 36 kD. These bands supposedly represented the CF1 α, β, and γ subunit. MgATPase activity of NaBr-treated membranes, expressed as release of µmol Pi h^{-1} mg Chl^{-1} (± SE, *n* = 3), was not detectable (n.d.). The membranes incubated with CF1, followed by several washing steps, showed MgATPase, indicating reconstitution (reconst.) of CF1 to the membrane. (B) CF1-deficient membranes retained electron transfer capability. Membrane vesicles (100 µg Chl mL^{-1}) were incubated for 10 min with 10 µM venturicidin (vtcd) which blocks the CFo H^+ channel (Zhang et al. 1993). Switching on actinic red light (open arrow) induced ACMA fluorescence quenching as a measure of membrane vesicle acidification in venturicidin-treated samples only. In darkness (black arrow) the ΔpH dissipated slowly.

3.2.2 Treatment of the isolated CF1 with singlet oxygen

Isolated CF1 shows ATP hydrolysis enhanced by several treatments (Richter et al. 1984). Exposure *in vitro* was carried out to analyze if CF1 served as the primary target portion affected during $^1O_2$-induced activity attenuation of isolated thylakoids (section 3.1). Incubation with DTT and $CuCl_2$ yielded reduced and oxidized enzyme (Samra et al. 2006), respectively, whereas reduced CF1 showed roughly 7-fold higher MgATPase (Table 3).

Table 3: *In vitro* affection of CF1 MgATPase by $^1O_2$.
[a]Oxidation (100 µM $CuCl_2$) and reduction (50 mM DTT) of 3.75 µM CF1 were carried out over night at 25 °C in 5 mM Tricine-NaOH (pH 8.0), 3 mM ATP and 2 mM EDTA. [b]Rates are expressed as µmol Pi released min^{-1} mg $protein^{-1}$ (± SE; *n* = 3) and assays were carried out in 50 mM Tricine-NaOH (pH 8.0), 50 mM Na_2SO_3, 3 mM ATP and 1.5 mM $MgCl_2$. Samples (1.25 µM CF1) were illuminated in presence of RB for 1 min after DTT/$CuCl_2$ removal via gel filtration.

CF1 redox state[a]	MgATPase activity upon RB treatment[b]			
	0 µM RB	1 µM RB	2 µM RB	4 µM RB
oxidized	4.1 (± 0.2)	3.9 (± 0.1)	3.4 (± 0.1)	2.2 (± 0.2)
residual activity	*100%*	*94%*	*83%*	*54%*
reduced	29.2 (± 0.6)	21.5 (± 0.4)	17.0 (± 0.7)	8.2 (± 1.0)
residual activity	*100%*	*74%*	*58%*	*28%*

Like observations *in situ* (Figure 13), elevation of catalytic activity by a reduction step was also observed when CF1 was assayed *in vitro* (Table 3). An analysis of CF1 affection in respect to γ subunit redox state revealed that, in contrast to observations *in situ*, the oxidized enzyme was less susceptible to $^1O_2$. However, the data supported the hypothesis that affection by $^1O_2$ observed *in situ* was mainly the result of oxidative damage of the CF1 portion.

Nevertheless, the data did not indicate precisely which subunits were oxidized by $^1O_2$, thus affecting activity of CF1. Interestingly, only the γ subunit showed an altered gel electrophoresis behavior on SDS-PAGE upon $^1O_2$ treatment (Figure 18). In line with this observation, appearance of a new γ subunit isoform was reported previously in a two-dimensional separation approach of Arabidopsis *flu* thylakoid proteins (Mahler et al. 2007). A change of electrophoresis pattern has also been described for other proteins exposed to reactive oxygen species (Vougier et al. 2004).

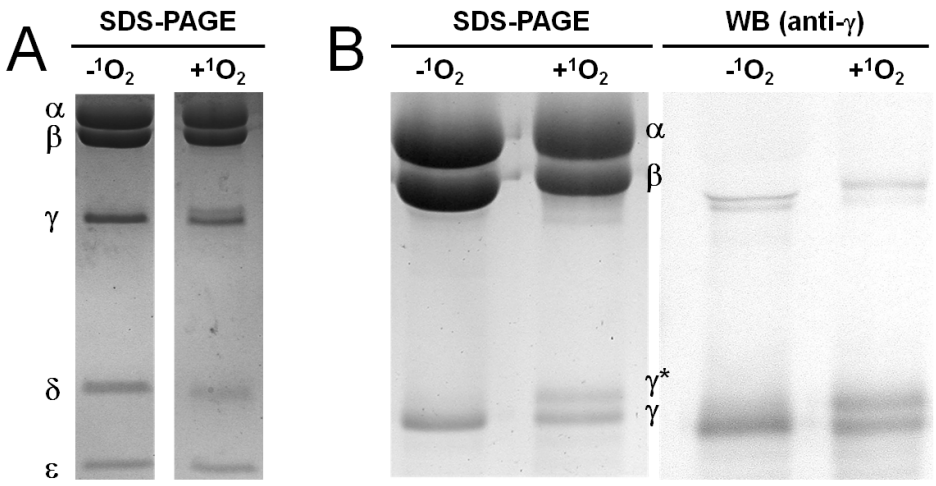

Figure 18: SDS-PAGE analysis of $^1O_2$-treated CF1 illuminated for 1 min at 4 µM RB. The gels were stained with Coomassie and contained ca. 7 µg of protein per lane. (A) The Coomassie signal of the δ subunit decreased slightly and a new isoform of the γ subunit was observed in treated samples on a 15% polyacrylamide gel. (B) Enhanced separation of the newly formed γ subunit (γ*) is shown on a 12% polyacrylamide gel. Immunodetection on a Western Blot (WB) with polyclonal antibodies raised against the γ subunit confirmed the new isoform as γ-specific.

3.2.3 Molecular dissection and reassembly of the spinach CF1 portion

Suggested cross-link hypothesis between residues of the γ and ε subunits upon $^1O_2$ exposure (section 4.1) could not be disproved so far, since $^1O_2$-induced activity attenuation was also observed after treatment of CF1 *in vitro*, demanding for a detailed analysis of the soluble enzyme. In order to delimitate putatively involved ε-residues, the subunit was removed, yielding CF1-ε (Figure 19). The subunit-deficient enzyme was assayed for residual activity upon $^1O_2$ treatment (Table 4).

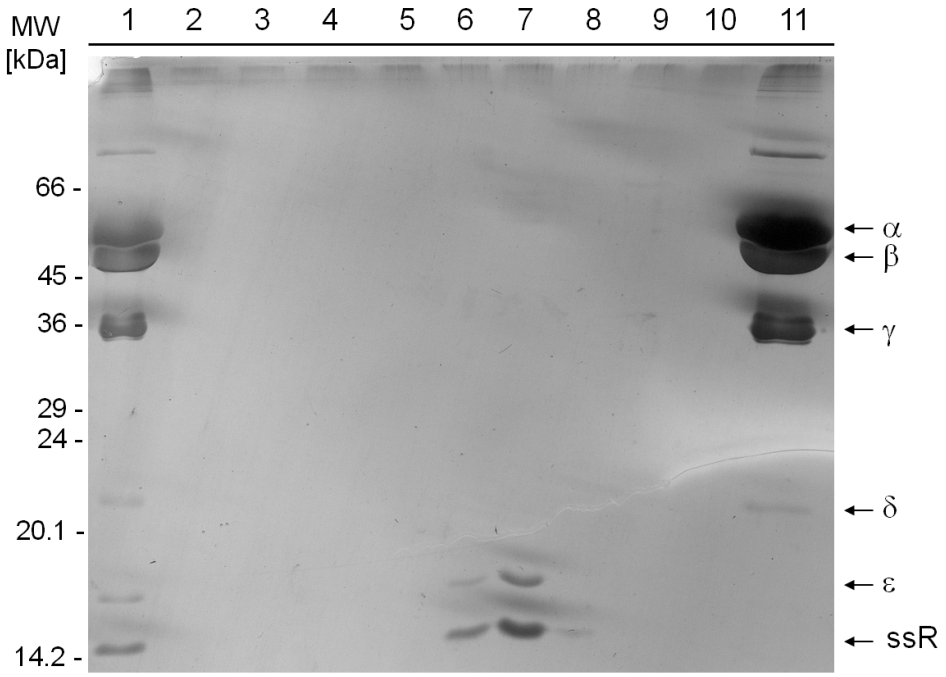

Figure 19: SDS-PAGE analysis showing dissection of the ε subunit from spinach CF1 and purification of CF1-ε. Silver-stained gels contained in lanes 1: ca. 7 µg CF1 protein after overnight reduction step; 2: flow through during protein loading step; 3-5: flow through of column wash; 6-8: alcoholic elution flow through containing the ε subunit and small subunit of RuBisCO (ssR); 9-10: flow through of column wash; 11: ca. 7 µg of CF1-ε protein eluted at high salt conditions.

Table 4: *In vitro* affection of CF1-ε ATPase by $^1O_2$.
[a]MgATPase was performed as in Table 3. CaATPase is described in section 2.2.13. [b]Oxidation and reduction of CF1-ε was carried out as in Table 3. [c]Rates are expressed as µmol Pi released min^{-1} mg $protein^{-1}$ (± SE; *n* = 3). RB treatment carried out as in Table 3.

	redox	ATPase activity[c]		*residual*
cation[a]	state[b]	0 µM RB	4 µM RB	*activity*
Mg^{2+}	oxidized	18.3 (± 1.6)	6.4 (± 2.7)	*35%*
	reduced	40.2 (± 0.6)	6.2 (± 1.2)	*15%*
Ca^{2+}	oxidized	15.7 (± 1.1)	3.8 (± 1.2)	*24%*
	reduced	30.7 (± 1.1)	3.8 (± 0.7)	*12%*

Unlike CF1, ATPase rates in presence of Ca^{2+} are detectable if ε is removed from the enzyme (Richter et al. 1984). This catalytic property of the subunit-deficient enzyme was later used to monitor reassembly efficiency (see Figure 20 below). Regardless if Mg^{2+} or Ca^{2+} were present in the assay, a decline of ATPase was observed by the ε subunit-deficient enzyme upon treatment with $^1O_2$ (Table 4). The enhanced $^1O_2$ impact on reduced enzyme *in vitro* (Table 3) was consistent in the ε subunit-deficient enzyme (Table 4). Again, these observations opposed the findings of redox state-dependent activity decline *in situ* (section 3.1).

The ε subunit obtained by the alcoholic wash of column-bound CF1 (Figure 19) retained its ability to rebind to the subunit-deficient enzyme (Richter et al. 1984). Since ε did not appear to be involved in $^1O_2$-mediated activity attenuation (Table 4), this preparation feature was beneficial in order to reassemble recombinant ROS-tolerant CF1 with native ε subunits. An estimated concentration of the ε-polypeptide was obtained by SDS-PAGE and Bradford assay since preparations were contaminated with the small subunit of RuBisCO (Figure 19). The method of continuous variation, also known as Job plot, was performed to demonstrate binding of the isolated subunit to ε-deficient CF1 (Figure 20). Taking account of an estimated ε subunit concentration, the results were in good agreement with earlier findings (Richter et al. 1985) showing maximum binding of ε at a roughly equal molar ratio to CF1-ε.

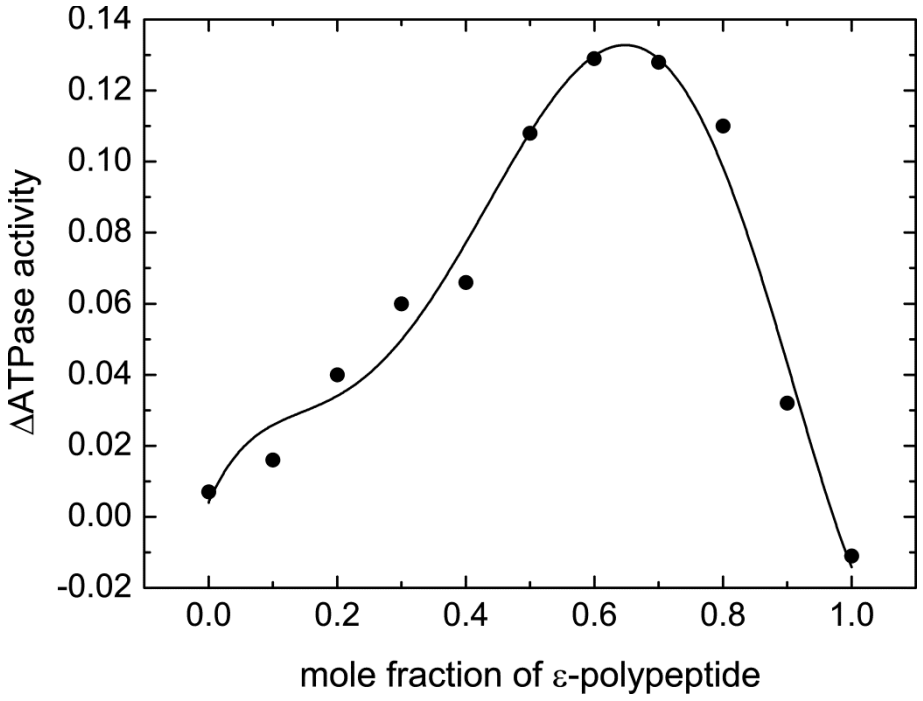

Figure 20: Job plot for the binding of the ε-polypeptide to CF1-ε. CF1-ε and ε were mixed in different proportions while the total protein concentration (5.65×10^{-4} M) was kept constant. ATPase activity (colorimetric Pi determination at 740 nm) in the presence of Ca^{2+} was inhibited by ε binding to CF1-ε (Richter et al. 1984). The difference in Pi release (A_{740nm}) between each sample and that of a control without ε added is shown.

A similar protocol (Richter et al. 1986) was applied in order to yield the catalytically active core complex consisting of $\alpha_3\beta_3\gamma$ (CF1-δε, Figure 21). Both minor subunits were removed by increasing ionic strength. Since the δ subunit anchors CF1 to CFo on the membrane (Groth and Strotmann 1999), CF1-δε represents the minimal set of subunits necessary for ATP hydrolysis *in vitro*. Like the ε-deficient enzyme (Table 4), CF1-δε was susceptible to $^1O_2$ (Figure 22).

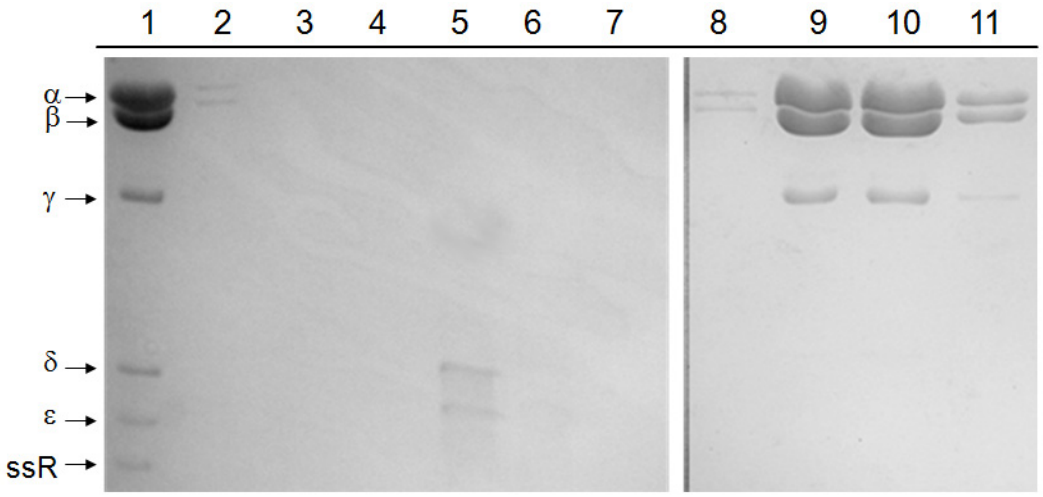

Figure 21: SDS-PAGE analysis showing dissection of the minor δ and ε subunits from spinach CF1 and purification of CF1-δε. Coomassie-stained gels contained in lanes 1: ca. 7 µg CF1 protein after overnight reduction step. The sample was contaminated with small subunit of RuBisCO (ssR); 2: flow through during protein loading on DEAE-cellulose column; 3-4: flow through of column wash; 5: alcoholic elution flow through at increased ionic strength containing the δ and ε subunit; 6-8: flow through of column wash; 9-11: fractions of eluted CF1-δε protein at high salt conditions.

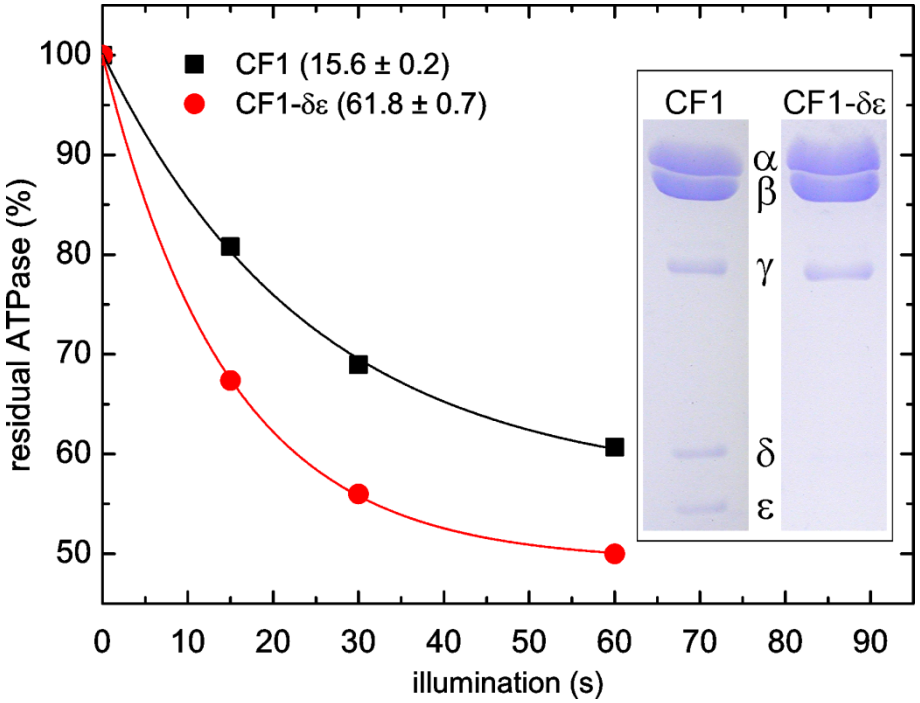

Figure 22: $^1O_2$-induced *in vitro* affection of MgATPase by CF1 and CF1-δε. $^1O_2$ was generated by illumination in presence of 2 µM RB. 2.5 µM of the enzyme was pre-treated for 2 h and 25 °C in TA buffer and 20 mM DTT. Activities in brackets are expressed as µmol Pi released min^{-1} mg $protein^{-1}$ (*n* = 3, ± SE). The inset shows a polyacrylamide gel containing 6 µg of purified protein stained with Coomassie.

Affection of CF1-δε indicated that deleterious $^1O_2$ impact on CF1 occurred within α, β or γ subunits. However, *in vitro* findings (Figure 18) suggested the latter, being the most promising candidate. Accordingly, CF1-δε was further dissected molecularly (Gao et al. 1995; Sokolov et al. 1999) in order to obtain native purified CF1 $\alpha_3\beta_3$ hexamer (Figure 23).

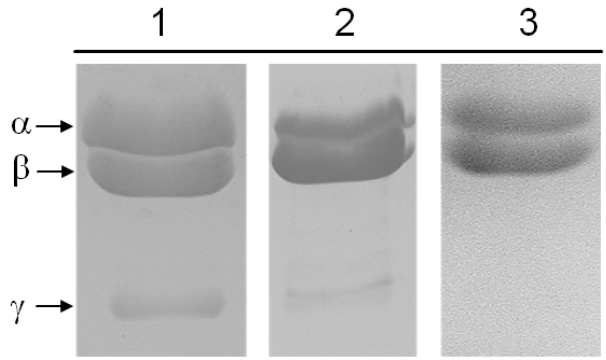

Figure 23: Purification of CF1 $\alpha_3\beta_3$ complex shown on polyacrylamide gel stained with Coomassie. CF1-δε (lane 1) was applied on a hydroxylapatite column to remove most of the γ subunit (lane 2). In a second purification step, traces of γ impurities were removed via DEAE cellulose column chromatography, yielding pure $\alpha_3\beta_3$ (lane 3).

By following several protocols (Gao et al. 1995; He et al. 2008; Sokolov et al. 1999), CF1 was reassembled from its building blocks. The $\alpha_3\beta_3$ hexamer was reassembled with solubilized recombinant γ subunit wild type protein (section 3.4), yielding catalytically active $\alpha_3\beta_3\gamma$ (Table 5). Both building blocks showed no MgATPase if assayed separately. Poor activity of $\alpha_3\beta_3$ was in good correspondence with earlier reports (Gao et al. 1995), indicating that the γ subunit is essential to drive ATP hydrolysis. Accordingly, the reassembled complex consisting of $\alpha_3\beta_3\gamma$ showed MgATPase activity (Table 5). Reassembly efficiency of $\alpha_3\beta_3\gamma$ appeared to be high because samples showed similar activity compared to the same set of subunits in native CF1-δε. Compared to CF1, incubation of the δε mixture (Figure 21, lane 5) with $\alpha_3\beta_3\gamma$ assemblies yielded a slightly higher active $\alpha_3\beta_3\gamma\delta\varepsilon$ complex (Table 5).

Table 5: Reassembly of CF1 monitored by MgATPase rates using native isolated and recombinant subunits. [a]native protein, [b]recombinant protein, [c]mixture of native and recombinant protein [d]Assay carried out as in Table 3. Rates are expressed as µmol Pi released min^{-1} mg $protein^{-1}$ (± SE, *n* = 3). The activity of some samples was not detectable (n.d.).

protein	CF1[a]	CF1-δε[a]	$\alpha_3\beta_3$[a]	γ[b]	$\alpha_3\beta_3\gamma$[c]	$\alpha_3\beta_3\gamma\delta\varepsilon$[c]
MgATPase[d]	5.0 (± 1.2)	19.8 (± 1.6)	n.d.	n.d.	20.2 (± 0.9)	8.2 (± 0.6)

There exist several lines of evidence (Figure 18, Figure 22) that the γ subunit might play a crucial role in $^1O_2$-induced activity decline of the enzyme. With help of the assembly approach (Gao et al. 1995; Sokolov et al. 1999) it could be shown (Table 6) that activity of the enzyme attenuated, if the γ subunit was exclusively exposed to $^1O_2$. The results were in line with observations of $^1O_2$-exposed $\alpha_3\beta_3\gamma$ (Figure 22).

Table 6: Activity attenuation of $\alpha_3\beta_3\gamma$ referring to $^1O_2$ exposure of the γ subunit prior assembly. [a]γ subunit not exposed to $^1O_2$ prior assembly [b]γ subunit exposed to $^1O_2$ prior assembly [c]Assay carried out as in Table 3 and rates are expressed as µmol Pi released min^{-1} mg $protein^{-1}$ (± SE, *n* = 3).

protein	$\alpha_3\beta_3\gamma^a$	$\alpha_3\beta_3\gamma^b$	*residual activity* (a/b)
MgATPase[c]	18.7 (± 0.5)	11.7 (± 0.2)	*63%*

3.3 Mapping of putative ROS targets and mass spectrometric analysis of CF1

3.3.1 Mapping of putative targets by using a model structure of the CF1 γ subunit

Based on the results (Figure 18, Figure 22, Table 6), the main focus of target mapping lied on the γ subunit. However, especially particular tyrosines within nucleotide binding sites at the interfaces between α and β subunits (Abrahams et al. 1994) were additionally considered as potential targets (Davies 2003).

A high resolution structure of the chloroplast F1 γ subunit is not available. Therefore, a homology model based on mitochondrial and bacterial F1 γ subunit structures has been developed (Richter et al. 2005). This model served as a platform for spatial mapping of putative $^1O_2$ targets which was based on reported ROS/protein interactions with tyrosine, histidine and tryptophan, as well as cysteine and methionine (Davies 2003). An amino acid sequence alignment of sixteen F1 γ subunits (Figure 24A) resulted in a sequence identity of only 7.4%. Such low identity is in good agreement with other alignments (Nakamoto et al. 1992) which have indicated that most of the conserved residues are restricted to the amino and carboxyl termini and a small central region. These regions were part of the structurally conserved terminal alpha-helical elements and a γ protrusion loop. These elements contained a set of highly conserved methionines and a cysteine in close proximity. The ROS target mapping approach revealed that these sulfur-containing amino acids formed a cluster located at the "neck" region of the γ subunit that protruded from the $\alpha_3\beta_3$ hexamer (Figure 24B, Figure 24C). In the course of this work the cluster is referred to as *target cluster*. The residues are highly

conserved in other γ subunits and can be found in several published structures, for example, those of bacterial (Cingolani and Duncan 2011; PDB ID: 3OAA), yeast mitochondrial (Stock et al. 1999; PDB ID: 2XOK) and bovine mitochondrial (Rees et al. 2009; PDB ID: 2WSS) F1 γ subunits (Figure 25). Depending on the organism, the cluster consists of each one or two methionines located on both termini, and a central cysteine. The residues are placed near the second “catch” region of the empty and ADP-containing β subunits that forms a contact with the γ subunit (Abrahams et al. 1994; Pu and Karplus 2008; Samra et al. 2008).

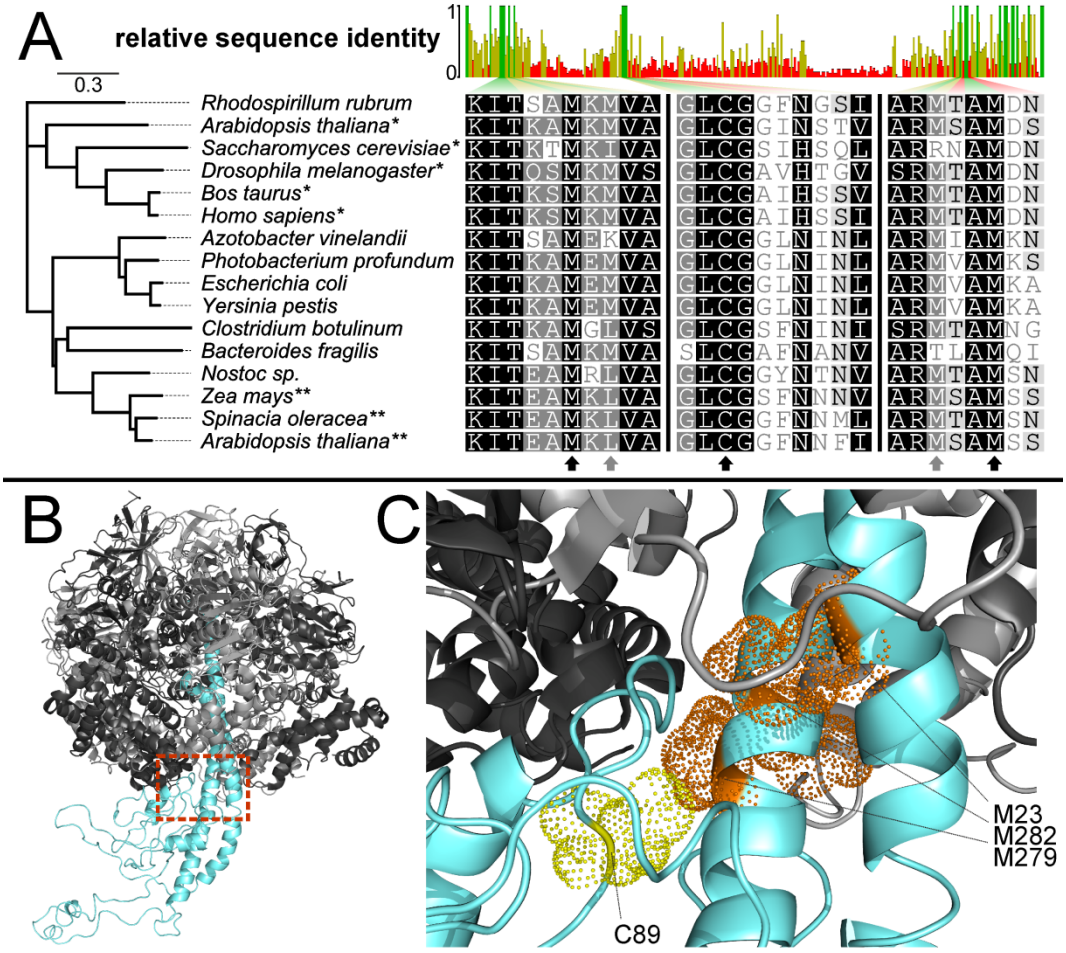

Figure 24: Alignment and mapping of putative ROS targets. (A) Amino acid sequence alignment and phylogenetic tree of 16 bacterial, mitochondrial (*) and chloroplast (**) F-ATP synthase γ subunits. The scale bar represents the number of amino acid substitutions per site. The upper part shows a full sequence alignment overview with identical (green), semi-conserved (olive) and non-conserved (red) regions. Three alignment excerpts of the N-terminus, the central region and the C-terminus are shown in the lower part. Decreasing similarity of aligned residues is scaled from black to white background. The black and grey arrows below the N-terminal sequence TxxMx[MLIK]V indicate conserved (spinach γM23) and semi-conserved methionines, respectively. The black arrow below the central domain excerpt marks a conserved cysteine (spinach γC89). The grey and black arrows below the C-terminal sequence R[MRT]xAMx highlight semi-conserved (spinach γM279) and conserved (spinach γM282) methionines, respectively. (B) Alignment of crystal structures from spinach CF1 α (light grey) and β (dark grey) subunits, and the γ subunit homology model (cyan) was carried out as described under 2.2.15. (C) Magnification of the dashed square from (B) shows the conserved cluster of terminal methionines in orange and the central cysteine in yellow.

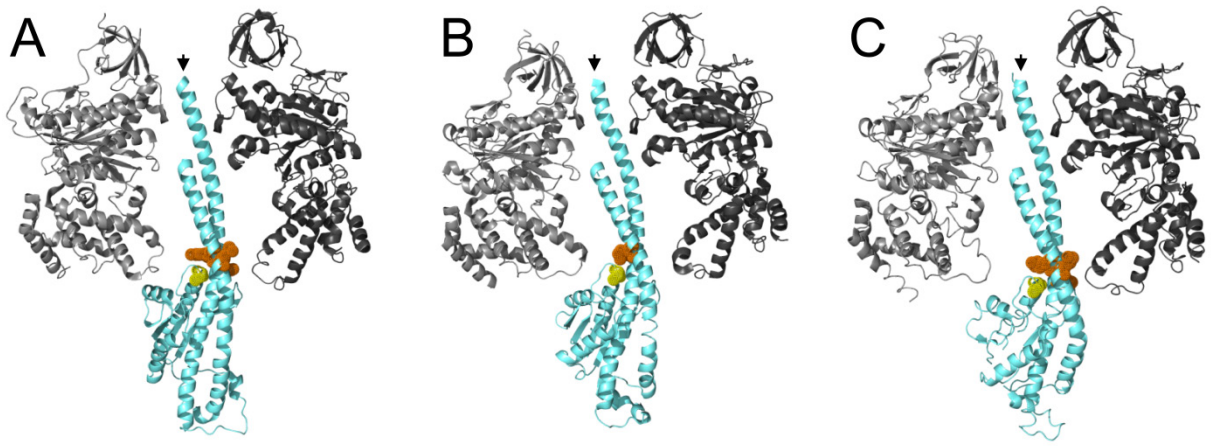

Figure 25: Cross-sections through parts of F1 crystal structures indicating the suggested ROS *target cluster*. The γ subunit (cyan) harbors the suggested ROS target methionines (orange) and cysteine (yellow), presented as dots. Black arrows indicate the γ subunit C-terminus. Subunits α (light grey) and β (dark grey) are shown. The *target cluster* is located at the "neck region" of the γ subunit. (A) *Escherichia coli* F1 (Cingolani and Duncan 2011; PDB ID: 3OAA), (B) *Saccharomyces cerevisiae* mitochondrial F1 (Stock et al. 1999; PDB ID: 2XOK), and (C) *Bos taurus* mitochondrial F1 (Rees et al. 2009; PDB ID: 2WSS) are shown.

3.3.2 Mass spectrometry analysis of CF1 oxidation

Due to their sulfur atoms, methionine and cysteine are easily oxidized. Therefore, these two residues are major sites of protein oxidation (Davies 2005). Methionine is successively oxidized at the sulfur center, forming methionine sulfoxide (mono-oxidation) and methionine sulfone (di-oxidation). Reactions with cysteines within proteins are more diverse and result in the formation of a disulfide or oxyacid derivatives, such as tri-oxidized sulfonic acid. Using LC-ESI-MS/MS, ROS treated CF1 was analyzed for oxidized amino acid residues. In general, ROS treatment resulted mainly in oxidation of α, β and γ subunits whereas degrees of δ and ε subunit oxidation were less affected (Figure 26). Table 7 summarizes a brief overview which highlights oxidation susceptibility of particular residues, initially considered to be potential functional targets (Figure 24). Mass spectrometric measurements revealed further potential targets which are discussed and mutationally analyzed in detail below.

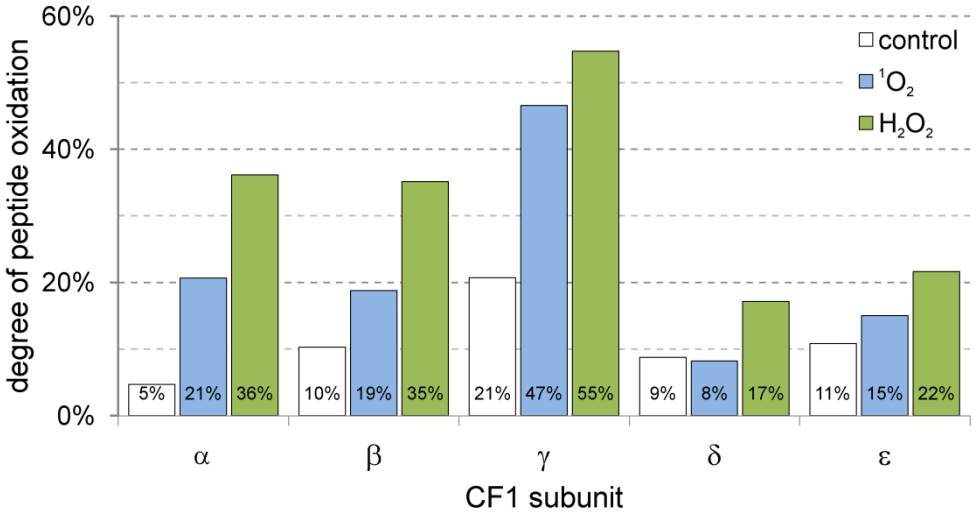

Figure 26: Relative oxidation of CF1 subunit peptides detected via mass spectrometry. Conditions are defined under methods. All detected peptide peaks were accounted for analysis. Database search included single and multiple oxidations of tyrosine, tryptophan, histidine, methionine and cysteine. Exemplary measurements of control, $^1O_2$-treated and H_2O_2-treated samples are shown. The α, β and γ subunits were more susceptible towards oxidation than the δ and ε subunit. In general, H_2O_2 treatment resulted in higher amounts of oxidized peptides detected.

Table 7: Overview of mass spectrometry analysis.
[a]Particular residues in the CF1 β and γ subunits were oxidized. In control samples, most residues were not oxidized (×), whereas single (✓) and multiple oxidations (✓✓) were detected primarily in $^1O_2$- and H_2O_2-treated samples. Furthermore, certain peptide fragments containing particular residues could not be detected (-) in the measurements. A detailed description and spectra are given in the text below.

residue[a]	control	$^1O_2$	H_2O_2
γM23	×	✓	-
γC89	×	✓	✓
γM95	×/✓	✓	✓
γH187	×	×	×
γC199	×	-	✓
γC205	-	-	-
γM279	×	✓/✓✓	✓/✓✓
γM282	×	✓/✓✓	✓/✓✓
βY362	×	✓	×
βH384	×	✓	×
βY385	×	✓	×

Detailed mass spectrometric data clearly indicated that the proposed candidates of the conserved sulfurous γ subunit amino acid cluster were specifically oxidized upon $^1O_2$ exposure (Figure 27, Figure 28) since control samples did not contain modified cluster residues (Figure 29, Figure 30). After treating the samples with $^1O_2$, N-terminal γM23 was oxidized to sulfoxide (Figure 27A), whereas the C-terminal methionines were mutually affected: Peptide fragments containing a pair of γM279 and γM282 sulfoxides were detected (Figure 28A). Additionally, fragments containing a mixture of methionine sulfoxide and methionine sulfone (Figure 28B) were identified. Methionine sulfone of either γM279 or γM282 was only observed if the other methionine was mono-oxidized. Moreover, the formation of a sulfonic acid derivative of γC89 was determined after $^1O_2$ exposure (Figure 27B). In this particular fragment oxidation of γM95 was also found in non-exposed samples (Figure 30B). This methionine will be further analyzed and discussed in section 3.6 and 4.5, respectively.

Particular amino acid oxidations within other CF1 subunits were also considered to be involved in activity attenuation. In fact, observed oxidized CF1 βY362 (Figure 31A) and CF1 βH384/βY385 (Figure 32A) were good candidates. The aromatic rings of tyrosine and histidine react with $^1O_2$ in different ways not yet fully understood (Davies 2004; Kim et al. 2008b). The two tyrosines mentioned correspond to bovine MF1 βY345 and βY368, being residues of the catalytic and non-catalytic nucleotide binding site, respectively (Cross et al. 1987).

In a second approach, the oxidation pattern of CF1 was analyzed after exposure to H_2O_2. Unfortunately, the fragment containing γM23 could not be detected in treated samples, neither in a modified nor in a non-modified state. As described for $^1O_2$, oxidation of C-terminal γM279 and γM282 (Figure 33) and γC89 (Figure 34A) was observed. Furthermore, tri-oxidation of regulatory γC199 (Figure 34B) was discovered.

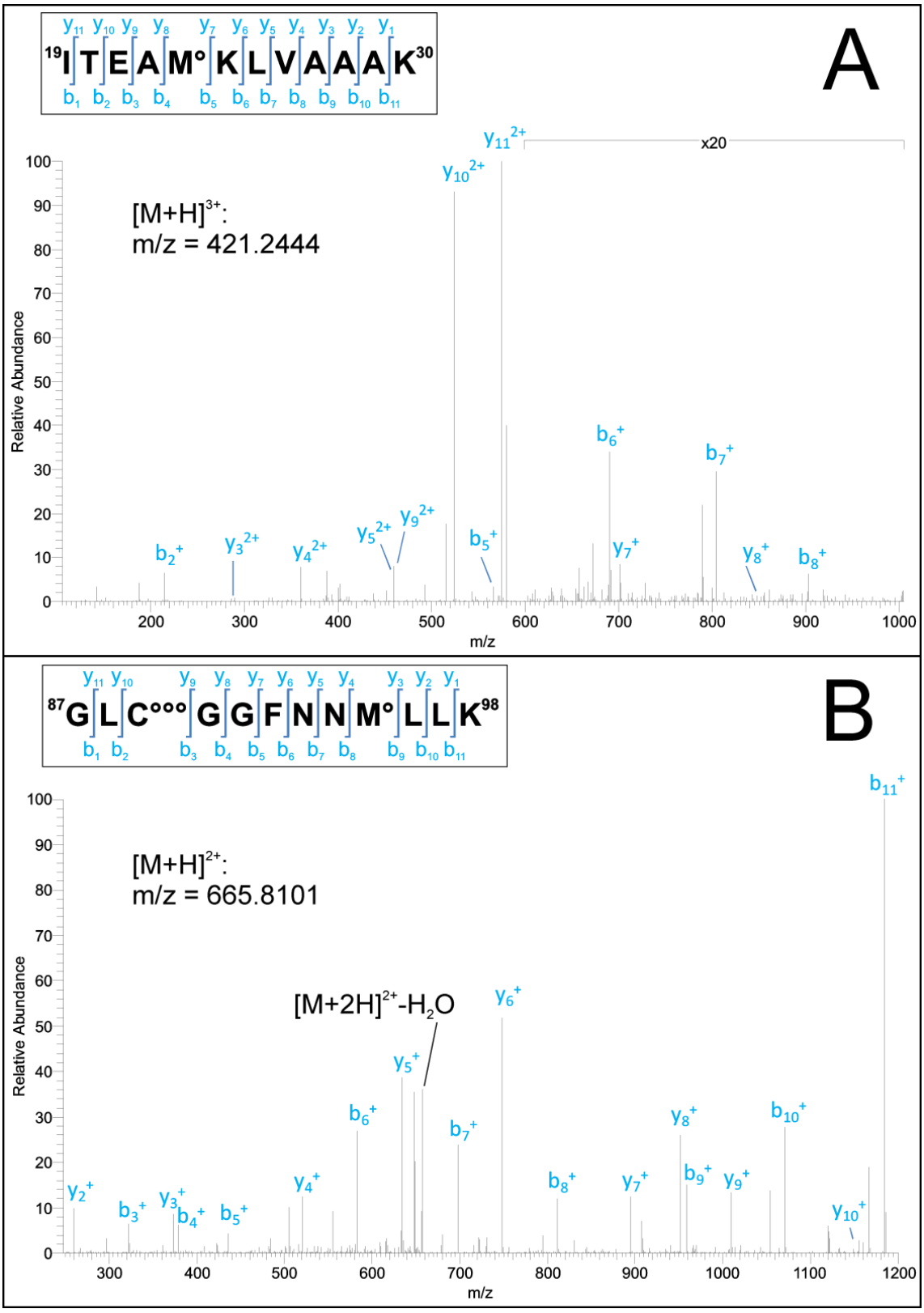

Figure 27: Mass spectrometric analysis of $^{1}O_2$-induced γ subunit modifications of γM23 and γC89. NanoLC-ESI/MS/MS average spectra of γ subunit peptides are shown, highlighting mono-oxidation (°) and tri-oxidation (°°°). The b- and y-ion series are labeled. (A) Peptide ^{19}ITEAMKLVAAAK^{30} contained mono-oxidized γM23. (B) The peptide ^{87}GLCGGFNNMLLK^{98} was tri-oxidized on γC89 and mono-oxidized on γM95.

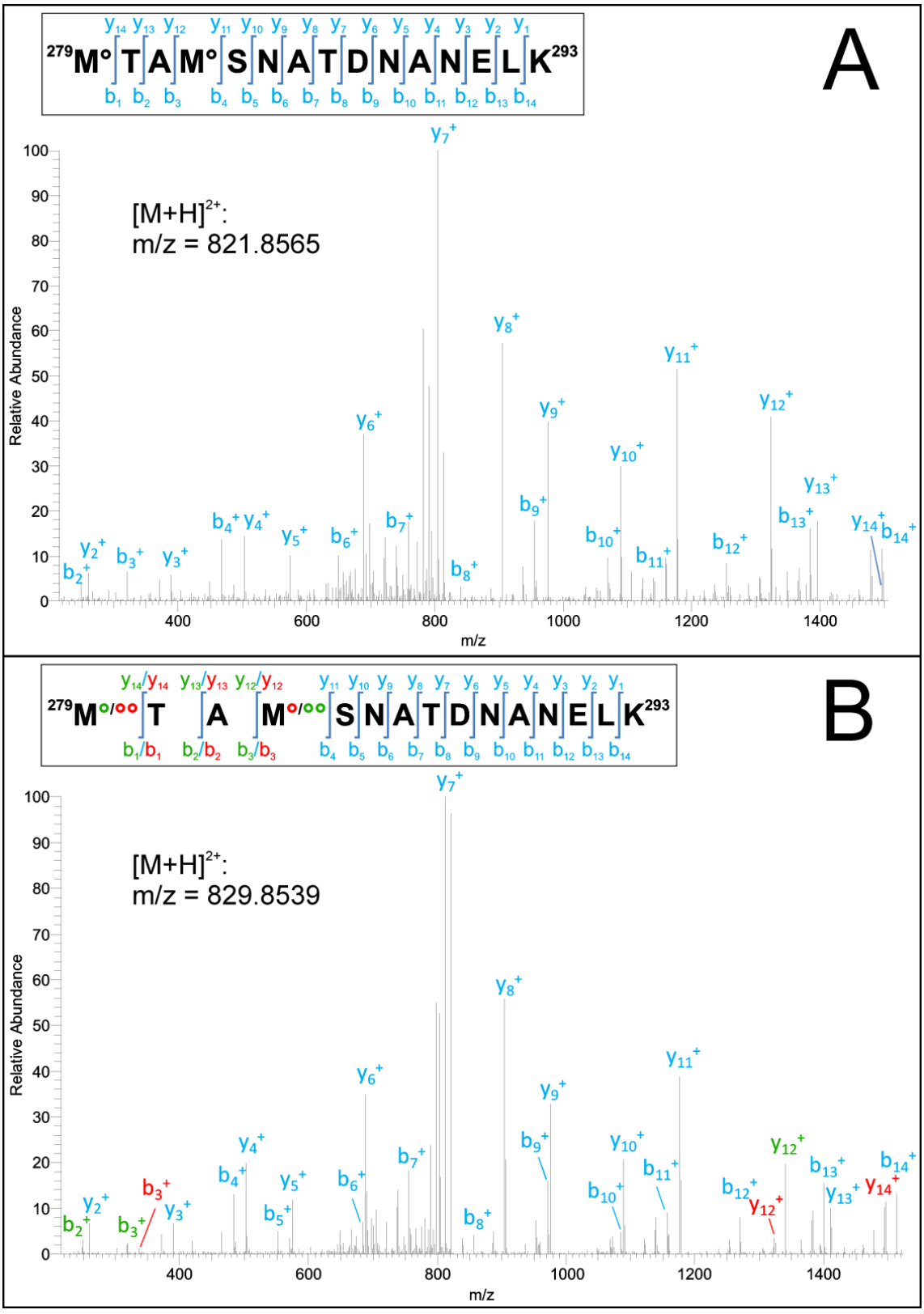

Figure 28: Mass spectrometric analysis of $^1O_2$-induced γ subunit modifications of the C-terminal methionines. NanoLC-ESI/MS/MS average spectra of γ subunit peptides are shown, highlighting mono-oxidation (°) and di-oxidation (°°). The b- and y-ion series are labeled. (A) Peptide ^{279}MTAMSNATDNANELK^{293} contained both mono-oxidized γM279 and γM282. (B) Peptide ^{279}MTAMSNATDNANELK^{293} was mono-oxidized on γM279 and di-oxidized on γM282. Alternatively, γM279 was di-oxidized and γM282 was mono-oxidized. Both cases could be distinguished with the y_{12}-y_{14} ions and with the b_1-b_3 ions. The typical ions for both possibilities were present in this MS/MS indicating both detected modifications. Green b- and y-ions: typical ions for γM279 mono-oxidized and γM282 di-oxidized; red b- and y-ions: typical ions for γM279 di-oxidized and γM282 mono-oxidized.

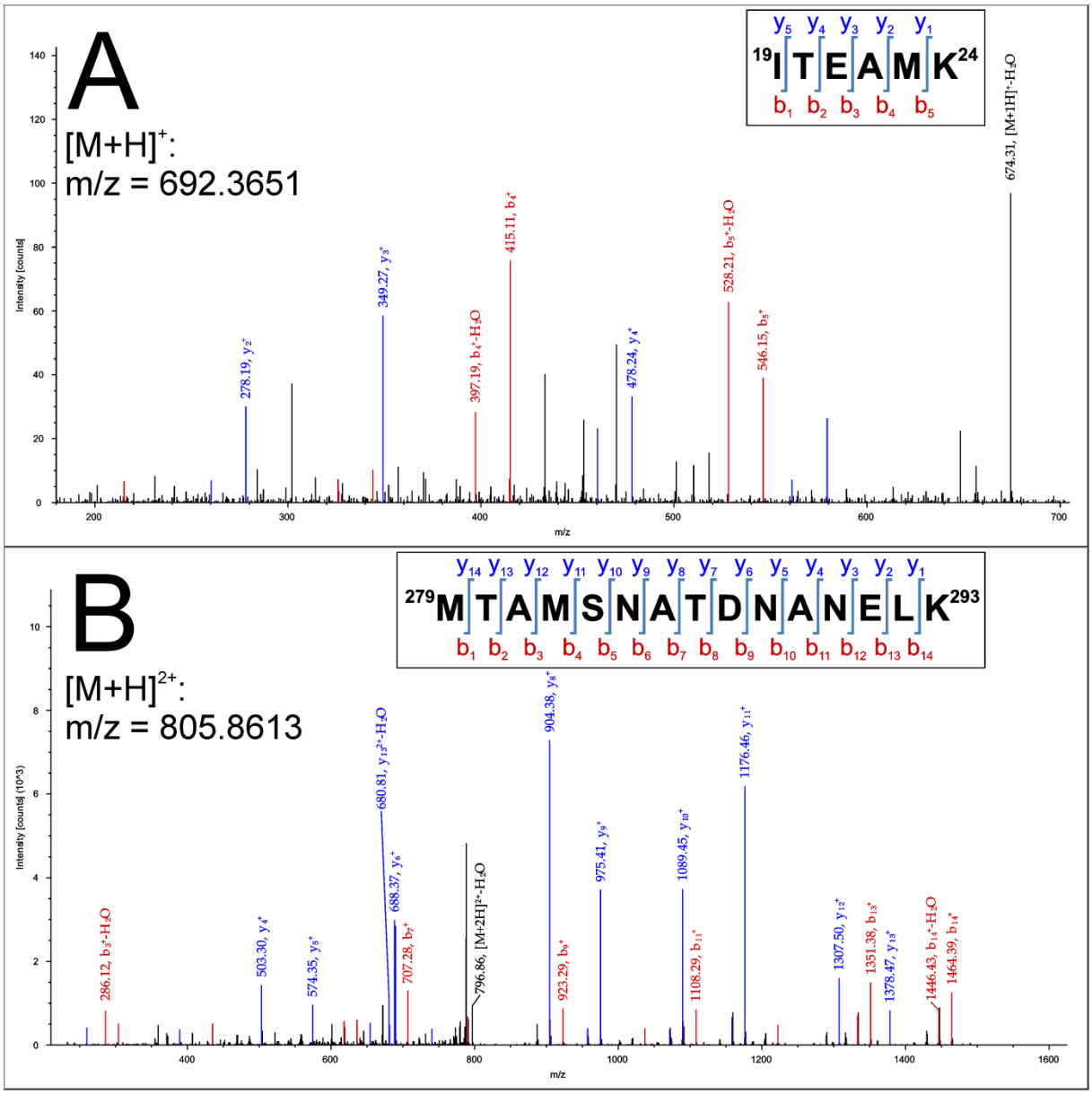

Figure 29: Mass spectrometric analysis of amino acid modifications in non-treated control samples showing NanoLC-ESI/MS/MS average spectra of γ subunit peptides. The b- and y-ion series are labelled. Cluster methionines γM23, γM279 and γM282 were not oxidized as shown in peptides (A) ^{19}ITEAMK^{24} and (B) ^{279}MTAMSNATDNANELK^{293}.

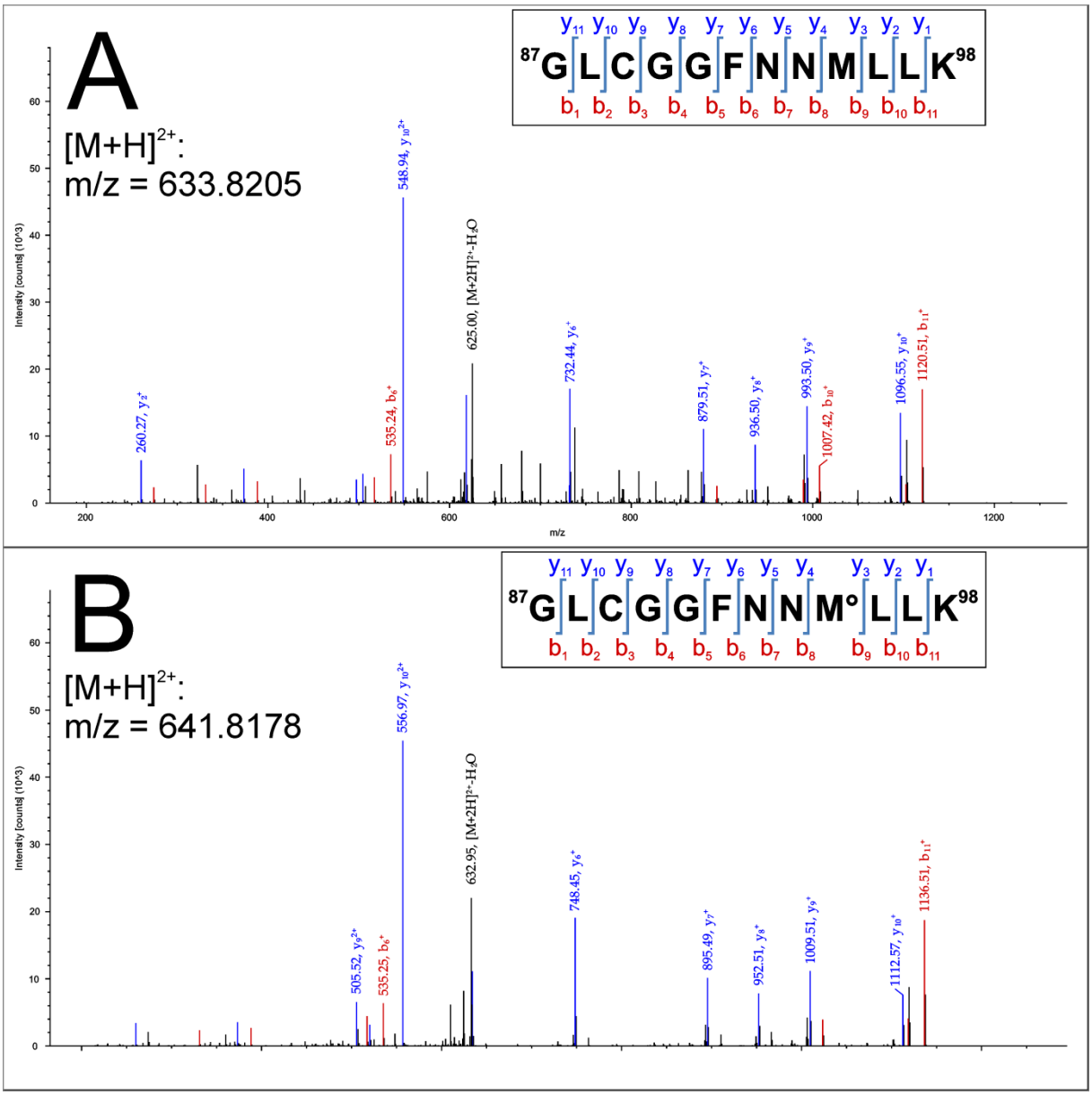

Figure 30: Mass spectrometric analysis of amino acid modifications in non-treated control samples showing NanoLC-ESI/MS/MS average spectra of γ subunit peptides. The b- and y-ion series are labelled. Cluster cysteine γC89 was not oxidized as shown in peptides (A) ^{87}GLCGGFNNMLLK^{98} and (B) ^{87}GLCGGFNNMLLK^{98}, whereas this non-treated sample contained mono-oxidized (°) γM95.

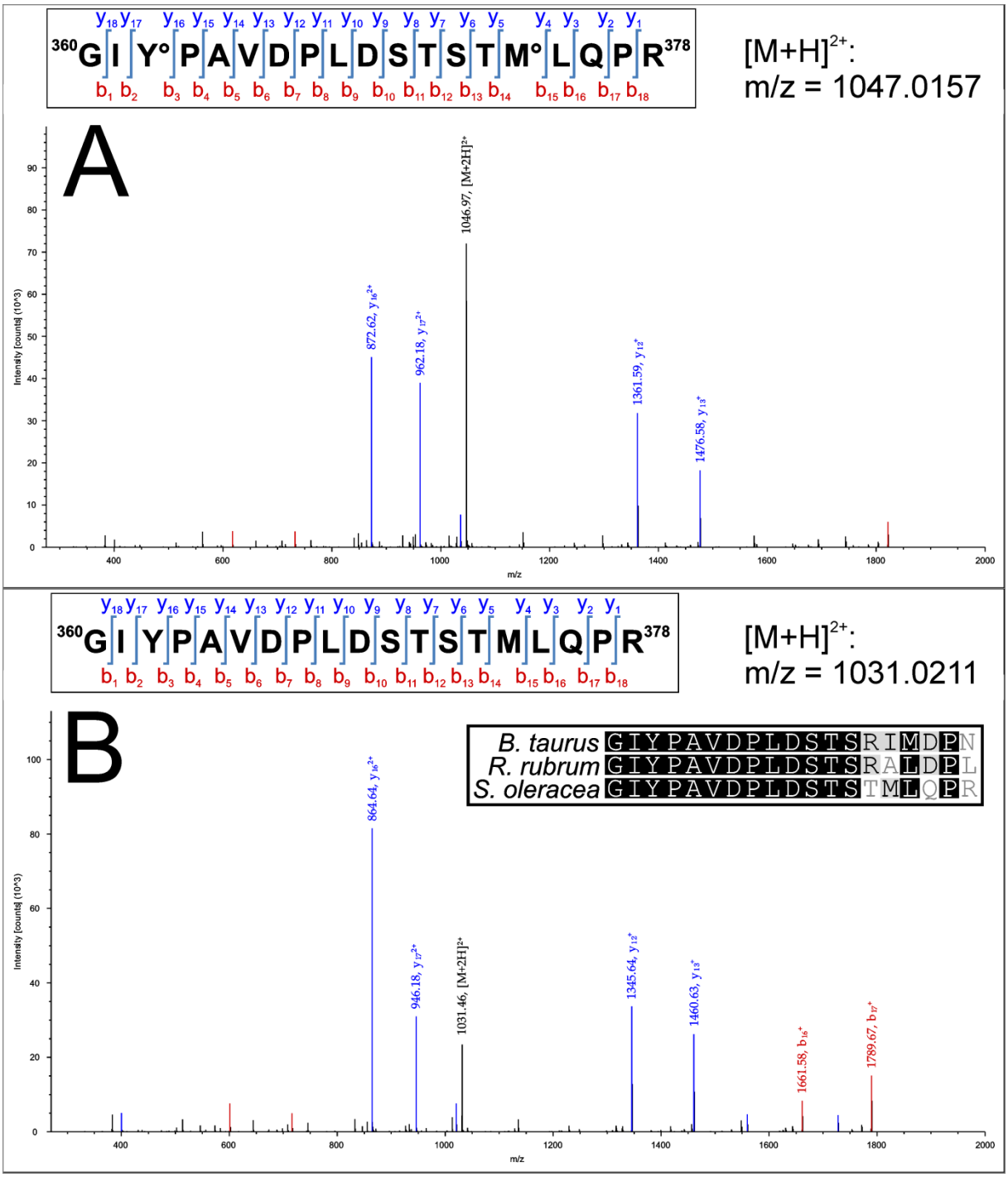

Figure 31: Mass spectrometric analysis of nucleotide binding site residues of the CF1 β subunit. NanoLC-ESI/MS/MS average spectra are shown. Mono-oxidations (°) are highlighted. The b- and y-ion series are labeled. (A) In $^1O_2$-exposed samples the peptide ^{360}GIYPAVDPLDSTSTMLQPR^{378} contained mono-oxidized βY362 and βM374. (B) In non-treated samples peptide ^{360}GIYPAVDPLDSTSTMLQPR^{378} contained no modified residues. The inset shows an alignment of the corresponding β subunit peptide sequences from bovine mitochondrial, *Rhodospirillum rubrum* and spinach chloroplast F1.

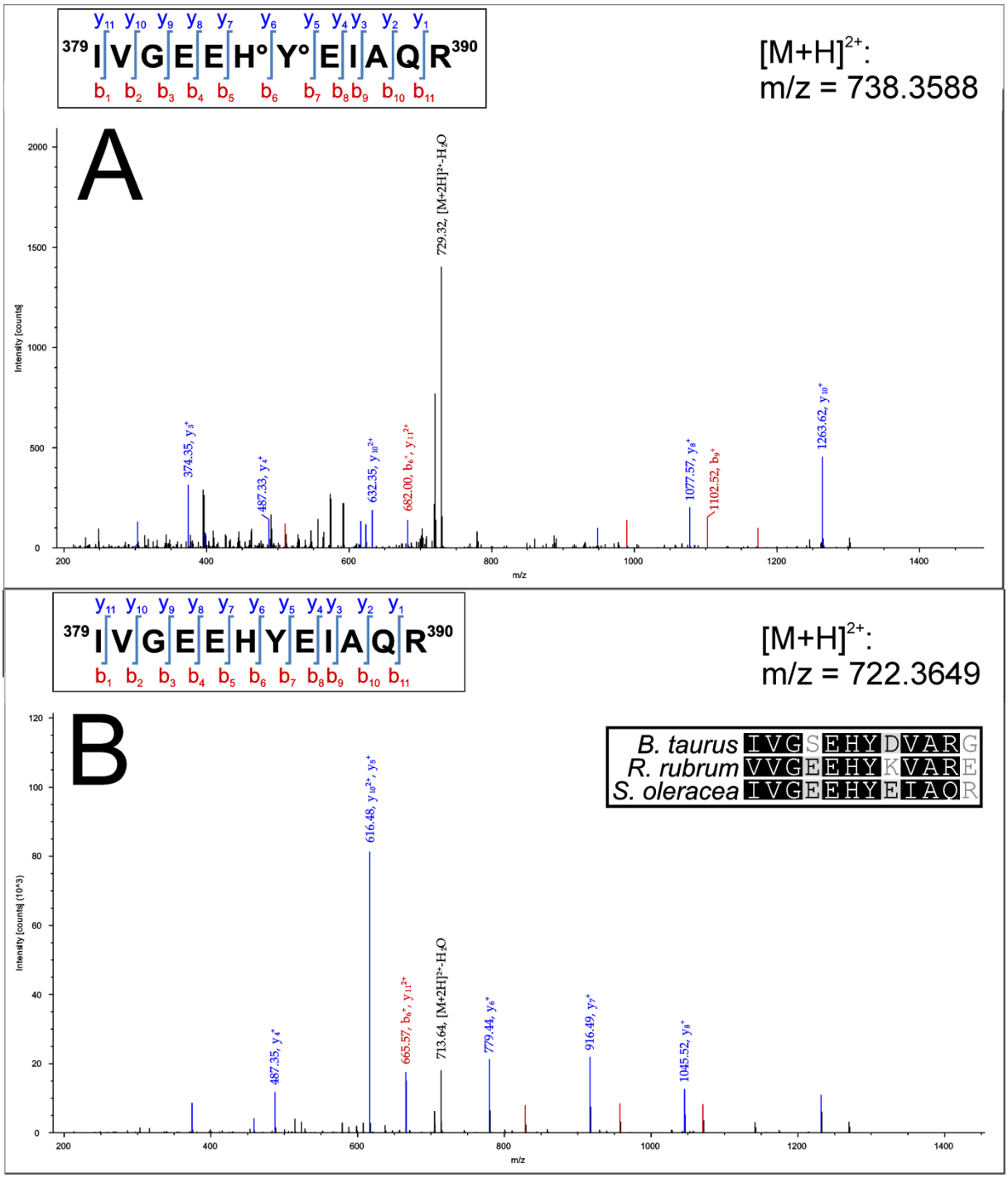

Figure 32: Mass spectrometric analysis of nucleotide binding site residues of the CF1 β subunit. NanoLC-ESI/MS/MS average spectra are shown. Mono-oxidations (°) are highlighted. The b- and y-ion series are labeled. (A) In $^1O_2$-exposed samples peptide ^{379}IVGEEHYEIAQR^{390} contained mono-oxidized βH384 and βY385. (B) In non-treated samples peptide ^{379}IVGEEHYEIAQR^{390} contained no modified residues. The inset shows an alignment of the corresponding β subunit peptide sequences from bovine mitochondrial, *Rhodospirillum rubrum* and spinach chloroplast F1.

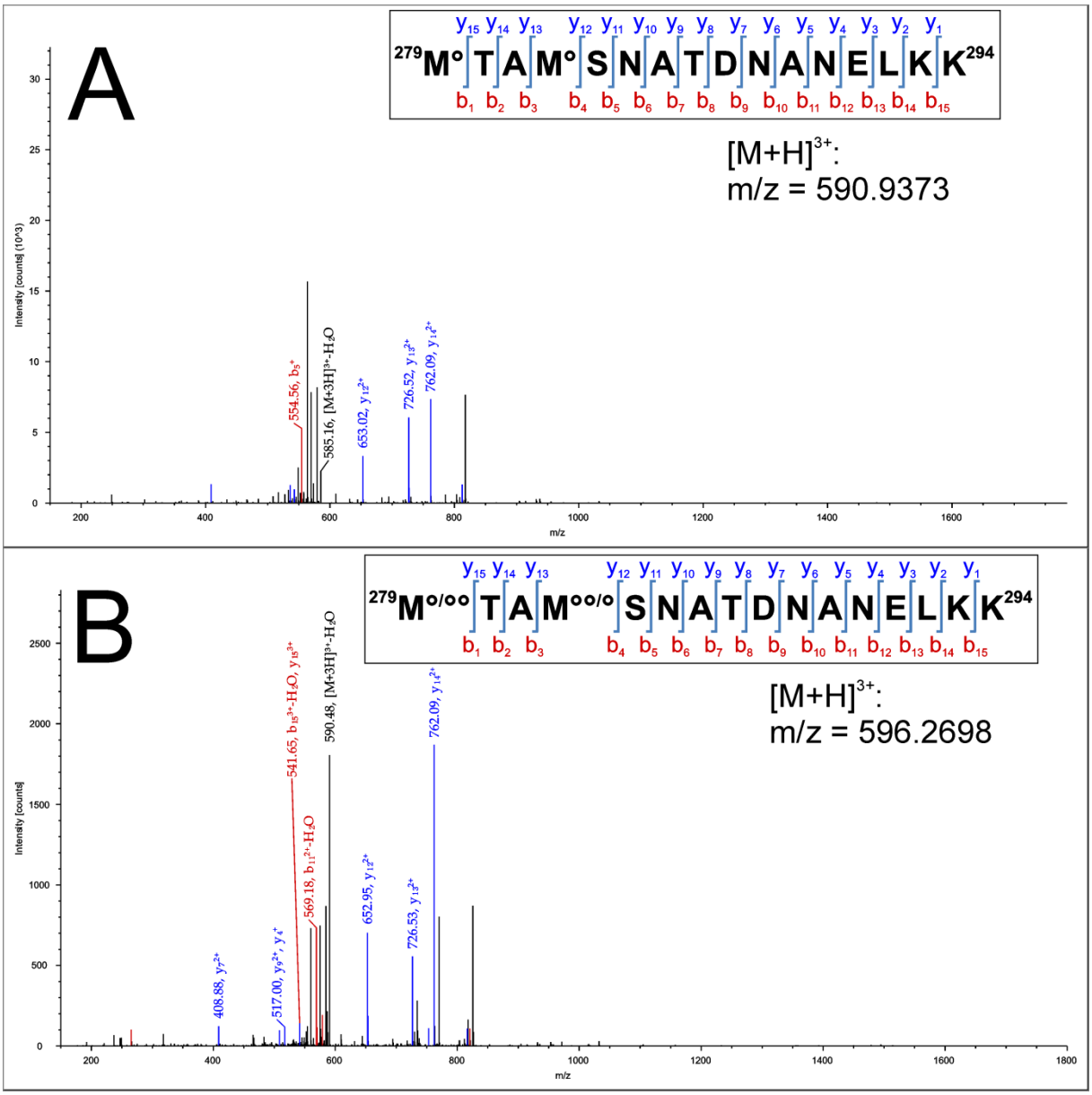

Figure 33: Mass spectrometric analysis of hydrogen peroxide-induced γ subunit modifications of C-terminal methionines. NanoLC-ESI/MS/MS average spectra of γ subunit peptides are shown highlighting mono-oxidation (°) and di-oxidation (°°). The b- and y-ion series are labeled. (A) The peptide ^{279}MTAMSNATDNANELKK^{294} contained both mono-oxidized γM279 and γM282. (B) The peptide ^{279}MTAMSNATDNANELK^{294} contained mono-oxidized γM279 and di-oxidized γM282. Alternatively, γM279 was di-oxidized and γM282 was mono-oxidized. The typical ions for both possibilities were present in this MS/MS indicating both detected modifications.

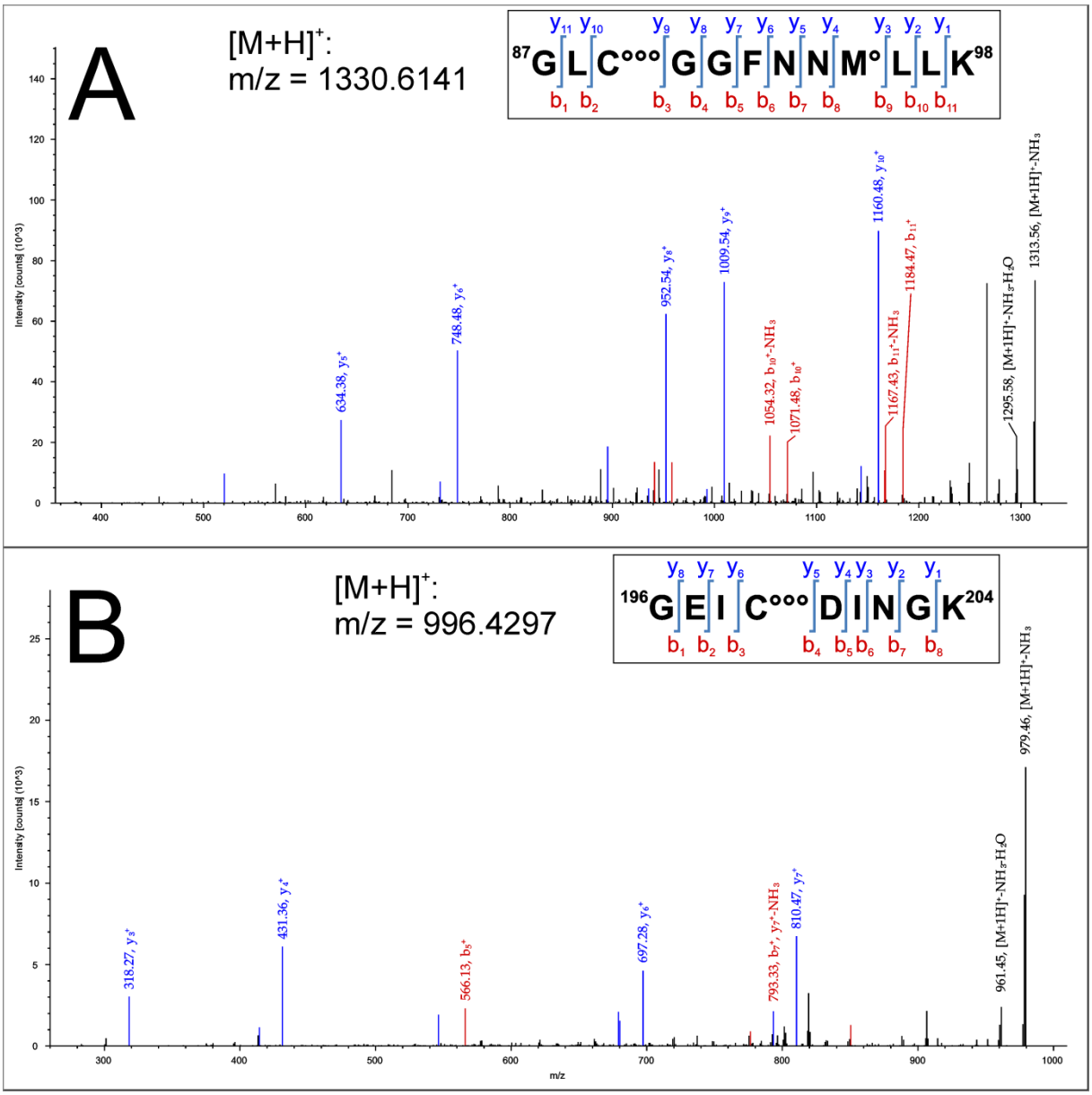

Figure 34: Mass spectrometric analysis of hydrogen peroxide-induced γ subunit modifications of γC89 and γC199. NanoLC-ESI/MS/MS average spectra of γ subunit peptides are shown highlighting mono-oxidation (°) and tri-oxidation (°°°). The b- and y-ion series are labeled. (A) Peptide ^{87}GLCGGFNNMLLK^{98} was tri-oxidized on γC89 and mono-oxidized on γM95. (B) Peptide ^{196}GEICDINGK^{204} contained tri-oxidized γC199.

3.4 The hybrid F1: Site-directed mutagenesis, expression, purification and assembly

As suitable substitutes, leucine for methionine and alanine for cysteine, were chosen. In a previous study of homologous EcF1 γ subunit mutants these substitutions displayed minimal effects *in vivo* (Shin et al. 1992). Regarding γM279 and γM282 (see section 3.3.2), a mutual oxidation pattern was observed, similar to observations with methionine-methionine dipeptides (Miller et al. 1998). Therefore, single mutants of these particular residues were not investigated. The proposed histidine target γH187 (section 4.1) was mutated to glutamine which is found at the corresponding position in monocots and the green algae *Chlamydomonas reinhardtii* (Figure 35).

The protocol used for purification of inclusion bodies, following expression in *E. coli*, yielded clean protein preparations (Figure 36) that were later used for reassembly.

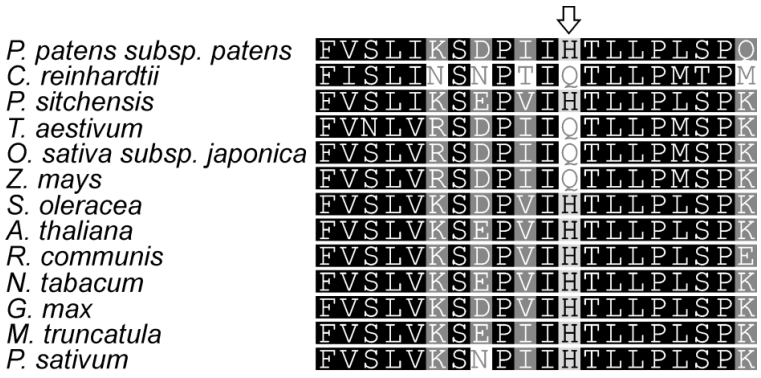

Figure 35: Alignment extraction of various CF1 γ subunits highlighting a conserved histidine (arrow) at the position of spinach numbering γH187. The residue was substituted in the γH187Q mutant. Sequences correspond to an altered peptide fragment detected via MALDI-TOF in $^1O_2$-treated Arabidopsis *flu* (Mahler et al. 2007).

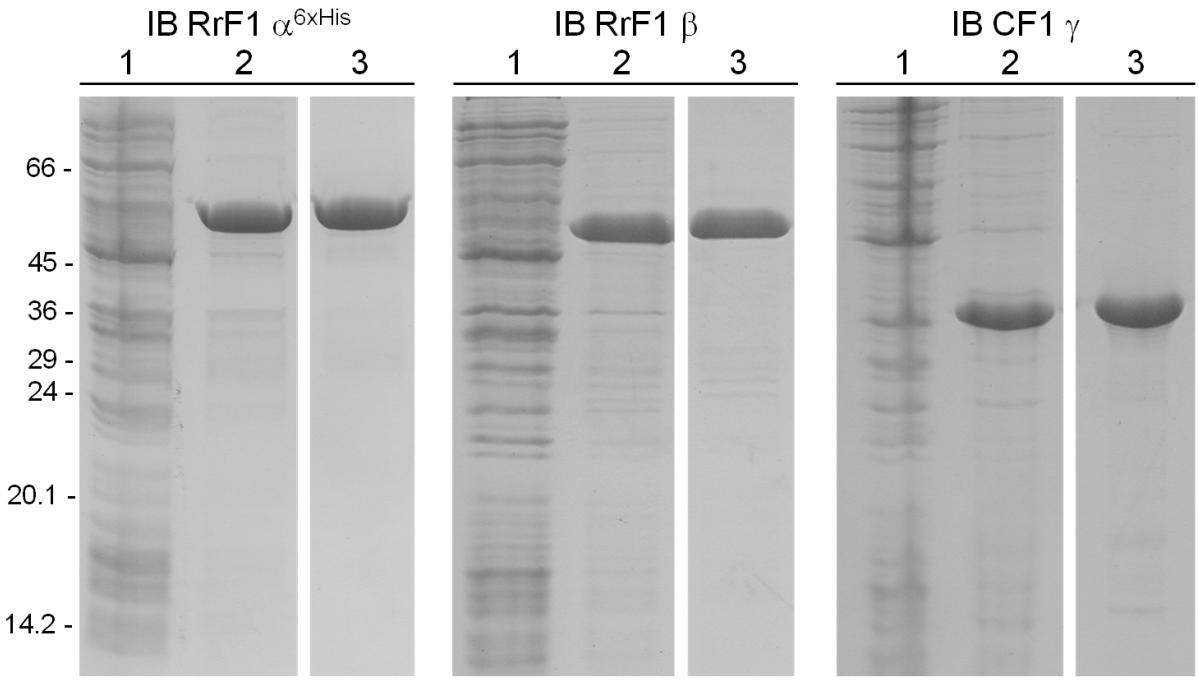

Figure 36: Inclusion body purification. *Rhodospirillum rubrum* F1 (RrF1) and spinach chloroplast F1 (CF1) subunits were expressed and purified as inclusion bodies (IB), used for the hybrid F1 assembly approach. Polyacrylamide gels were stained with Coomassie and contained an aliquot of *E. coli* cells prior (lane 1) and after (lane 2) induction with IPTG, as well as washed and purified IB (lane 3).

Initial experiments were carried out with purified hybrid F1 to set up an analytical approach on impact of H_2O_2. It could be shown that, as well as $^1O_2$ treatment, the mild oxidant H_2O_2 caused visible alterations of the γ subunit on SDS-PAGE (Figure 37). However, all mutants tested in this study showed this effect (not shown).

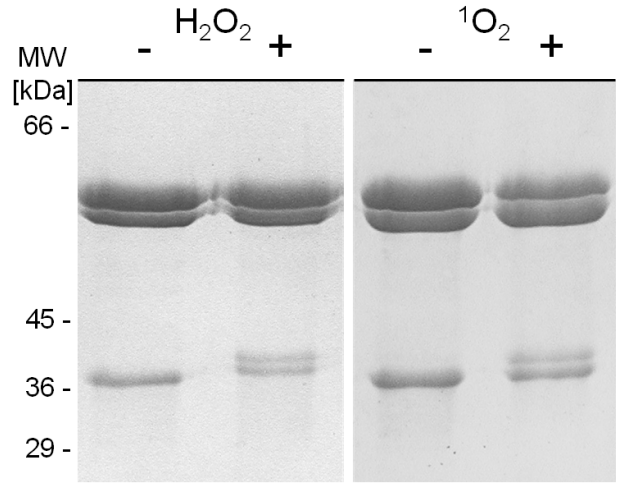

Figure 37: Protein pattern of purified hybrid F1 visualized by SDS-PAGE. Gels were stained with Coomassie and contained ca. 7 µg of protein per lane. Both treatments with H_2O_2 (at 50 mM for 60 min and 37 °C) and $^1O_2$ (30 s illumination at 2 µM RB) resulted in an additional γ subunit isoform, resembling results from Figure 18.

3.5 The hybrid F1: Mutant characterization of catalytic properties

3.5.1 The effect of oxyanions on MgATP hydrolysis

According to numerous studies, especially on γM23 (Bandyopadhyay and Allison 2004; Feniouk et al. 2007; Omote et al. 1999; Shin et al. 1992), the region of the proposed ROS targets plays a critical role in enzyme functionality. For this reason, attempts were made to characterize the hybrid F1 mutants apart from ROS response.

Oxyanions, such as bicarbonate or sulfite, are thought to compete with metalbinding ligands within the nucleotide binding pocket, thus leading to faster release of ADP (Du and Boyer 1990). MgATPase stimulation by sulfite is caused by release of bound inhibitory ADP which is stabilized by free Mg^{2+} in photosynthetic and mitochondrial F1 (Malyan 1981; Murataliev and Boyer 1994). It should be noted that release of inhibitory MgADP is facilitated by the ΔpH when F1 is attached to the membrane (Du and Boyer 1990). The propensity of hybrid F1 mutant assemblies to entrap inhibitory MgADP in a catalytic site during turnover was analyzed by monitoring the stimulatory effect of sulfite on MgATP hydrolysis (Table 8).

Table 8: The stimulatory effect of sulfite on MgATP hydrolysis by hybrid F1.
[a]Hybrid F1 assemblies were purified and assayed as described in section 2.2.6.
[b]Expressed as µmol Pi released min^{-1} mg $protein^{-1}$. Assay conditions are described under 2.2.13. Errors are SE with *n* = 3. 25 mM Na_2SO_3 was present where indicated.
[c]The stimulation factor describes the ratio of MgATPase activity in the presence of sulfite to the activity without sulfite.

protein preparation[a]	MgATPase activity[b]		sulfite stimulation factor[c]
	- sulfite	+ sulfite	
$\alpha_3\beta_3\gamma^{wild\ type}$	9.5 (± 0.3)	41.0 (± 0.5)	4.3
$\alpha_3\beta_3\gamma^{M23L}$	4.8 (± 0.2)	36.3 (± 0.7)	7.6
$\alpha_3\beta_3\gamma^{M279+282L}$	2.1 (± 0.3)	23.5 (± 0.3)	11.2
$\alpha_3\beta_3\gamma^{M23+279+282L}$	5.9 (± 0.4)	61.4 (± 0.5)	10.5
$\alpha_3\beta_3\gamma^{C89A}$	8.1 (± 0.3)	34.6 (± 0.4)	4.3
$\alpha_3\beta_3\gamma^{M23+279+282L/C89A}$	1.9 (± 0.3)	26.6 (± 0.3)	14.2
$\alpha_3\beta_3\gamma^{C199+205A}$	16.7 (± 0.4)	61.1 (± 0.2)	3.7

In the wild type assembly, a roughly 4-fold increase in MgATPase activity was observed upon addition of sodium sulfite, resembling previous observations of hybrid F1 under similar experimental conditions (He et al. 2007). Mutation of cluster component methionines significantly enhanced the stimulatory effect of sulfite ranging from 1.8-fold (γM23L) to 2.6-fold (γM279+282L) over that of the wild type assembly. This indicated that the corresponding mutants bound MgADP more tightly. Sulfite stimulation in γC199+205A and γC89A

assemblies was rather indistinguishable from wild type. In line with the latter observation, the quadruple cluster mutant γM23+279+282L/γC89A revealed no substantially additive stimulatory effect by a γC89A substitution compared to γM23+279+282L.

3.5.2 *The effect of γ disulfide redox-modulation on MgATP hydrolysis*

In higher plant chloroplasts, ATP hydrolysis is regulated by two γ-cysteines, designated as C199 and C205 in spinach (Richter 2004). If oxidized, both cysteines form a disulfide bridge, resulting in low ATP hydrolysis, whereas disulfide cleavage by reduction stimulates ATP hydrolysis. It is assumed that redox-modulation of the two regulatory γ-cysteines is accompanied with dynamic structural changes within the dithiol domain, consequently affecting inter-domain movement of the γ subunit during rotational catalysis (Richter 2004; Richter et al. 2005).

A second mutant characterization attempt was made to analyze the implications of proposed domain movements upon γ disulfide reduction (Table 9).

Table 9: The response of γ subunit mutants to reducing/oxidizing conditions. [a]Hybrid F1 assemblies were purified and assayed as described under 2.2.6. [b]Expressed as µmol Pi released min^{-1} mg $protein^{-1}$. Assay conditions as described under 2.2.13. Errors are SE with n = 3. 25 mM Na_2SO_3 was present. Reduction (10 mM DTT) and oxidation (100 µM $CuCl_2$) was carried out for 60 min and 37 °C. [c]Ratios of reduced to oxidized MgATPase is shown.

protein preparation[a]	MgATPase activity[b] reduced	oxidized	reduced/ oxidized[c]
$\alpha_3\beta_3\gamma^{wild\ type}$	90.0 (± 0.6)	52.0 (± 1.0)	1.73
$\alpha_3\beta_3\gamma^{M23L}$	57.9 (± 0.8)	57.7 (± 0.8)	1.00
$\alpha_3\beta_3\gamma^{M279+282L}$	27.8 (± 0.6)	29.1 (± 1.1)	0.96
$\alpha_3\beta_3\gamma^{M23+279+282L}$	81.3 (± 0.9)	81.8 (± 0.9)	0.99
$\alpha_3\beta_3\gamma^{C89A}$	77.9 (± 1.8)	55.9 (± 0.9)	1.39
$\alpha_3\beta_3\gamma^{M23+279+282L/C89A}$	44.2 (± 0.9)	41.1 (± 0.8)	1.08
$\alpha_3\beta_3\gamma^{C199+205A}$	78.6 (± 0.7)	99.0 (± 0.5)	0.79

MgATPase activitiy of oxidized hybrid F1 wild type in the presence of sulfite was slightly below oxidized γM23L and γC89A. Although no bacterial redox-modulation is established, activity ratios to the wild type resembled observations of corresponding EcF1 mutants (Shin et al. 1992). If leucines at position 279 and 282 were introduced, oxidized ATPase activity dropped

roughly by 50% compared to the wild type (see oxidized γM279+282L). However, this strong detrimental effect was recovered by an additional γM23L substitution (γM23+279+282L) which resulted in an approximate 1.5-fold MgATPase compared wild type. Although γC89A resembled wild type, the potency of γM23L recovery in γM23+279+282L was significantly weakened by an additional γC89A substitution (see oxidized γM23+279+282L/γC89A).

Consistent with previous hybrid F1 studies (Samra et al. 2008), reduction of wild type γ subunit strongly enhanced ATP hydrolysis. Despite interplay of evolutionary diverged subunits, the extent of DTT-induced activation in the wild type hybrid F1 was comparable with CF1 core assemblies (Samra et al. 2006). Substitution of leucine for methionine in the cluster region strongly diminished ATPase activation upon γ disulfide reduction (see γM23L, γM279+282L and γM23+279+282L). In the γC89A this effect was less pronounced. Reduced γC199+205A mutants showed lower activities compared to $CuCl_2$-treated samples. A similar effect was described previously with CF1 $\alpha_3\beta_3\gamma$ assemblies lacking the regulatory cysteine region (Samra et al. 2006). In that case, alkylation of the thiols, following reduction, blocked the inhibition. However, in hybrid F1 γC199+205A of this study the DTT-induced inhibition could not be abolished by alkylation of the remaining γ-cysteines with N-ethylmaleimide prior to the reduction step (not shown).

3.6 The hybrid F1: MgATPase upon exposure to singlet oxygen

An empirical approach was undertaken by assembling hybrid F1 enzymes lacking γ-residues that were confirmed to be modified by $^1O_2$ (Figure 27, Figure 28). The approximate locations of introduced mutations are shown in Figure 38.

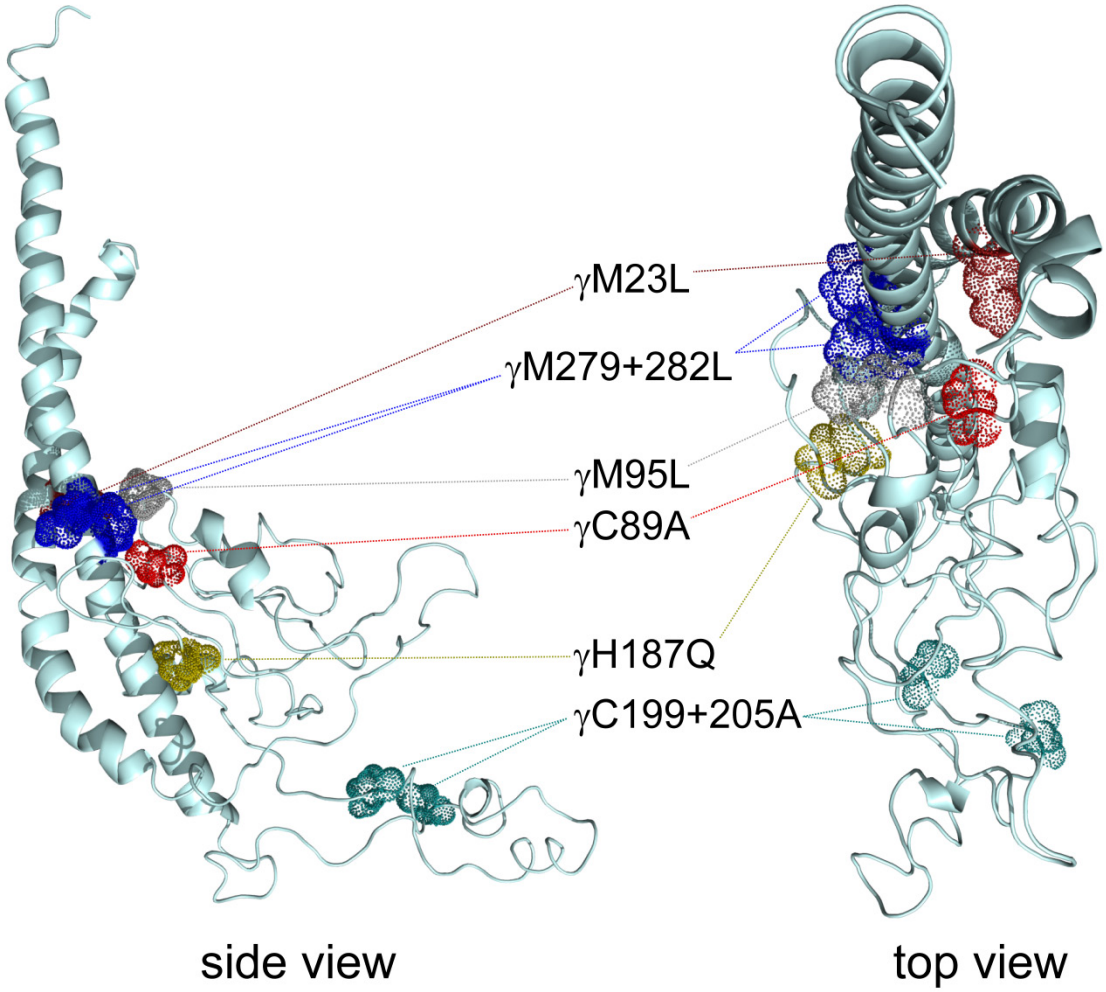

Figure 38: Indication of γ subunit mutations tested in this study. Approximate locations are based on the γ subunit model structure (Richter et al. 2005). The color coding is proceeded in Figure 39 and Figure 41.

Activity attenuations of methionine-cysteine cluster mutants showed that these assemblies were still susceptible to $^1O_2$, but in different ways (Figure 39A). The most striking resistance was observed in the γM23L enzyme, whereas γC89A tended to be slightly more susceptible than wild type. The γM279+282L was, if at all, only slightly more tolerant than the wild type, so were γM23+279+282L and γM23+279+282L/γC89A. Interestingly, γM279+282L response seemed to be dominant over γM23L since the gain of γM23L resistance was absent in both, the γM23+279+282L and γM23+279+282L/γC89A combination mutants. Gain of γM23L resistance was preserved when combined with wild type-like γM95L in γM23+95L assemblies (Figure 39B). Since disulfides can be generated upon protein exposure to certain ROS (Davies 2005), a γC199+205A construct (Samra et al. 2006) was assayed (Figure 39B) which lacks the disulfide forming regulatory cysteines. It turned out that the γC199+205A enzyme tended to be marginally more susceptible to $^1O_2$ than the wild type. This indicated that activity attenuation in the wild type was not a result of successive $^1O_2$-mediated disulfide

formation between γC199 and γC205. In contrast to initial suggestions (section 4.1), substituting the conserved single γ-histidine with glutamine in the γH187Q did not alter the response, demonstrating that the histidine was not a functional target of $^1O_2$.

A reaction feature of $^1O_2$ is the pH dependence of target rate constants (Wilkinson et al. 1995). Especially histidines react more slowly at lower pH (Bisby et al. 1999; Davies 2003). More resistant *target cluster* mutants were observed when exposure to $^1O_2$ was carried out at pH 6.0 (Figure 39C) instead of pH 8.0 (as in Figure 39A). The γM23L mutant showed almost no pH-dependent tolerance effect and only minor differences were observed upon changing pH with γC89A, the enzyme being slightly more tolerant toward oxidation at the lower pH. The remaining multiple cluster mutants were significantly less sensitive when exposed to $^1O_2$ at lower pH. Interestingly, all mutants harboring γM279+282L showed the greatest increase in tolerance at pH 6 (Figure 39C). There was a slight indication of an additive effect in the triple γM23+279+282L mutant assembly compared to the corresponding terminal mutants γM23L and γM279+282L. Furthermore, substitution of γC89A had no additional effect in the quadruple γM23+279+282L/γC89A mutant compared to γM23+279+282L. When comparing pH-dependent activity attenuation of the wild type, only a small difference was observed, i.e. an exposure for 1 min resulted in residual activities of 51% (pH 8.0) and 48% (pH 6.0), respectively.

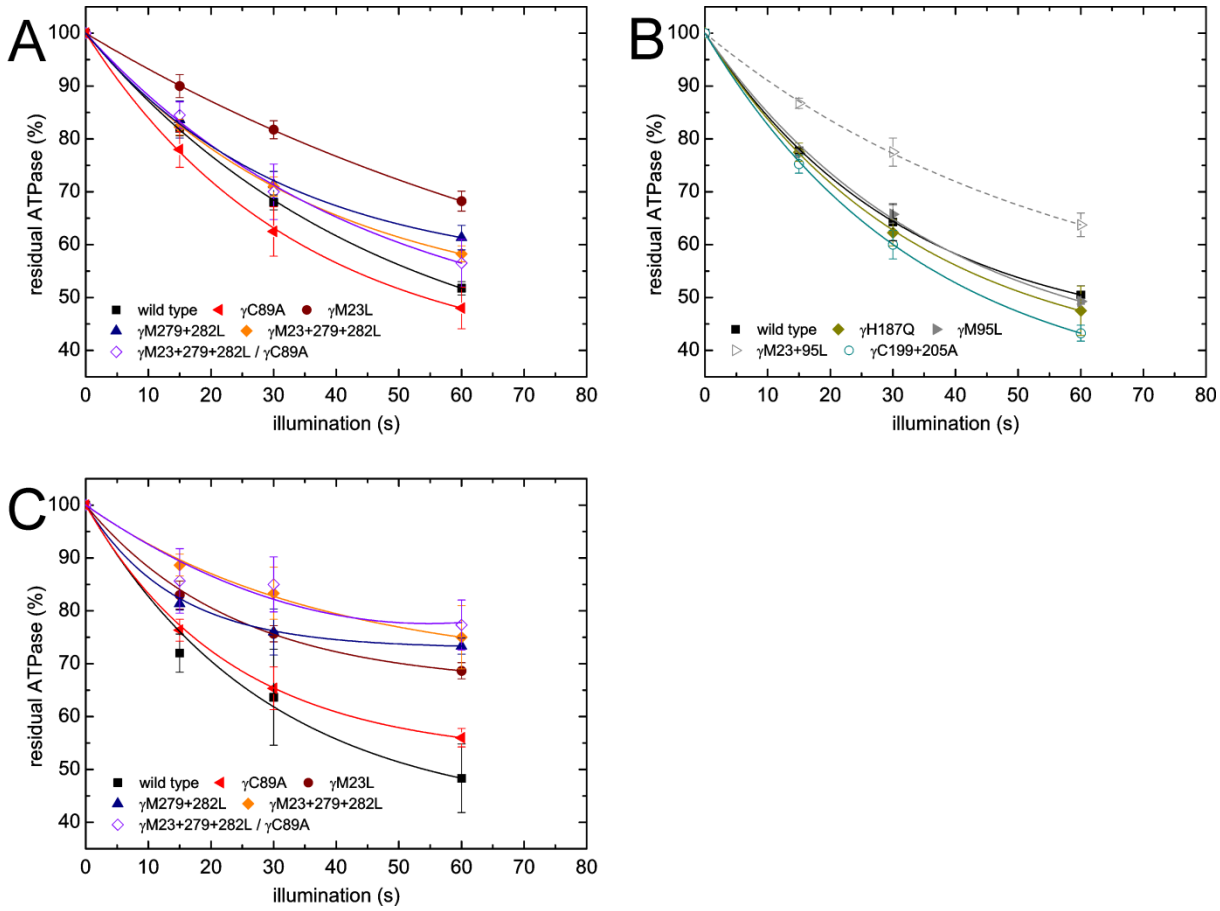

Figure 39: $^1O_2$ lowered the MgATP hydrolysis by recombinant hybrid F1 assemblies. Illumination was carried out in presence of 2 µM RB. Residual activities (± SD) relative to the control were plotted against exposure time. (A) Combinations of γ-methionine-cysteine cluster mutants were compared to wild type ($^1O_2$ generation at pH 8.0, *n* = 4). (B) Activity of the γH187Q mutant declined comparably to wild type assemblies, whereas γC199+205A was slightly more susceptible under reaction conditions as in (A). Single γM95L and the combination γM23+95L showed no effect compared to wild type and γM23L from (A), respectively. (C) pH effect on $^1O_2$-exposed combinations of γ-methionine-cysteine cluster mutants compared to wild type (pH 6.0, *n* = 3).

Similarly, $^1O_2$-induced oxidations of nucleotide binding site residues in the CF1 β subunit (Figure 31A, Figure 32A) did not affect MgATPase in the corresponding hybrid F1 (Figure 40).

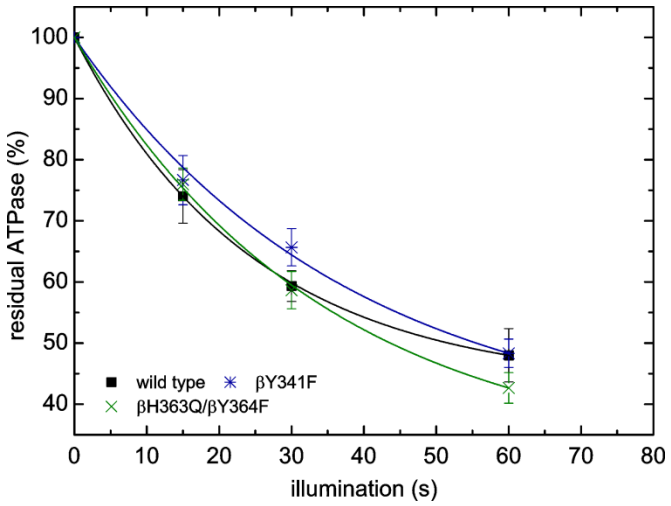

Figure 40: $^1O_2$ lowered the MgATP hydrolysis by recombinant hybrid F1 β subunit mutants. Illumination was carried out in presence of 2 µM RB. Homologous RrF1 mutations of the modified spinach CF1 β subunit tyrosines and histidine (Figure 31, Figure 32) were introduced. The impact of $^1O_2$ on the mutants was comparable to the wild type. Residual activities (± SD, *n* = 3) relative to the control were plotted against exposure time at pH 8.0.

3.7 The hybrid F1: MgATPase upon exposure to hydrogen peroxide

In a second approach, the cluster-substituted hybrid F1 was exposed to hydrogen peroxide. The data indicated that a significant decrease in activity resulted from an impact of oxidized cluster residues (Figure 41A). Equal contributions yielded similar tolerances of γC89A, γM279+282L and γM23+279+282L, respectively. In contrast to the effect of $^1O_2$ (Figure 39), the absence of γM23 led to a small decrease in inhibition only (Figure 41A). Similarly, neither enhanced tolerance by γM23L was observed in the triple mutant γM23+279+282L when compared to the γM279+282L mutant. This was in line with the almost H_2O_2-tolerant γM279+282L/γC89A that harbored γM23 as the only potential *target cluster* component. However, the most striking effect was observed in the quadruple cluster mutant γM23+279+282L/γC89A that rendered the enzyme nearly insensitive to H_2O_2. On the contrary, exposing wild type hybrid F1 to lower concentrations of 1 mM H_2O_2 (Figure 41B) yielded a slightly activated enzyme which showed successive ATPase attenuation with increasing H_2O_2 concentrations. The quadruple cluster mutant γM23+279+282L/γC89A showed a higher extent of activation with little, if any inhibition occurring at higher H_2O_2 concentrations. Since H_2O_2 does not react with histidines, absence of the residue in γH187Q had no effect on susceptibility (Figure 41C). Even though a sulfonic acid derivative within the redox-regulatory core element was detected (Figure 34B), no implications on H_2O_2 tolerance were observed in γC199+205A (Figure 41C).

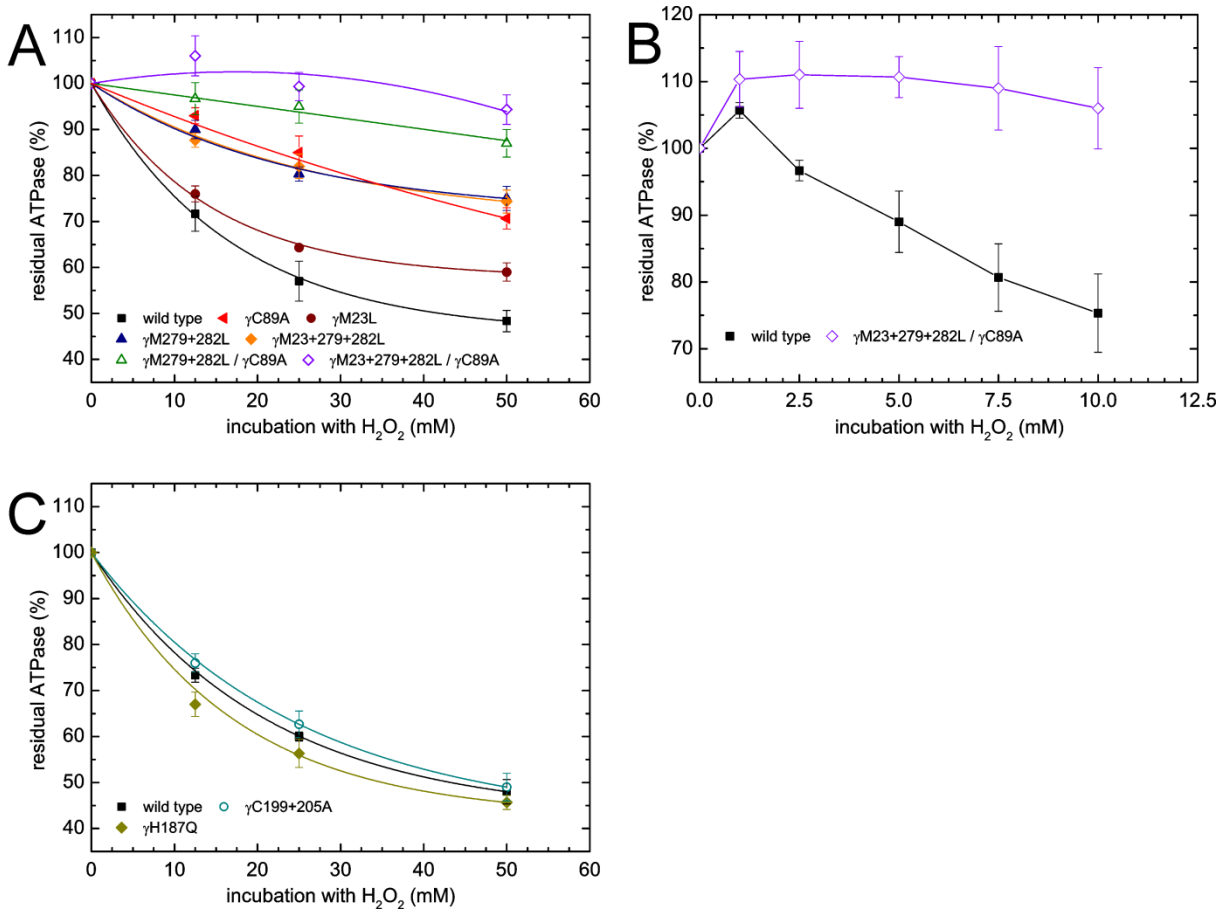

Figure 41: Hydrogen peroxide lowered the MgATP hydrolysis by recombinant hybrid F1 assemblies. Residual activities (± SD, *n* = 3) relative to the control were plotted against exposure to increasing concentrations of H_2O_2. (A) Combinations of γ-methionine-cysteine cluster mutants were compared to wild type. (B) Comparison of wild type with γM23+279+282L/γC89A at lower concentrations of H_2O_2. 1 mM H_2O_2 caused a slight initial ATPase activation of 10% and 6% observed in γM23+279+282L/γC89A and the wild type assembly, respectively. With increasing concentrations, the assemblies showed activities as outlined in (A). (C) The activity of γH187Q and γC199+205A assemblies declined like wild type.

3.8 The hybrid F1: MgADP binding propensity upon exposure to ROS

As shown in this study, even minimally perturbing mutations of the γ subunit methionine-cysteine cluster dramatically changed catalytic properties and ROS sensitivity of the enzyme. It remains elusive by which means ROS provoked activity decline. One possibility could be that reactive oxygen affects MgADP binding and release. Thus, sulfite stimulation of MgATPase was assayed in ROS-treated hybrid F1. The whole set of residues involved in $^1O_2$-induced enzyme affection could not be identified completely since the quadruple cluster mutant showed significant susceptibility under all conditions tested. Accordingly, mutant nucleotide exchange assays were not carried out. However, MgATPase stimulation by sulfite in the wild type was not affected upon exposure to $^1O_2$ (Table 10), although RB treatment for 1 min slightly lowered the stimulatory sulfite effect.

The data in Figure 41A suggested that H_2O_2-induced enzyme affection was caused by oxidation of the γ subunit methionine-cysteine cluster. Therefore, γM23+279+282L/γC89A served as control in the H_2O_2-dependent MgADP release assay shown in Table 11. Again, the data indicated that H_2O_2-induced loss of activity did not seem to be a result of enhanced inhibitory MgADP binding. Both, the ROS-impaired wild type enzyme and the quadruple mutant showed a small increase of sulfite-induced H_2O_2 resistance.

Table 10: The effect of sulfite on MgATP hydrolysis by $^1O_2$-exposed hybrid F1 wild type.
[a]Singlet oxygen was released at pH 8.0 during illumination in the presence of 2 µM RB. [b]Expressed as µmol Pi released min^{-1} mg $protein^{-1}$. Assay conditions as described under 2.2.13. Errors are SE with *n* = 3. 25 mM Na_2SO_3 was present where indicated. [c]The value is obtained by setting activity after $^1O_2$ treatment relative to activity of the non-treated control. [d]The stimulation factor describes the ratio of MgATPase activity in the presence of sulfite to the activity without sulfite.

$^1O_2$ release by RB[a]	MgATPase[b]		*residual activity*[c]		sulfite stimulation factor[d]
	- sulfite	+ sulfite	- sulfite	+ sulfite	
0 s	8.7 (± 0.3)	36.0 (± 0.6)	*100%*	*100%*	4.1
15 s	6.8 (± 0.3)	28.9 (± 0.8)	*78%*	*80%*	4.3
60 s	4.7 (± 0.1)	17.1 (± 0.4)	*54%*	*48%*	3.6

Table 11: The stimulatory effect of sulfite on MgATP hydrolysis by H_2O_2-exposed hybrid F1.
[a]Hybrid F1 assemblies were purified and assayed as described under 2.2.6. [b]H_2O_2 treatment (50 mM) is described under 2.2.10. [c]Expressed as µmol Pi released min^{-1} mg $protein^{-1}$. Assay conditions as described under 2.2.13. Errors are SE with *n* = 3. 25 mM Na_2SO_3 was present where indicated. [d]The value is obtained by setting activity after H_2O_2 treatment relative to activity of the non-treated control. [e]The stimulation factor describes the ratio of MgATPase activity in the presence of sulfite to the activity without sulfite. [f]The resistance factor describes the ratio of residual activity upon H_2O_2 in the presence of sulfite to residual activity without sulfite.

		MgATPase[c]				
protein preparation[a]	Na_2SO_3	-		+		resistance factor[f]
	H_2O_2[b]	-	+	-	+	
$\alpha_3\beta_3\gamma^{wild\ type}$		7.9 (± 0.3)	2.7 (± 0.2)	33.1 (± 0.2)	15.0 (± 0.2)	1.3
	residual activity[d]		*34%*		*45%*	
	sulfite stimulation factor[e]		4.2		5.6	
$\alpha_3\beta_3\gamma^{M23+279+282L/C89A}$		2.7 (± 0.3)	2.1 (± 0.1)	26.8 (± 0.4)	23.4 (± 0.2)	1.1
	residual activity[d]		*78%*		*87%*	
	sulfite stimulation factor[e]		9.8		11.0	

4 Discussion

A central element of the study was identification of specific target sites of ROS within CF1CFo. In the course of the project convincing proof was found that oxidation of a group of interacting γ subunit residues was responsible for activity attenuation. Since this markedly conserved cluster of highly ROS-sensitive amino acids is located at a critical position and of functional importance, it is likely that these key residues might serve as a sensor for increasing ROS concentrations within the chloroplast. Thus, affection of ADP/ATP ratio and/or the thylakoid ΔpH might have further implications on the regulation of the photosynthetic machinery in general.

4.1 *In situ* affection of CF1CFo by singlet oxygen

Within minutes, $^1O_2$ has a massive impact on the chloroplast ATP synthase *in situ*. It could be shown that the selected concentrations of RB to generate $^1O_2$ mostly preserved membrane integrity. Therefore, $^1O_2$-dependent loss of ATP-driven thylakoid acidification caused by excessive H^+ leakage could be ruled out. Both, ATP synthesis and hydrolysis by CF1CFo are simultaneously affected. Interestingly, the magnitude of $^1O_2$ impact on ATP hydrolysis and ATP-driven H^+ translocation is dependent on the redox state of regulatory γ-cysteines. The widely accepted model of ATPase activity regulation proposes conformational changes within γ subunit (McCarty and Fagan 1973; Richter 2004; Schumann et al. 1985), the ε subunit (Johnson and McCarty 2002; Richter and McCarty 1987) and among ε and γ subunit (Richter and Gao 1996). A recently modeled structure (Richter et al. 2005) of the regulatory γ subunit segment suggests a compact closed conformation of the inactive/oxidized state compared to the reduced state (Figure 2). Based on these assumptions, three possible conclusions might explain the γ subunit redox state-dependent affection of CF1CFo.

(a) Intra-subunit cross-links could be formed by targeting γH187, thus resulting in loss of CF1CFo activity. At least in spinach and Arabidopsis, γH187 is the only histidine in the γ subunit (Figure 35). Interestingly, a previous mass spectrometric approach revealed $^1O_2$-induced alterations in a peptide fragment between γF176 and γK195, containing γH187 (Mahler et al. 2007). $^1O_2$ preferentially interacts with tyrosine, tryptophan, methionine, cysteine and histidine (Spikes and Knight 1970; Straight and Spikes 1985), whereas histidine has the highest rate constant for an interaction with $^1O_2$ at physiological pH (Davies 2004). Furthermore, $^1O_2$-mediated histidine cross-links with cysteines and lysines are reported (Balasubramanian et al. 1990; Dillon et al. 1993; Guptasarma et al. 1992; Shen et al. 1996a; Shen et al. 1996b; Verweij and Vansteveninck 1982). The histidine-containing fragment habors several lysines (Figure 35) and is directly neighboring the redox regulatory region

(Samra et al. 2006), supposed to be in closer spatial vicinity to γH187 in the compact oxidized conformation (Figure 2D). Thus, intra-subunit histidine-cysteine cross-links could be favoured in the oxidized state, resulting in enhanced activity attenuation.

(b) Alternatively, the "light site" γC89 (Richter and Gao 1996) could serve as a target involved in activity attenuation. It was shown that labelling of this particular residue by bulky maleimides is only accomplished in illuminated thylakoids (Moroney et al. 1980; Nalin et al. 1983). Thus, light-dependent labelling by maleimides implicates structural changes around γC89 upon illumination. It should be noted that light-dependent structural changes within the enzyme coincide with a structural imprint by *in vivo* reduction of the regulatory cysteines via thioredoxin (Dann and McCarty 1992; Mills and Mitchell 1982). Accordingly, the structural imprint of γ-disulfide (Figure 2D) might promote deleterious impact of γC89 oxidation in $CuCl_2$-treated samples.

(c) Polyacrylamide gel electrophoresis of thylakoid protein revealed that $^1O_2$ supposedly directly interacts with the γ subunit. Enzyme activity is regulated by the interaction strength between γ and inhibitory ε subunit (Evron et al. 2000), whereas oxidized CF1 shows lower ATPase due to higher of affinity of γ for the ε subunit (Duhe and Selman 1990; Soteropoulos et al. 1992). However, it could not be excluded that exposure to $^1O_2$ induced an increase of interaction strength between those two subunits, probably via cross-link formation, thus resulting in lower MgATPase. Likewise, cross-linking of γ and ε subunits in *E. coli* F1 results in a loss of ATPase activity (Tsunoda et al. 2001). As a result of tight interactions between γ and ε under oxidized conditions, cross-linking might be favored. This could explain increased susceptibility of oxidized thylakoids. Interestingly, trypsin treatment loosens the interaction at specific positions between ε and γ subunit (Hightower and McCarty 1996; Soteropoulos et al. 1992). In theory, this should impede cross-link formation. Nevertheless, trypsin had no effect on the magnitude of affection by $^1O_2$ in the oxidized state. This contradicted inter-subunit cross-link hypothesis, although spatial range of the affected site(s) might not be changed by trypsin cleavage of the γ subunit at all.

Considerations above mainly focus on the hydrolysis of ATP, a convenient feature to characterize enzyme properties. Instead, CF1CFo primarily acts as an ATP synthase *in vivo*, also affected in thylakoid experiments. A decreased photophosphorylation capacity of chloroplasts upon oxidative stress would potentially alter ADP/ATP ratio in the plant which then could function as a signal. Nevertheless, detailed information of targeted residues is necessary to design *in vivo* study experiments.

4.2 CF1 *in vitro*: Isolation, molecular dissection and affection by singlet oxygen

Pinpointing functional $^1O_2$ targets within the multisubunit thylakoid ATP synthase is aggravated by several facts. Generation of a ΔpH (Ort and Oxborough 1992; Richter and Gao 1996), rotation of certain subunits during catalysis (Richter 2004), and redox-modulation of the regulatory cysteines γC199 and γC205 (Richter et al. 2005), altogether have implications on the structure of the enzyme. Thus, the surrounding environment of putative targets, which is a crucial reaction parameter (Davies 2004; Michaeli and Feitelson 1994; Zhang and Kalonia 2007), is constantly changed. Accordingly, a formerly concealed residue might become a target upon exposure to the surface. Alternatively, structurally flexible residues might react spontaneously with other groups nearby in a $^1O_2$-dependent manner. If affection by $^1O_2$ was dependent on the redox state of the CF1 γ subunit, which is believed to coincide with structural changes (Figure 2), a detailed *in vitro* study is expected to gain additional information of enzyme affection. A sophisticated molecular dissection ruled out subunits that were not involved in oxidative damage.

First of all, the catalytically active CF1 portion was isolated which, as a matter of course, *in vitro* exclusively hydrolyzes ATP (Richter et al. 1984). H^+ translocation, not subject to the following considerations, depends on both portions, CF1 and CFo. The findings ascribe CF1 to be the main target portion. A comparison of enzyme affection *in vitro* and *in situ* should be carefully interpreted. Assuming that accessibility, and thus reactivity, of putative targets is determined by the structure of the enzyme, several distinct parameters are changed when analyzing isolated CF1. Likewise, in isolated CF1 the strain of pmf no longer influences both, nucleotide exchange on the α/β subunit interface and solvent exposure of particular ε and γ subunit regions (Richter and Gao 1996). Limited comparison could be exemplified by controversial findings of the γ subunit redox state with regard to $^1O_2$ impact. In thylakoids, enzyme activity was more affected in oxidized samples, whereas isolated CF1 was more resistant to $^1O_2$ when γ-cysteines were oxidized. It might be that structure-defining conditions, such as pmf and γ subunit redox state, act in concert. Thus, the set of accessible putative $^1O_2$ targets is co-determined by several distinct factors. When analyzing γ subunit redox state-dependent affection in illuminated thylakoids, the pmf parameter contributed to the enzyme response. This parameter, however, has been eliminated when CF1 activity was redox-dependently analyzed *in vitro*. Thus, different sets of targets might become accessible upon γ subunit redox-modulation under both conditions.

The stepwise disassembly of CF1, followed by $^1O_2$-dependent ATPase assays, reinforced initial assumptions that the γ subunit might be a good candidate serving as the main target involved in loss of activity. Due to its asymmetric structure (Abrahams et al. 1994), the rotating γ stalk drives nucleotide exchange by interacting with the β subunit, a process known

as *binding change mechanism* proposed by Boyer (1993). Given that, early enzyme affection by $^1O_2$ would be of biological significance, targeting of the rotating γ subunit should attenuate activity more efficiently than modifying several critical residues on the six nucleotide binding sites on the α and β subunits.

It should be noted that, although no detailed studies on CFo have been performed yet, the membrane-embedded portion is supposed to play a minor role as a target for $^1O_2$, also interacting with lipids (Davies 2004; Girotti and Kriska 2004; Martinez et al. 2003). Coupling of CFo and CF1 during catalytic turnover is accomplished by the N-terminal domain of the CF1 ε subunit (Cingolani and Duncan 2011). In line with a suggested minor role of CFo, the presence of the coupling ε subunit had no implications on activity attenuation of the enzyme *in vitro*. Due to redundancy of the ε subunit in CF1 affection, it is very unlikely that $^1O_2$-induced loss of H^+ translocation was mainly caused by aggravation of coupling efficiency.

4.3 Mapping of putative ROS targets and mass spectrometric analysis of CF1

A very promising outcome of the target mapping approach was the cluster-like orientation of various highly conserved potential amino acid targets of the γ subunit (Figure 24, Figure 25). The overall structure of the rotating γ stalk is very similar in F-ATP synthase enzymes (Gibbons et al. 2000). Alpha-helical elements at the N- and C-terminal end act like a bearing coated by the $\alpha_3\beta_3$ hexamer. The central polypeptide sequence forms a rather globular protruding foot which interacts with the Fo subunit ring. The proposed γ subunit *target cluster* is located at a point of contact between γ and β subunit (Abrahams et al. 1994; Pu and Karplus 2008; Samra et al. 2008), in general referred to as “catch”. Besides of another catch (Abrahams et al. 1994), it is believed that rotational substeps of γ depend on these interactions (Gibbons et al. 2000). As suggested above (section 4.2), targeting of the enzyme during oxidative stress would result in inactivation more efficiently if the rotating γ stalk, rather than nucleotide binding sites, was subject to modifications. Accordingly, the proposed targets would be good candidates to serve as a ROS-sensing element due to their critical location for catalytic turnover. The highly conserved character of the cluster supports the suggested role as a sensory element, since F-ATP synthase, most likely, share a common ancestor (Richter 2004) and ROS co-emerged with oxygenic photosynthesis several billion years ago (Hohmann-Marriott and Blankenship 2011). Finally, it should be noted that methionines in general are very susceptible for a broad range of oxidants (Davies 2005). However, the initially proposed main target for $^1O_2$ impact, γH187 (section 4.1), was not oxidized.

4.4 The hybrid F1: Mutant characterization of catalytic properties

The results of the methionine-cluster mutants presented in the sulfite stimulation approach are in good agreement with earlier studies describing MgATPase activation by detergent-stimulated MgADP release in TF1 $\alpha_3\beta_3\gamma$ from the thermophilic *Bacillus* PS3. Therein, methionines, that are homologous to spinach CF1 γM23 and γM282, were substituted for cysteine or lysine (Bandyopadhyay and Allison 2004). Similarly, a study of *Rhodobacter capsulatus* F1 (Feniouk et al. 2007) proposes stabilization of the ADP-inhibited state of the enzyme by γM23K.

Recent γ subunit cross-linking studies nearby (Samra et al. 2008) and within the methionine-cluster (Bandyopadhyay and Allison 2004) suggest that there are no large-scale movements between the terminal γ subunit alpha-helices during rotation in the ATP hydrolysis direction. Concomitantly, the integrity of this helical γ-region is supposed to be crucial for ADP release during rotation (Bandyopadhyay and Allison 2004; Feniouk et al. 2007; Samra et al. 2008; Sun et al. 2004) because it is part of a β-γ contact point (Abrahams et al. 1994; Pu and Karplus 2008; Samra et al. 2008). There are alternative explanations for deviations of β-γ interactions in the mutants, suggesting that electrostatic (Al-Shawi et al. 1997; Feniouk et al. 2007; Ketchum et al. 1998) or hydrophobic (Bandyopadhyay and Allison 2004) parameters likely play a role. By substituting leucine for methionine and alanine for cysteine, the hydrophobic character of the cluster was preserved to a certain extent. According to the results presented here, hydrophobicity of the corresponding γ-residues seemed to play a minor role in adjusting the *binding change mechanism*.

Regardless of proposed γ subunit redox-modulated structural changes, integrity of the highly conserved cluster of amino acids was essential. Probably, these amino acids somehow forwarded the information produced by redox-regulation since the remote cluster is not part of the disulfide-containing domain (Figure 2, Figure 38). Nevertheless, the observations on γ disulfide redox-modulation did not take account of the ε subunit which is also considered to regulate activity (Richter 2004). Furthermore, it should be emphasized that observed activities did not allow prediction of membrane-attached enzyme characteristics. It should be mentioned that initial activity rates of hybrid F1 assayed in the ROS tolerance approach (section 3.6, 3.7) were similar to MgATPase after $CuCl_2$ treatment (not shown) suggesting that assembly procedure yielded oxidized regulatory γ-cysteines.

Summarizing characterization of general catalytic mutant features, it turned out that (a) the introduced amino acid substitutions had the potential to influence remote dynamic interactions during catalytic turnover. Especially cluster methionines located in the terminal alpha-helices of the γ subunit (Figure 24C) seemed to be involved in *binding change*

mechanism. (b) Additionally, the cluster appeared to be a set of highly dynamic interacting residues and the effect of certain substitutions was obviously dominant over others. Similarly, in an earlier study the interaction between these particular alpha-helical regions of *E. coli* F1 γ subunit has been described (Nakamoto et al. 1993) and showed recovery of energy coupling in the deficient γM23K mutant by introducing a γR242C second-site mutation, which is the homolog to spinach γR278.

4.5 The hybrid F1: MgATPase upon exposure to singlet oxygen

It is challenging to establish a connection between the potential role of F-ATP synthase in maintaining ROS homeostasis (Houstek et al. 2006; Kanazawa and Kramer 2002) and its concurrent susceptibility, as shown above (section 3.1). Unlike previous experiments analyzing nitrative stress (Fujisawa et al. 2009; Haynes et al. 2010), susceptibility of F-ATPase caused by ROS could not be linked to any specific targets. However, recent studies of fungal mitochondrial F1 identified a defined tryptophan on the α subunit as a functional ROS target (Rexroth et al. 2012). The approach made in section 3.6 revealed that (1) all of the mutants tested still showed significant activity attenuation upon $^1O_2$ exposure, and (2) that this effect is mainly dependent on the oxidation of a defined methionine-cysteine cluster. (3) This cluster appeared as a group of mutually dependent residues. Therefore it is difficult to pinpoint single targets playing a defined role in the reaction. Instead, the cluster should be regarded as a whole. Accordingly, three possible conclusions could be drawn to interpret the results in Figure 39.

(a) Changing the cluster by partial mutation might cause altered catalytic impact upon oxidation. Hence, increased sensitivity in γC89A could be observed. Likewise, formerly tolerant γM23L was not persistent in γM23+279+282L because of enhanced deleterious impact of the latter oxidized disrupted *target cluster*.

(b) Enduring susceptibility of γM23+279+282L/γC89A strongly demanded for existence of functional targets remote of the suggested cluster. In fact, amino acid oxidations within the other CF1 subunits were observed as well, e.g. CF1 βY362 (Figure 31A) and CF1 βH384/βY385 (Figure 32A). The two tyrosines, which correspond to bovine MF1 βY345 and βY368, are residues of the catalytic and non-catalytic nucleotide binding site, respectively (Cross et al. 1987). However, substitutions of non-target phenylalanines (and glutamine) for the homologous RrF1 β-tyrosines (and β-histidine) did not result in altered $^1O_2$ susceptibility of the corresponding hybrid F1 assemblies. Recently, it was shown that both β-tyrosines are the primary targets responsible for nitrative stress susceptibility, whereas γ-methionine modification was not detected (Fujisawa et al. 2009; Haynes et al. 2010). The challenge of

identifying yet unknown functional targets is aggravated since oxidation of a residue can also occur spontaneously and without affecting enzyme functionality (Levine et al. 1999; Walsh et al. 1978). Thus, it cannot be ruled out that, for instance, γM95 might be highly susceptible towards spontaneous oxidation but without effect, since absence of γM95 did not alter enzyme functionality upon oxidation.

(c) The cluster region appears to be critical for general enzyme functionality. Therefore, the introduced mutations might have the potential to affect other and remote functional structures (section 4.4). Accordingly, it cannot be ruled out that concealed potential $^1O_2$ target residues were experimentally changed to functional $^1O_2$ targets. Theoretically, this would challenge conclusion (a) by implying that cluster residues themselves are supposedly "concealed" in the wild type and only become "functional" in disrupted cluster mutants. Nevertheless, every single cluster residue was specifically oxidized upon $^1O_2$ treatment (section 3.3.2) and modified experimental conditions at lower pH undermine theoretical restrictions of concealed targets within the cluster itself. Taking this into consideration, overlapping of both conclusions still cannot be excluded. Candidates which might serve as new functional ROS targets could be highly reactive histidines within the enzyme. Several observations supported this assumption. Suggesting this particular amino acid, advantage was taken that histidine reacts much slower at non-physiological lower pH (Bisby et al. 1999; Davies 2003; Heldt et al. 1973). Accordingly, lowering histidine reactivity at pH 6 in hybrid F1 wild type did not alter susceptibility. Thus, new functional targets were revealed while analyzing the mutants. Likewise, γM23L, considerably more tolerant under both conditions, was less efficient in functionalizing targets since almost no pH-dependent effect was observed. In γC89A, lowering reactivity of new targets at pH 6 could explain the observed gain of tolerance. Dominant mutations of C-terminal γM279 and γM282 were supposedly most efficient in manifesting histidine targets. Thus, enzymes harboring these mutations showed the largest pH-dependent sensitivity.

4.6 The hybrid F1: MgATPase upon exposure to hydrogen peroxide

Recently (Triantaphylides et al. 2008), $^1O_2$ was considered the most potent ROS involved in photo-oxidative damage in plants, whereas its reactivity with proteins is not fully understood yet (Davies 2003; Wardman and Vonsonntag 1995; Wright et al. 2002). Compared to $^1O_2$, the interaction of H_2O_2 with proteins is less versatile since it reacts with cysteines and methionines only, thus serving as a poor oxidant (Imlay 2003). The initially proposed existence of a ROS-sensitive γ subunit amino acid cluster was clearly validated in the H_2O_2 approach. Indications were provided that slight initial activation was caused by oxidation processes remote from the ROS *target cluster*. Physiological relevance of slight activation

remains elusive. For the first time, notably ROS-tolerant ATP synthase could be designed. The remarkably straightforward set of targets within the rotary stalk of this key bioenergetic enzyme is intriguing. Supporting mechanical deliberations above (section 4.2), efficient affection is rather accomplished by evolutionary placement of a rotating ROS-sensory element than ROS-modifiable nucleotide binding site residues. In the course of my project I realized how much work has been done already to unravel energy coupling between ATP hydrolysis and H^+ translocation. Especially the Futai laboratory published several ground-breaking mutant studies on EcF1 γM23 (reviewed in Futai 2006), which is considered to play a crucial role in energy coupling. Based on these findings, coupling effects were analyzed in various F-ATP synthase systems using partially homologous mutants to the constructs I analyzed. However, ROS have never been attributed to these highly conserved critical γ-residues before. Coincidentally, particular indications of $^1O_2$-induced uncoupling were observed at the beginning of the project (section 3.1.4) when no further information of specific targets was available yet. Taking account of other recent findings (Fujisawa et al. 2009; Haynes et al. 2010), there is growing interest in post-translational modifications of F-ATP synthase.

Regardless of yet unknown targets, it should be noted that the ultimate fate of ROS exposure was a loss of enzyme activity. On the other hand, the aftereffects of amino acid oxidations within a disrupted cluster seemed to be different, depending on the ROS applied. Especially absence of γM23 and γC89 during oxidative enzyme modification resulted in inverted responses upon $^1O_2$ and H_2O_2 stress (Figure 39C, Figure 41A) which could be explained by proposed conclusions (section 4.5). According to the suggestions above, ROS-specific reactivity of formerly concealed targets caused inverted responses. Additionally, ROS-specific impact of a γM23- and γC89-disrupted cluster on catalytic activity could also be considered. In this context it should be noted that among the mutants tested, sulfite-stimulated MgATPase by γM23L and γC89A enzymes was most similar to wild type (Table 9).

4.7 The hybrid F1: MgADP binding propensity upon exposure to ROS

The critical location of the cluster (Figure 35C), its involvement in dynamic wide-ranging interactions within the enzyme (Table 8, Table 9) and its susceptibility to ROS (Figure 27, Figure 28, Figure 33, Figure 34) were clearly evident. Although methionine sulfoxide is more hydrophilic than methionine (Davies 2005) and some authors consider hydrophobicity of the cluster region to be involved in MgADP release (Bandyopadhyay and Allison 2004), no enhanced propensity to entrap inhibitory MgADP upon ROS exposure could be observed.

4.8 Perspective

For the first time, indications are provided that this key bioenergetic enzyme was adapted to emerging ROS by evolving a readily modifiable set of F1 γ subunit targets. The outcome strongly demands for sophisticated *in vivo* studies, such as initially mentioned NPQ analysis of plants expressing ROS-tolerant chloroplast ATP synthase (section 1.3). By choosing an appropriate light/temperature regime to generate ROS, comparative NPQ analysis could be carried out. Assuming that ATP synthase serves as a ROS-modifiable element *in vivo*, affection would alter $g H^+$ of thylakoid membranes. Thus, under these conditions ROS-tolerant mutants are not supposed to display protective NPQ rates as the wild type. Other proposed *in vivo* studies are based on the assumption that oxidative affection of the enzyme alters ADP/ATP ratio. Since ROS act as a signal and extensive analysis on gene regulation has been carried out (Glaeser et al. 2011; Kim et al. 2008a; Laloi et al. 2007; Neill et al. 2002), it would be tempting to speculate if several genes are expressed differently in presence of a ROS-tolerant ATP synthase. At least in plants, certain genes are regulated by the level of ATP or ADP. For instance, transcription of genes encoding for the D1 and D2 protein of PSII is mediated by ADP-dependent phosphorylation (Danon and Mayfield 1994; Kim et al. 1999). These experiments might ascribe ROS-susceptible ATP synthase to a regulatory element which contributes to environmental responses under oxidative stress.

Initial *in vivo* experiments should be carried out in prokaryotic model systems first. These studies could back up the suggested general concept that F1 γ subunit harbors a highly conserved ROS-sensing element. Furthermore, extensive mutant coupling analysis of ATP hydrolysis and H^+ translocation could be carried out efficiently. In general, re-investigation of the mutants in bacteria could eliminate potential artifacts of the hybrid F1 assembly system. The hybrid F1 is a suitable rapid system for broad range mutant analysis but the assemblies were suggested to contain fewer contacts between γ subunit and the $\alpha_3\beta_3$ hexamer (He et al. 2008).

Suggesting yet elusive details on the molecular mechanism of ROS impact, disturbance of subunit cooperativity apart from nucleotide binding (section 3.8) might play a role. Additional mutations apart from ROS *target cluster* residues could help to unravel further details. It was described that methionine sulfoxide formation in alpha-helical regions of proteins can have helix-breaking effects (Bigelow and Squier 2005). Assuming that this might be the case at least for spinach CF1 γM279 and γM282, C-terminal γ subunit catch interactions with an anionic loop of the β subunit could be perturbed (Greene and Frasch 2003). In line with this suggestion, hybrid F1 studies of CF1 γ subunit mutants in this region showed loss of MgATPase (He et al. 2007). Apart from other potential impacts of helix-breaking events, steric clashes might also result directly from oxidized methionines. A particular β-γ contact is

formed by residues of and around the γ subunit ROS *target cluster* (Abrahams et al. 1994). ROS-induced γ subunit modifications could dramatically interfere with subunit cooperativity during rotation at this catch region (Mnatsakanyan et al. 2009). It is believed that the catch assists in closing catalytic sites upon nucleotide binding at the α/β interface. Assistance is accomplished by catch interaction with an acidic sequence in the C-terminal domain of the β subunit, termed DELSEED motif according to its amino acid sequence. However, the DELSEED motif is not essential for activity (Hara et al. 2000) and corresponding mutants could provide additional information regarding enzyme affection by ROS.

Aberration of higher plant redox-regulation of the enzyme (section 3.5.2) might be a potential drawback when designing *in planta* studies with current γ subunit constructs. Although physiological relevance is still a matter for debate, Arabidopsis redox-regulation mutants are detrimental to photosynthesis and growth under low light conditions (Wu et al. 2007). Again, second-site mutations could overcome aberration of redox-regulation. Similarly, energy coupling, which demands complex subunit cooperativity, was reported to be recoverd by second-site mutations in the γ subunit (Nakamoto et al. 1993).

5 Abbreviations

abbreviation	name
ΔpH	transmembrane H^+ gradient
$^1O_2$	singlet oxygen
$^3O_2$	triplet oxygen (i.e. molecular ground state of oxygen)
9-AA	9-aminoacridine
ACMA	9-amino-6-chloro-2-methoxyacridine
ADP	adenosine 5'-(trihydrogen diphosphate)
ATP	Adenosine-5'-triphosphate
cDNA	complementary deoxyribonucleic acid
CDS	protein coding sequence
CF1	chloroplast F1
CFo	chloroplast Fo
Chl	chlorophyll
DCMU	3-(3,4-dichlorophenyl)-1,1-dimethylurea
DTT	dithiothreitol
E. coli	*Escherichia coli*
EcF1	*E. coli* F1
EDTA	2,2',2'',2'''-(Ethane-1,2-diyldinitrilo)tetraacetic acid
F1	coupling factor-1, first identified particle that restored oxidative phosphorylation
Fo	coupling factor-o, insoluble F1-binding factor sensitive to antibiotic oligomycin
gH^+	proton efflux conductance of the thylakoid membrane
H_2O_2	hydrogen peroxide
HPLC	high performance liquid chromatography
hybrid F1	recombinant photosynthetic F1 of RrF1 $\alpha_3\beta_3$ and *Spinacia oleracea* CF1 γ subunit
IPTG	Isopropyl β-D-1-thiogalactopyranoside
MES	2-(N-morpholino)-ethanesulfonic acid
MF1	mitochondrial F1
NPQ	non-photochemical quenching
$O_2^{\bullet-}$	superoxide
$OH^{\bullet}$	hydroxyl radical
OSCP	Oligomycin sensitivity-conferring protein
PCR	polymerase chain reaction
Pi	hydrated inorganic phosphate
pmf	proton motive force
PSI, PSII	photosystem I, photosystem II
RB	Rose Bengal
ROS	reactive oxygen species
RNO	*p*-nitrosodimethylaniline
RuBisCO	Ribulose-1,5-bisphosphate carboxylase oxygenase
RrF1	*Rhodospirillum rubrum* F1
SD	standard deviation
SE	standard error
spinach	*Spinacia oleracea*
TCA	trichloroacetic acid
TF1	F1 from thermophilic *Bacillus* PS3
Tricine	N-(2-Hydroxy-1,1-bis(hydroxymethyl) ethyl) glycine
Tris	2-Amino-2-hydroxymethyl-propane-1,3-diol
v/v	volume per volume

6 References

Abrahams, J.P., Leslie, A.G., Lutter, R. and Walker, J.E. (1994) Structure at 2.8 A resolution of F1-ATPase from bovine heart mitochondria. *Nature* 370: 621-628.

Adam-Vizi, V. and Chinopoulos, C. (2006) Bioenergetics and the formation of mitochondrial reactive oxygen species. *Trends Pharmacol Sci* 27: 639-645.

Al-Shawi, M.K., Ketchum, C.J. and Nakamoto, R.K. (1997) Energy coupling, turnover, and stability of the FoF1 ATP synthase are dependent on the energy of interaction between γ and β subunits. *J Biol Chem* 272: 2300-2306.

Apel, K. and Hirt, H. (2004) Reactive oxygen species: Metabolism, oxidative stress, and signal transduction. *Annu Rev Plant Biol* 55: 373-399.

Arnon, D.I. (1949) Copper enzymes in isolated chloroplasts. Polyphenoloxidase in *Beta vulgaris*. *Plant Physiol* 24: 1-15.

Bakker-Grunwald, T. and van Dam, K. (1973) The energy level associated with the light-triggered Mg 2+ -dependent ATPase in spinach chloroplasts. *Biochim Biophys Acta* 292: 808-814.

Balasubramanian, D., Du, X. and Zigler, J.S. (1990) The reaction of singlet oxygen with proteins, with special reference to crystallins. *Photochem Photobiol* 52: 761-768.

Bandyopadhyay, S. and Allison, W.S. (2004) γM23K, γM232K, and γL77K single substitutions in the TF1-ATPase lower ATPase activity by disrupting a cluster of hydrophobic side chains. *Biochemistry* 43: 9495-9501.

Bienert, G.P., Schjoerring, J.K. and Jahn, T.P. (2006) Membrane transport of hydrogen peroxide. *Biochim Biophys Acta* 1758: 994-1003.

Bigelow, D.J. and Squier, T.C. (2005) Redox modulation of cellular signaling and metabolism through reversible oxidation of methionine sensors in calcium regulatory proteins. *Biochim Biophys Acta* 1703: 121-134.

Bisby, R.H., Morgan, C.G., Hamblett, I. and Gorman, A.A. (1999) Quenching of singlet oxygen by Trolox C, ascorbate, and amino acids: Effects of pH and temperature. *Journal of Physical Chemistry A* 103: 7454-7459.

Boyer, P.D. (1993) The binding change mechanism for ATP synthase - some probabilities and possibilities. *Biochim Biophys Acta* 1140: 215-250.

Bradford, M.M. (1976) Rapid and sensitive method for quantitation of microgram quantities of protein utilizing principle of protein-dye binding. *Analytical Biochemistry* 72: 248-254.

Bratt, C.E., Arvidsson, P.O., Carlsson, M. and Akerlund, H.E. (1995) Regulation of violaxanthin de-epoxidase activity by pH and ascorbate concentration. *Photosynth Res* 45: 169-175.

Cadenas, E. (1989) Biochemistry of oxygen toxicity. *Annu Rev Biochem* 58: 79-110.

Cingolani, G. and Duncan, T.M. (2011) Structure of the ATP synthase catalytic complex F1 from *Escherichia coli* in an autoinhibited conformation. *Nat Struct Mol Biol* 18: 701-707.

Cross, R.L., Cunningham, D., Miller, C.G., Xue, Z.X., Zhou, J.M. and Boyer, P.D. (1987) Adenine-nucleotide binding-sites on beef-heart F1 ATPase - Photoaffinity-labeling of β subunit Tyr-368 at a noncatalytic site and β Tyr-345 at a catalytic site. *Proc Natl Acad Sci U S A* 84: 5715-5719.

Cruz, J.A., Harfe, B., Radkowski, C.A., Dann, M.S. and McCarty, R.E. (1995) Molecular dissection of the ε subunit of the chloroplast ATP synthase of spinach. *Plant Physiol* 109: 1379-1388.

Dann, M.S. and McCarty, R.E. (1992) Characterization of the activation of membrane-bound and soluble CF1 by thioredoxin. *Plant Physiol* 99: 153-160.

Danon, A. and Mayfield, S.P. (1994) ADP-dependent phosphorylation regulates RNA-binding in vitro: implications in light-modulated translation. *EMBO J* 13: 2227-2235.

Davenport, J.W. and McCarty, R.E. (1984) An analysis of proton fluxes coupled to electron transport and ATP synthesis in chloroplast thylakoids *Biochim Biophys Acta* 766: 363-374.

Davies, M.J. (2003) Singlet oxygen-mediated damage to proteins and its consequences. *Biochem Bioph Res Co* 305: 761-770.

Davies, M.J. (2004) Reactive species formed on proteins exposed to singlet oxygen. *Photochem Photobiol Sci* 3: 17-25.

Davies, M.J. (2005) The oxidative environment and protein damage. *Biochim Biophys Acta* 1703: 93-109.

DeLano, W.L. and Lam, J.W. (2005) PyMOL: A communications tool for computational models. *Abstr Pap Am Chem S* 230: U1371-U1372.

Demmig-Adams, B. and Adams, W.W. (1992) Photoprotection and other responses of plants to high light stress. *Annu Rev Plant Physiol Plant Mol Biol* 43: 599-626.

DeRosa, M.C. and Crutchley, R.J. (2002) Photosensitized singlet oxygen and its applications *Coordination Chemistry Reviews* 233-234: 351-371.

Digel, J.G., Kishinevsky, A., Ong, A.M. and McCarty, R.E. (1996) Differences between two tight ADP binding sites of the chloroplast coupling factor-1 and their effects on ATPase activity. *J Biol Chem* 271: 19976-19982.

Digel, J.G., Moore, N.D. and McCarty, R.E. (1998) Influence of divalent cations on nucleotide exchange and ATPase activity of chloroplast coupling factor-1. *Biochemistry* 37: 17209-17215.

Dillon, J., Chiesa, R., Wang, R.H. and Mcdermott, M. (1993) Molecular changes during the photooxidation of alpha-crystallin in the presence of uroporphyrin. *Photochem Photobiol* 57: 526-530.

Dismukes, G.C., Klimov, V.V., Baranov, S.V., Kozlov, Y.N., DasGupta, J. and Tyryshkin, A. (2001) The origin of atmospheric oxygen on Earth: the innovation of oxygenic photosynthesis. *Proc Natl Acad Sci U S A* 98: 2170-2175.

Dowling, D.K. and Simmons, L.W. (2009) Reactive oxygen species as universal constraints in life-history evolution. *Proc Biol Sci* 276: 1737-1745.

Drummond, A.J., Ashton, B., Buxton, S., Cheung, M., Cooper, A., et al. (2011) Geneious v5.4, Available from http://www.geneious.com/.

Du, Z.Y. and Boyer, P.D. (1990) On the mechanism of sulfite activation of chloroplast thylakoid ATPase and the relation of ADP tightly bound at a catalytic site to the binding change mechanism. *Biochemistry* 29: 402-407.

Duhe, R.J. and Selman, B.R. (1990) The dithiothreitol-stimulated dissociation of the chloroplast coupling factor-1 ε subunit is reversible. *Biochim Biophys Acta* 1017: 70-78.

Evron, Y., Johnson, E.A. and McCarty, R.E. (2000) Regulation of proton flow and ATP synthesis in chloroplasts. *J Bioenerg Biomembr* 32: 501-506.

Evron, Y. and McCarty, R.E. (2000) Simultaneous measurement of ΔpH and electron transport in chloroplast thylakoids by 9-aminoacridine fluorescence. *Plant Physiol* 124: 407-414.

Evron, Y. and Pick, U. (1997) Modification of sulfhydryl groups in the γ subunit of chloroplast coupling factor-1 affects the proton slip through the ATP synthase. *Plant Physiol* 115: 1549-1555.

Feniouk, B.A., Rebeechi, A., Giovannini, D., Anefors, S., Mulkidjanian, A.Y., Junge, W., Tunina, P. and Melandri, A. (2007) Met23Lys mutation in subunit γ of FoF1-ATP synthase from *Rhodobacter capsulatus* impairs the activation of ATP hydrolysis by proton motive force. *Biochim Biophys Acta* 1767: 1319-1330.

Fischer, B.B., Krieger-Liszkay, A., Hideg, E., Snyrychova, I., Wiesendanger, M. and Eggen, R.I. (2007) Role of singlet oxygen in chloroplast to nucleus retrograde signaling in *Chlamydomonas reinhardtii*. *FEBS Lett* 581: 5555-5560.

Fujisawa, Y., Kato, K. and Giulivi, C. (2009) Nitration of tyrosine residues 368 and 345 in the β subunit elicits FoF1-ATPase activity loss. *Biochem J* 423: 219-231.

Futai, M. (2006) Our research on proton pumping ATPases over three decades: Their biochemistry, molecular biology and cell biology. *P Jpn Acad B-Phys* 82: 416-438.

Gao, F., Lipscomb, B., Wu, I.M. and Richter, M.L. (1995) *In vitro* assembly of the core catalytic complex of the chloroplast ATP synthase. *J Biol Chem* 270: 9763-9769.

Gibbons, C., Montgomery, M.G., Leslie, A.G.W. and Walker, J.E. (2000) The structure of the central stalk in bovine F-1-ATPase at 2.4 angstrom resolution. *Nat Struct Biol* 7: 1055-1061.

Girault, G., Berger, G., Galmiche, J.M. and Andre, F. (1988) Characterization of 6 nucleotide-binding sites on chloroplast coupling factor-1 and one site on its purified β subunit. *J Biol Chem* 263: 14690-14695.

Girotti, A.W. and Kriska, T. (2004) Role of lipid hydroperoxides in photo-oxidative stress signaling. *Antioxid.Redox Signal.* 6: 301-310.

Glaeser, J., Nuss, A.M., Berghoff, B.A. and Klug, G. (2011) Singlet oxygen stress in microorganisms. *Adv Microb Physiol* 58: 141-173.

Gomis-Ruth, F.X., Moncalian, G., Perez-Luque, R., Gonzalez, A., Cabezon, E., de la Cruz, F. and Coll, M. (2001) The bacterial conjugation protein TrwB resembles ring helicases and F1-ATPase. *Nature* 409: 637-641.

Gräber, P., Schlödder, E. and Witt, H.T. (1977) Conformational change of the chloroplast ATPase induced by a transmembrane electric field and its correlation to phosphorylation. *Biochim Biophys Acta* 461: 426-440.

Greene, M.D. and Frasch, W.D. (2003) Interactions among γR268, γQ269, and the β subunit catch loop of *Escherichia coli* F1-ATPase are important for catalytic activity. *J Biol Chem* 278: 51594-51598.

Groth, G. and Pohl, E. (2001) The structure of the chloroplast F1-ATPase at 3.2 angstrom resolution. *J Biol Chem* 276: 1345-1352.

Groth, G. and Strotmann, H. (1999) New results about structure, function and regulation of the chloroplast ATP synthase (CFoCF1). *Physiol Plant* 106: 142-148.

Guptasarma, P., Balasubramanian, D., Matsugo, S. and Saito, I. (1992) Hydroxyl radical mediated damage to proteins, with special reference to the crystallins. *Biochemistry* 31: 4296-4303.

Hangarter, R.P., Jones, R.W., Ort, D.R. and Whitmarsh, J. (1987) Stoichiometries and energetics of proton translocation coupled to electron-transport in chloroplasts. *Biochim Biophys Acta* 890: 106-115.

Hara, K.Y., Noji, H., Bald, D., Yasuda, R., Kinosita, K. and Yoshida, M. (2000) The role of the DELSEED motif of the β subunit in rotation of F1-ATPase. *J Biol Chem* 275: 14260-14263.

Haynes, V., Traaseth, N.J., Elfering, S., Fujisawa, Y. and Giulivi, C. (2010) Nitration of specific tyrosines in FoF1 ATP synthase and activity loss in aging. *American journal of physiology. Endocrinology and metabolism* 298: E978-987.

He, F., Samra, H.S., Johnson, E.A., Degner, N.R., McCarty, R.E. and Richter, M.L. (2008) C-Terminal mutations in the chloroplast ATP synthase γ subunit impair ATP synthesis and stimulate ATP hydrolysis. *Biochemistry* 47: 836-844.

He, F., Samra, H.S., Tucker, W.C., Mayans, D.R., Hoang, E., Gromet-Elhanan, Z., Berrie, C.L. and Richter, M.L. (2007) Mutations within the C-terminus of the gamma subunit of the photosynthetic F-1-ATPase activate MgATP hydrolysis and attenuate the stimulatory oxyanion effect. *Biochemistry* 46: 2411-2418.

Heldt, H.W., Werdan, K., Milovanc.M and Geller, G. (1973) Alkalization of chloroplast stroma caused by light-dependent proton flux into thylakoid space. *Biochim Biophys Acta* 314: 224-241.

Hightower, K.E. and McCarty, R.E. (1996) Proteolytic cleavage within a regulatory region of the γ subunit of chloroplast coupling factor-1. *Biochemistry* 35: 4846-4851.

Hohmann-Marriott, M.F. and Blankenship, R.E. (2011) Evolution of photosynthesis. *Annu Rev Plant Biol* 62: 515-548.

Houstek, J., Pickova, A., Vojtiskova, A., Mracek, T., Pecina, P. and Jesina, P. (2006) Mitochondrial diseases and genetic defects of ATP synthase. *Biochim Biophys Acta* 1757: 1400-1405.

Imlay, J.A. (2003) Pathways of oxidative damage. *Annu Rev Microbiol* 57: 395-418.

Johnson, E.A. and McCarty, R.E. (2002) The carboxyl terminus of the ε subunit of the chloroplast ATP synthase is exposed during illumination. *Biochemistry* 41: 2446-2451.

Junge, W. (1970) The critical electric potential difference for photophosphorylation. Its relation to the chemiosmotic hypothesis and to the triggering requirements of the ATPase system. *Eur J Biochem* 14: 582-592.

Kamienietzky, A. and Nelson, N. (1975) Preparation and properties of chloroplasts depleted of chloroplast coupling factor-1 by sodium bromide treatment. *Plant Physiol* 55: 282-287.

Kanazawa, A. and Kramer, D.M. (2002) *In vivo* modulation of nonphotochemical exciton quenching (NPQ) by regulation of the chloroplast ATP synthase. *Proc Natl Acad Sci U S A* 99: 12789-12794.

Kato-Yamada, Y., Noji, H., Yasuda, R., Kinosita, K., Jr. and Yoshida, M. (1998) Direct observation of the rotation of ε subunit in F1-ATPase. *J Biol Chem* 273: 19375-19377.

Ketchum, C.J., Al-Shawi, M.K. and Nakamoto, R.K. (1998) Intergenic suppression of the γM23K uncoupling mutation in FoF1 ATP synthase by βGlu-381 substitutions: the role of the β380DELSEED386 segment in energy coupling. *Biochem J* 330: 707-712.

Kim, C., Meskauskiene, R., Apel, K. and Laloi, C. (2008a) No single way to understand singlet oxygen signalling in plants. *EMBO Rep* 9: 435-439.

Kim, J., Rodriguez, M.E., Guo, M., Kenney, M.E., Oleinick, N.L. and Anderson, V.E. (2008b) Oxidative modification of cytochrome c by singlet oxygen. *Free Radical Biology and Medicine* 44: 1700-1711.

Kim, M., Christopher, D.A. and Mullet, J.E. (1999) ADP-Dependent phosphorylation regulates association of a DNA-binding complex with the barley chloroplast psbD blue-light-responsive promoter. *Plant Physiol* 119: 663-670.

Laloi, C., Stachowiak, M., Pers-Kamczyc, E., Warzych, E., Murgia, I. and Apel, K. (2007) Cross-talk between singlet oxygen- and hydrogen peroxide-dependent signaling of stress responses in Arabidopsis thaliana. *Proc Natl Acad Sci U S A* 104: 672-677.

Larkin, M.A., Blackshields, G., Brown, N.P., Chenna, R., McGettigan, P.A., et al. (2007) Clustal W and clustal X version 2.0. *Bioinformatics* 23: 2947-2948.

Levine, R.L., Berlett, B.S., Moskovitz, J., Mosoni, L. and Stadtman, E.R. (1999) Methionine residues may protect proteins from critical oxidative damage. *Mechanisms of Ageing and Development* 107: 323-332.

Lin, T.Y. and Wu, C.H. (2005) Activation of hydrogen peroxide in copper(II)/amino acid/H_2O_2 systems: effects of pH and copper speciation. *J Catal* 232: 117-126.

Mahler, H., Wuennenberg, P., Linder, M., Przybyla, D., Zoerb, C., Landgraf, F. and Forreiter, C. (2007) Singlet oxygen affects the activity of the thylakoid ATP synthase and has a strong impact on its γ subunit. *Planta* 225: 1073-1083.

Malyan, A.N. (1981) Chloroplasts ATPase CF1 - Allosteric regulation by ADP and Mg^{2+} ions. *Photosynthetica* 15: 474-483.

Martinez, G.R., Loureiro, A.P., Marques, S.A., Miyamoto, S., Yamaguchi, L.F., Onuki, J., Almeida, E.A., Garcia, C.C., Barbosa, L.F., Medeiros, M.H. and Di Mascio, P. (2003) Oxidative and alkylating damage in DNA. *Mutat.Res.* 544: 115-127.

McCallum, J.R. and McCarty, R.E. (2007) Proton flux through the chloroplast ATP synthase is altered by cleavage of its γ subunit. *Biochim Biophys Acta* 1767: 974-979.

McCarty, R.E. (2005) ATP synthase of chloroplast thylakoid membranes: a more in depth characterization of its ATPase activity. *J Bioenerg Biomembr* 37: 289-297.

McCarty, R.E. (2006) The decay of the ATPase activity of light plus thiol-activated thylakoid membranes in the dark. *J Bioenerg Biomembr* 38: 67-74.

McCarty, R.E., Evron, Y. and Johnson, E.A. (2000) The Chloroplast ATP synthase: A rotary enzyme? *Annu Rev Plant Physiol Plant Mol Biol* 51: 83-109.

McCarty, R.E. and Fagan, J. (1973) Light-stimulated incorporation of N-ethylmaleimide into coupling factor-1 in spinach chloroplasts. *Biochemistry* 12: 1503-1507.

Michaeli, A. and Feitelson, J. (1994) Reactivity of singlet oxygen toward amino acids and peptides. *Photochem Photobiol* 59: 284-289.

Miller, B.L., Kuczera, K. and Schoneich, C. (1998) One-electron photooxidation of N-methionyl peptides. Mechanism of sulfoxide and azasulfonium diastereomer formation through reaction of sulfide radical cation complexes with oxygen or superoxide. *Journal of the American Chemical Society* 120: 3345-3356.

Mills, J.D. and Mitchell, P. (1982) Modulation of coupling factor ATPase activity in intact chloroplasts - Reversal of thiol modulation in the dark. *Biochim Biophys Acta* 679: 75-83.

Mills, J.D., Ort, D.R. and Yocum, C.F. (1996) The regulation of chloroplast ATP synthase, CFoCF1. In *Oxygenic Photosynthesis: The Light Reactions (Advances in Photosynthesis)* pp. 469-485. Kluwer, Dordrecht/Boston/London.

Mittler, R. (2002) Oxidative stress, antioxidants and stress tolerance. *Trends Plant Sci* 7: 405-410.

Mnatsakanyan, N., Krishnakumar, A.M., Suzuki, T. and Weber, J. (2009) The role of the βDELSEED-loop of ATP synthase. *J Biol Chem* 284: 11336-11345.

Moroney, J.V., Andreo, C.S., Vallejos, R.H. and McCarty, R.E. (1980) Uncoupling and energy transfer inhibition of photophosphorylation by sulfhydryl reagents. *J Biol Chem* 255: 6670-6674.

Mulkidjanian, A.Y., Makarova, K.S., Galperin, M.Y. and Koonin, E.V. (2007) Inventing the dynamo machine: the evolution of the F-type and V-type ATPases. *Nature reviews. Microbiology* 5: 892-899.

Muller, P., Li, X.P. and Niyogi, K.K. (2001) Non-photochemical quenching. A response to excess light energy. *Plant Physiol* 125: 1558-1566.

Murataliev, M.B. and Boyer, P.D. (1994) Interaction of mitochondrial F1-ATPase with trinitrophenyl derivatives of ATP and ADP - Participation of 3rd catalytic site and role of Mg^{2+} in enzyme inactivation. *J Biol Chem* 269: 15431-15439.

Nakamoto, R.K., Maeda, M. and Futai, M. (1993) The γ subunit of the *Escherichia coli* ATP synthase - Mutations in the carboxyl-terminal region restore energy coupling to the amino-terminal mutant γMet-23-Lys. *J Biol Chem* 268: 867-872.

Nakamoto, R.K., Shin, K., Iwamoto, A., Omote, H., Maeda, M. and Futai, M. (1992) *Escherichia coli* FoF1-ATPase - Residues involved in catalysis and coupling. *Ann Ny Acad Sci* 671: 335-344.

Nalin, C.M., Beliveau, R. and McCarty, R.E. (1983) Selective modification of coupling factor-1 in spinach chloroplast thylakoids by a fluorescent maleimide. *J Biol Chem* 258: 3376-3381.

Nathanson, L. and Gromet-Elhanan, Z. (1998) Mutagenesis of β-Glu-195 of the *Rhodospirillum rubrum* F1-ATPase and its role in divalent cation-dependent catalysis. *J Biol Chem* 273: 10933-10938.

Neill, S., Desikan, R. and Hancock, J. (2002) Hydrogen peroxide signalling. *Curr Opin Plant Biol* 5: 388-395.

Nishiyama, Y., Allakhverdiev, S.I. and Murata, N. (2006) A new paradigm for the action of reactive oxygen species in the photoinhibition of photosystem II. *Biochim Biophys Acta* 1757: 742-749.

Niyogi, K.K. (1999) Photoprotection Revisited: Genetic and molecular approaches. *Annu Rev Plant Physiol Plant Mol Biol* 50: 333-359.

Niyogi, K.K. (2000) Safety valves for photosynthesis. *Curr Opin Plant Biol* 3: 455-460.

Omote, H., Sambonmatsu, N., Saito, K., Sambongi, Y., Iwamoto-Kihara, A., Yanagida, T., Wada, Y. and Futai, M. (1999) The γ subunit rotation and torque generation in F1-ATPase from wild-type or uncoupled mutant *Escherichia coli*. *Proc Natl Acad Sci U S A* 96: 7780-7784.

op den Camp, R.G., Przybyla, D., Ochsenbein, C., Laloi, C., Kim, C., et al. (2003) Rapid induction of distinct stress responses after the release of singlet oxygen in Arabidopsis. *Plant Cell* 15: 2320-2332.

Ort, D.R. and Oxborough, K. (1992) *In situ* regulation of chloroplast coupling factor activity. *Annu Rev Plant Physiol Plant Mol Biol* 43: 269-291.

Penefsky, H.S. (1977) Reversible binding of Pi by beef-heart mitochondrial adenosine-triphosphatase. *J Biol Chem* 252: 2891-2899.

Pu, J.Z. and Karplus, M. (2008) How subunit coupling produces the γ subunit rotary motion in F-1-ATPase. *Proc Natl Acad Sci U S A* 105: 1192-1197.

Rees, D.M., Leslie, A.G.W. and Walker, J.E. (2009) The structure of the membrane extrinsic region of bovine ATP synthase. *Proc Natl Acad Sci U S A* 106: 21597-21601.

Rexroth, S., Poetsch, A., Rogner, M., Hamann, A., Werner, A., Osiewacz, H.D., Schafer, E.R., Seelert, H. and Dencher, N.A. (2012) Reactive oxygen species target specific tryptophan site in the mitochondrial ATP synthase. *Biochim Biophys Acta* 1817: 381-387.

Richter, M.L. (2004) γ–ε interactions regulate the chloroplast ATP synthase. *Photosynth Res* 79: 319-329.

Richter, M.L. and Gao, F. (1996) The chloroplast ATP synthase: structural changes during catalysis. *J Bioenerg Biomembr* 28: 443-449.

Richter, M.L., Gromet-Elhanan, Z. and McCarty, R.E. (1986) Reconstitution of the H^+-ATPase complex of *Rhodospirillum rubrum* by the β subunit of the chloroplast coupling factor-1. *J Biol Chem* 261: 12109-12113.

Richter, M.L., Hein, R. and Huchzermeyer, B. (2000) Important subunit interactions in the chloroplast ATP synthase. *Biochim Biophys Acta* 1458: 326-342.

Richter, M.L. and McCarty, R.E. (1987) Energy-dependent changes in the conformation of the ε subunit of the chloroplast ATP synthase. *J Biol Chem* 262: 15037-15040.

Richter, M.L., Patrie, W.J. and McCarty, R.E. (1984) Preparation of the ε subunit and ε subunit-deficient chloroplast coupling factor-1 in reconstitutively active forms. *J Biol Chem* 259: 7371-7373.

Richter, M.L., Samra, H.S., He, F., Giessel, A.J. and Kuczera, K.K. (2005) Coupling proton movement to ATP synthesis in the chloroplast ATP synthase. *J Bioenerg Biomembr* 37: 467-473.

Richter, M.L., Snyder, B., McCarty, R.E. and Hammes, G.G. (1985) Binding stoichiometry and structural mapping of the ε-polypeptide of chloroplast coupling factor-1. *Biochemistry* 24: 5755-5763.

Sambongi, Y., Iko, Y., Tanabe, M., Omote, H., Iwamoto-Kihara, A., Ueda, I., Yanagida, T., Wada, Y. and Futai, M. (1999) Mechanical rotation of the c subunit oligomer in ATP synthase (FoF1): direct observation. *Science* 286: 1722-1724.

Samra, H.S., Gao, F., He, F., Hoang, E., Chen, Z.G., Gegenheimer, P.A., Berrie, C.L. and Richter, M.L. (2006) Structural analysis of the regulatory dithiol-containing domain of the chloroplast ATP synthase γ subunit. *J Biol Chem* 281: 31041-31049.

Samra, H.S., He, F., Degner, N.R. and Richter, M.L. (2008) The role of specific β–γ subunit interactions in oxyanion stimulation of the MgATP hydrolysis of a hybrid photosynthetic F-1-ATPase. *J Bioenerg Biomembr* 40: 69-76.

Schuldiner, S., Rottenberg, H. and Avron, M. (1972) Determination of pH in chloroplasts. 2. Fluorescent amines as a probe for the determination of pH in chloroplasts. *Eur J Biochem* 25: 64-70.

Schumann, J., Richter, M.L. and McCarty, R.E. (1985) Partial proteolysis as a probe of the conformation of the γ subunit in activated soluble and membrane-bound chloroplast coupling factor-1. *J Biol Chem* 260: 11817-11823.

Shapiro, A.B. and McCarty, R.E. (1990) Substrate binding-induced alteration of nucleotide binding site properties of chloroplast coupling factor-1. *J Biol Chem* 265: 4340-4347.

Shen, H.R., Spikes, J.D., Kopecekova, P. and Kopecek, J. (1996a) Photodynamic crosslinking of proteins .1. Model studies using histidine- and lysine-containing N-(2-hydroxypropyl) methacrylamide copolymers. *J Photoch Photobio B* 34: 203-210.

Shen, H.R., Spikes, J.D., Kopeckova, P. and Kopecek, J. (1996b) Photodynamic crosslinking of proteins .2. Photocrosslinking of a model protein-ribonuclease A. *J Photoch Photobio B* 35: 213-219.

Shin, K., Nakamoto, R.K., Maeda, M. and Futai, M. (1992) FoF1-ATPase γ subunit mutations perturb the coupling between catalysis and transport. *J Biol Chem* 267: 20835-20839.

Shindyalov, I.N. and Bourne, P.E. (1998) Protein structure alignment by incremental combinatorial extension (CE) of the optimal path. *Protein Eng* 11: 739-747.

Sokolov, M., Lu, L., Tucker, W., Gao, F., Gegenheimer, P.A. and Richter, M.L. (1999) The 20 C-terminal amino acid residues of the chloroplast ATP synthase γ subunit are not essential for activity. *J Biol Chem* 274: 13824-13829.

Soteropoulos, P., Suss, K.H. and McCarty, R.E. (1992) Modifications of the γ subunit of chloroplast coupling factor-1 alter interactions with the inhibitory ε subunit. *J Biol Chem* 267: 10348-10354.

Spikes, J.D. and Knight, M. (1970) Dye-Sensitized photo-oxidation of proteins. *Ann N Y Acad Sci* 171: 149-162.

Stock, D., Leslie, A.G.W. and Walker, J.E. (1999) Molecular architecture of the rotary motor in ATP synthase. *Science* 286: 1700-1705.

Straight, R.C. and Spikes, J.D. (1985) Photosensitized oxidation of biomolecules. In *Singlet Oxygen*. Edited by Frimer, A.A. pp. 91-143. CRC Press, Boca Raton.

Studier, F.W. and Moffatt, B.A. (1986) Use of bacteriophage T7 RNA polymerase to direct selective high-level expression of cloned genes. *J Mol Biol* 189: 113-130.

Sun, S.X., Wang, H.Y. and Oster, G. (2004) Asymmetry in the F-1-ATPase and its implications for the rotational cycle. *Biophys J* 86: 1373-1384.

Sunamura, E., Konno, H., Imashimizu-Kobayashi, M., Sugano, Y. and Hisabori, T. (2010) Physiological impact of intrinsic ADP inhibition of cyanobacterial FoF1 conferred by the inherent sequence inserted into the γ subunit. *Plant Cell Physiol* 51: 855-865.

Takizawa, K., Kanazawa, A. and Kramer, D.M. (2008) Depletion of stromal Pi induces high 'energy-dependent' antenna exciton quenching (q_E) by decreasing proton conductivity at CFo-CF1 ATP synthase. *Plant Cell Environ* 31: 235-243.

Taussky, H.H. and Shorr, E. (1953) A microcolorimetric method for the determination of inorganic phosphorus. *J Biol Chem* 202: 675-685.

Telfer, A., Bishop, S.M., Phillips, D. and Barber, J. (1994) Isolated photosynthetic reaction center of photosystem II as a sensitizer for the formation of singlet oxygen. Detection and quantum yield determination using a chemical trapping technique. *J Biol Chem* 269: 13244-13253.

Triantaphylides, C., Krischke, M., Hoeberichts, F.A., Ksas, B., Gresser, G., Havaux, M., Van Breusegem, F. and Mueller, M.J. (2008) Singlet oxygen is the major reactive oxygen species involved in photooxidative damage to plants. *Plant Physiol* 148: 960-968.

Tsunoda, S.P., Rodgers, A.J., Aggeler, R., Wilce, M.C., Yoshida, M. and Capaldi, R.A. (2001) Large conformational changes of the ε subunit in the bacterial F1Fo ATP synthase provide a ratchet action to regulate this rotary motor enzyme. *Proc Natl Acad Sci U S A* 98: 6560-6564.

Tucker, W.C., Schwarz, A., Levine, T., Du, Z.Y., Gromet-Elhanan, Z., Richter, M.L. and Haran, G. (2004) Observation of calcium-dependent unidirectional rotational motion in recombinant photosynthetic F-1-ATPase molecules. *J Biol Chem* 279: 47415-47418.

Verweij, H. and Vansteveninck, J. (1982) Model studies on photodynamic cross-linking. *Photochem Photobiol* 35: 265-267.

Vougier, S., Mary, J., Dautin, N., Vinh, J., Friguet, B. and Ladant, D. (2004) Essential role of methionine residues in calmodulin binding to *Bordetella pertussis* adenylate cyclase, as probed by selective oxidation and repair by the peptide methionine sulfoxide reductases. *J Biol Chem* 279: 30210-30218.

Walker, J.E. (1998) ATP Synthesis by Rotary Catalysis (Nobel lecture). *Angew Chem Int Ed* 37: 2308-2319.

Walsh, M., Stevens, F.C., Oikawa, K. and Kay, C.M. (1978) Circular dichroism studies on Ca^{2+}-dependent protein modulator oxidized with N-chlorosuccinimide. *Biochemistry* 17: 3928-3930.

Wardman, P. and Vonsonntag, C. (1995) Kinetic factors that vontrol the fate of thiyl radicals in cells. *Methods Enzymol* 251: 31-45.

Wilkinson, F., Helman, W.P. and Ross, A.B. (1995) Rate constants for the decay and reactions of the lowest electronically excited singlet-state of molecular oxygen in solution - An expanded and revised compilation. *J Phys Chem Ref Data* 24: 663-1021.

Wright, A., Bubb, W.A., Hawkins, C.L. and Davies, M.J. (2002) Singlet oxygen-mediated protein oxidation: Evidence for the formation of reactive side chain peroxides on Tyrosine residues. *Photochem Photobiol* 76: 35-46.

Wu, G., Ortiz-Flores, G., Ortiz-Lopez, A. and Ort, D.R. (2007) A point mutation in *atpC1* raises the redox potential of the Arabidopsis chloroplast ATP synthase γ subunit regulatory disulfide above the range of thioredoxin modulation. *J Biol Chem* 282: 36782-36789.

Yamamoto, H.Y. (1979) Biochemistry of the violaxanthin cycle in higher plants. *Pure Appl.Chem* 51 639-648.

Zhang, J. and Kalonia, D.S. (2007) The effect of neighboring amino acid residues and solution environment on the oxidative stability of tyrosine in small peptides. *Aaps Pharmscitech* 8: 176-183.

Zhang, S., Letham, D.D. and Jagendorf, A.T. (1993) Inhibition of thylakoid ATPase by venturicidin as an indicator of CF1CFo interaction. *Plant Physiol* 101: 127-133.

7 Acknowledgements

I would like to thank Dr. Forreiter for giving me the opportunity to work on this project.

Especially, the parts of my most recent work would not have been realized without mass spectrometric expertise of Dr. Andreas Römpp and Yvonne Schober from the Institute of Inorganic and Analytical Chemistry (Justus-Liebig-University). Thank you for the nice collaboration.

I also want thank all members of the department. It was fun to work while being surrounded by collaborative individuals who never hesitated to spend their time and equipment to help me out. Thank you, Andrea, Anna-Lena, George, Jo, Jon, Kathi, Mathias, Melanie, Tanja, Tina (in alphabetical order).

Special thanks go out to Benni with whom I spend most of the time during my studies. We had a blast the last couple of years, both in the lab and in the world outside.

My PhD project received several productive inputs from collaborative experts on the field. I would like to gratefully acknowledge Dr. Richard E. McCarty (The Johns Hopkins University, USA) and Dr. Mark L. Richter (The University of Kansas, USA) for a warm welcome in their labs. I was trained several activity detection assays and reassembly procedures, and received structural model data during a visit in Baltimore and an EMBO Short Term Fellowship in Lawrence, respectively.

Finally, I want to say “thank you” to all my friends and, especially, my family. You are the ones who enduringly supported me with affection and understanding throughout the years. Thank you.

Stellungnahme

Ich habe die vorgelegte Dissertation selbstständig und ohne unerlaubte fremde Hilfe und nur mit den Hilfen angefertigt, die ich in der Dissertation angegeben habe. Alle Textstellen, die wörtlich oder sinngemäß aus veröffentlichen Schriften entnommen sind, und alle Angaben, die auf mündlichen Auskünften beruhen, sind als solche kenntlich gemacht. Bei den von mir durchgeführten und in der Dissertation erwähnten Untersuchungen habe ich die Grundsätze guter wissenschaftlicher Praxis, wie sie in der „Satzung der Justus-Liebig-Universität Gießen zur Sicherung guter wissenschaftlicher Praxis“ niedergelegt sind, eingehalten.

_____

Felix Buchert